SUPPORTING INFORMATION FOR

Synthetically Reversible, Proton-Mediated Nitrite N–O Bond Cleavage at a Dicopper Core

Jose Martinez Fernandez,[†] Alireza Haji Seyed Javadi,[‡] Simon J. Teat,[‖] Thomas R. Cundari,[‡*] and T. Don Tilley[†*]

[†]Department of Chemistry, University of California, Berkeley, Berkeley, California 94720, United States; Chemical Sciences Division, Lawrence Berkeley National Laboratory, Berkeley, California 94720, United States

[‡]Department of Chemistry, Center for Advanced Scientific Computing and Modeling (CASCaM), University of North Texas, Denton, Texas 76203, United States

[‖]Advanced Light Source, Lawrence Berkeley National Laboratory, Berkeley, California 94720, United States

[*]Email: tdtilley@berkeley.edu
[*]Email: Thomas.Cundari@unt.edu

TABLE OF CONTENTS:

1) General Considerations

Instrumentation and Physical Methods. Unless otherwise stated, all reactions and manipulations were carried out under an inert nitrogen atmosphere achieved through standard Schlenk techniques or an MBraun glovebox. ^{1}H and ^{19}F NMR spectra were acquired at 25° C using a Bruker AV-500 spectrometer. ^{13}C and ^{15}N NMR spectra were acquired at 25°C using a Bruker AV-600 spectrometer. ^{1}H and ^{13}C NMR spectra were referenced to residual signals from the solvent. ^{13}C NMR spectra were recorded at 125 MHz. ^{19}F NMR spectra were recorded at 470 MHz and referenced to hexafluorobenzene (δ -164.9 ppm vs. $CFCl_3$). ^{15}N NMR spectra were recorded at 61 MHz and referenced to an external standard composed of $Na^{15}NO_2$ in H_2O (δ = 609.5 ppm vs. liquid NH_3) inside a sealed glass capillary. Samples for ESI-MS were prepared in THF and acquired on a PerkinElmer AxION 2 UHPLC-TOF spectrometer equipped with an ESI source in the positive ionization mode. Carbon, hydrogen, and nitrogen elemental analyses were performed by Dr. Elena Kreimer in the College of Chemistry's Microanalytical Facility at the University of California, Berkeley. Analysis was performed with a Perkin Elmer CHNS 2400 Series II analyzer. A Thermo Fisher Scientific Nicolet iS10 FTIR spectrometer was used to collect infrared spectra. Samples were encased in a KBr pellet prior to data acquisition. Abbreviations for IR spectroscopy are as follows: s, strong; m, medium; w, weak; br, broad. Cyclic voltammetry experiments were performed at 25 °C in a nitrogen-filled glovebox using a BASi EC Epsilon potentiostat/galvanostat and a PWR-3 Power Module. A 3 mm diameter glassy carbon working electrode, Pt wire counter electrode, and $Ag/AgNO_3$ reference electrode were employed. Details for computational modeling and X-ray crystallography appear in sections 8 - 9 and 10 respectively.

Materials. Solvents were dried and deaerated using a JC Meyers Phoenix solvent purification system and then stored over 3 Å molecular sieves. Tetrahydrofuran-d_8 (THF-d_8) was purchased from Cambridge Isotope Laboratories, degassed by three freeze-pump-thaw cycles, and stored over activated 3 Å molecular sieves for 72 hours before use. Tetrabutylammonium nitrite ($[^{n}Bu_4N][NO_2]$) was purchased from Sigma Aldrich, dried under vacuum (60 mTorr) for 48 hours, and recrystallized from a diethyl ether/THF solution at -30 °C. CoTPP was purchased from Sigma Aldrich and dried under vacuum (60 mTorr) for 48 hours prior to use. 2,7-bis(fluoro-di(2-pyridyl)methyl)-1,8-naphthyridine (DPFN),[1] $[Cu_2(\mu\text{-CO})DPFN][NTf_2]_2$,[2] $[Cu_2(\mu\text{-OH})_2DPFN][NTf_2]_2$,[3] $[Cu_2(\mu\text{-O}^{t}Bu)DPFN][NTf_2]$,[4] $[Cu_3(DPFN)_2][NTf_2]_3$,[5] and $[Cu_2(\mu\text{-MeCN})DPFN][NTf_2]_2$ (**1**)[1] were prepared and purified according to literature

procedures. All other chemicals were purchased from commercial suppliers and used as received.

2) Synthesis and Characterization

Synthesis of $[Cu_2(\mu\text{–}\kappa^1\text{:}\kappa^1\text{-}O_2N)DPFN][NTf_2]$ (2)

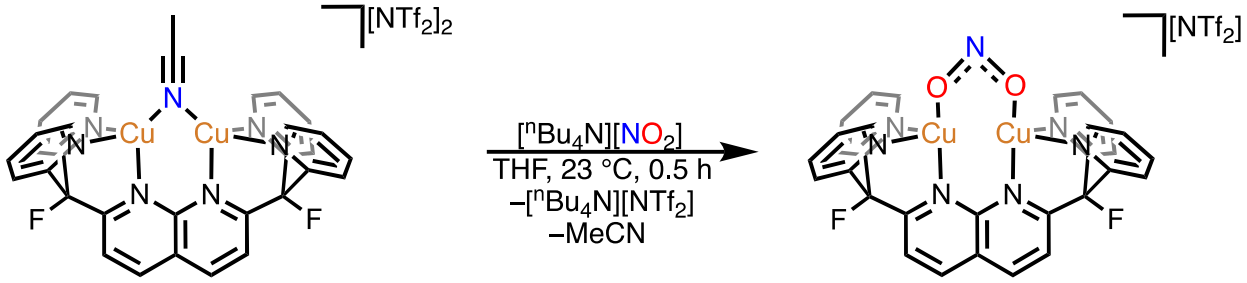

1 **2**

In a N_2-filled glovebox, a solution of $[n\text{Bu}_4\text{N}][NO_2]$ (0.023 g, 0.082 mmol, 1 equiv) in THF (2 mL) was added dropwise to a scintillation vial containing a solution of **1** (0.100 g, 0.0812 mmol) in THF (2 mL), being stirred by a magnetic stir bar. The bright orange solution immediately became dark red and was left to stir for 30 minutes at 23 °C. Volatiles were then removed under reduced pressure to afford a dark brown-red oil, which was subsequently triturated with diethyl ether (20 mL). The resulting brown powder was then allowed to settle, and the supernatant was carefully decanted. The powder was then washed with diethyl ether (2 x 1 mL) and pentane (2 x 1 mL) before being dried under vacuum for several hours to afford **2** as a light brown powder (0.076 g, 0.08 mmol, 98%). Layering diisopropyl ether over a saturated THF solution of the product at 23 °C afforded X-ray quality, black crystals of **2** after two days. **^{1}H NMR (500 MHz, THF-d_8):** δ 8.95 (d, *J* = 8.6 Hz, 2H, 4-naphth-C–*H*), 8.76 (d, *J* = 5.0 Hz, 4H, 6-pyridyl-C–*H*), 8.53 (dd, 8.6, 3.2 Hz, 2H, 3-naphth-C–*H*), 8.18 (dd, 8.1, 3.4 Hz, 4H, 3-pyridyl-C–*H*), 8.06 (td, 7.9, 1.8 Hz, 4H, 4-pyridyl-C–*H*), 7.53 (dd, 7.7, 5.0 Hz, 4H, 5-pyridyl-C–*H*). **^{19}F{^{1}H} NMR (470 MHz, THF-d_8):** δ –80.36 (s, 6F, –N(SO_2CF_3)$_2$), –172.90 (s, 2F, (pyridyl)$_2$(naphth)C–*F*). **^{13}C{^{1}H} NMR (125 MHz, THF-d_8):** δ 161.03 (d, *J* = 29.4 Hz, 2-naphth-*C*), 154.22 (d, *J* = 30.2 Hz, 2-pyridyl-*C*), 151.01 (8a-naphth-*C*), 150.22 (d, *J* = 3.2 Hz, 6-pyridyl-*C*-H), 142.40 (d, *J* = 4 Hz, 4-naphth-*C*–H), 140.25 (d, *J* = 3.2 Hz, 4-pyridyl-*C*–H), 125.76 (5-pyridyl-*C*–H), 125.06 (8a-naphth-*C*), 121.11 (d, *J* = 13.7 Hz, 3-pyridyl-*C*–H), 121.39 (q, *J* = 322 Hz, –N(SO_2CF_3)$_2$), 121.31 (d, *J* = 17.9 Hz, 3-naphthl-*C*–H) 94.42 (d, *J* = 186.6 Hz, pyridyl)$_2$(naphth)C–F). **^{15}N{^{1}H} NMR (61 MHz, THF-d_8):** δ 556.52 (s, $^{15}NO_2$). **IR (KBr, cm^{-1}):** 3074 (w), 1607 (s), 1593 (s), 1577 (m), 1546 (w), 1508 (m), 1465 (m), 1439 (m), 1405 (m), 1352 (s), 1309 (w), 1197 (s, br), 1136 (s), 1076 (s), 1062 (s), 1012 (m),

931 (w), 901 (w), 857 (m), 807 (w), 776 (s), 760 (w), 748 (w), 737 (m), 711 (w), 699 (m), 653 (m), 617 (s), 569 (s), 513 (s). **Anal. Calcd** for $C_{32}H_{20}Cu_2F_8N_8O_6S_2$: C, 40.21; H, 2.11; N, 11.72. Found: C, 40.39; H, 2.29; N, 11.40.

* The synthesis of $[Cu_2(\mu\text{–}\kappa^1\text{:}\kappa^1\text{-}O_2{}^{15}N)DPFN][NTf_2]$ employed excess $Na^{15}NO_2$ (remaining salt filtered after 30 minutes) instead of $[n Bu_4N][NO_2]$.

Synthesis of $Cu_2(\mu$-STol)DPFN][NTf_2] (3)

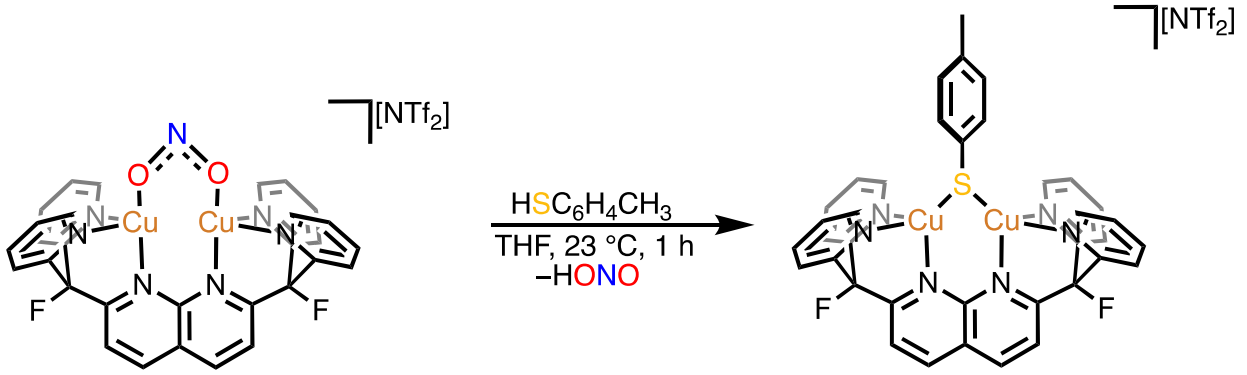

2 **3**

Under an inert atmosphere, 4-methylbenzenethiol (0.013 g, 0.11 mmol) was added to Schlenk flask containing a solution of **2** (0.100 g, 0.105 mmol) in THF (5 mL) being stirred by a magnetic stir bar at 23°C. The solution was stirred for 1 h which caused the color to change from black-red to dark orange. The solvent was then removed under reduced pressure and the remaining residue was washed with diethyl ether (3 x 5 mL). The resulting dark orange powder was redissolved in THF (5 mL) and filtered through Celite (1 cm height in a Pasteur pipette). Pentane was then allowed to diffuse into the solution at 23°C to yield X-ray quality, orange needle-shaped crystals of **3** (0.105 g, 0.102 mmol, 97%). **^{1}H NMR (600 MHz, THF-d_8):** δ 8.86 (d, *J* = 8.6 Hz, 2H, 4-naphth-C–*H*), 8.75 (s, 4H, 6-pyridyl-C–*H*), 8.47 (dd, *J* = 8.6, 3.3 Hz, 2H, 3-naphth-C–*H*), 8.15 (dd, *J* = 8.1, 3.3 Hz, 4H, 3-pyridyl-C–*H*), 8.02 (td, *J* = 7.9, 1.8 Hz, 4H, 4-pyridyl-C–*H*), 7.79 (d, *J* = 7.8 Hz, 4H, 2,6-tolyl-C–*H*), 7.44 (dd, *J* = 7.6, 5.0 Hz, 4H, 5-pyridyl-C–*H*), 6.98 (d, *J* = 7.7 Hz, 2H, 3,5-tolyl-C–*H*), 2.30 (s, 3H, tolyl methyl-C–*H*). **^{19}F{^{1}H} NMR (470 MHz, THF-d_8):** δ –80.25 (s, 6F, –N(SO_2CF_3)$_2$), –172.45 (s, 2F, (pyridyl)$_2$(naphth)C–*F*). **^{13}C{^{1}H} NMR (125 MHz, THF-d_8):** δ 161.00 (d, *J* = 29.4 Hz, 2-naphth-*C*), 154.64 (d, *J* = 29.9 Hz, 2-pyridyl-*C*), 151.53 (8a-naphth-*C*), 150.69 (6-pyridyl-*C*-H), 142.25 (d, *J* = 3.9 Hz, 4-naphth-*C*–H), 141.13 (4-tolyl-*C*), 140.06 (d, *J* = 3.5 Hz, 4-pyridyl-*C*–H), 134.69 (2,6-tolyl-*C*), 133.32 (1-tolyl-*C*), 129.72 (3,5-tolyl-*C*), 125.53 (5-pyridyl-*C*–H), 124.42 (8a-naphth-*C*), 121.36 (d, *J* = 14.4 Hz, 3-pyridyl-*C*–H), 121.49 (q, *J* = 323 Hz, –N(SO_2CF_3)$_2$), 120.61 (d, *J* = 17.3 Hz, 3-naphth-*C*–H), 94.37

(d, J = 187.3 Hz, pyridyl)$_2$(naphth)*C*–F), 21.16 (tolyl methyl-*C*–H). **IR (KBr, cm^{-1}):** 3070 (w), 2944 (w), 2865 (w), 1594 (s), 1576 (m), 1545 (w), 1503 (m), 1485 (m), 1464 (s), 1438 (m), 1354 (s), 1333 (s), 1295 (w), 1227 (m), 1196 (s), 1135 (m), 1075 (m), 1057 (s), 1011 (w), 928 (w), 858 (m), 808 (m), 771 (s), 755 (m), 739 (m), 711 (m), 699 (m), 687 (m), 644 (w), 616 (s), 570 (s), 497 (m). **Anal. Calcd** for $C_{39}H_{27}Cu_2F_8N_7O_4S_3$: C, 45.35; H, 2.63; N, 9.49. Found: C, 45.21; H, 2.77; N, 9.32.

Synthesis of [Cu$_2$(μ-NO)(μ-OH)DPFN][NTf$_2$]$_2$ (4)

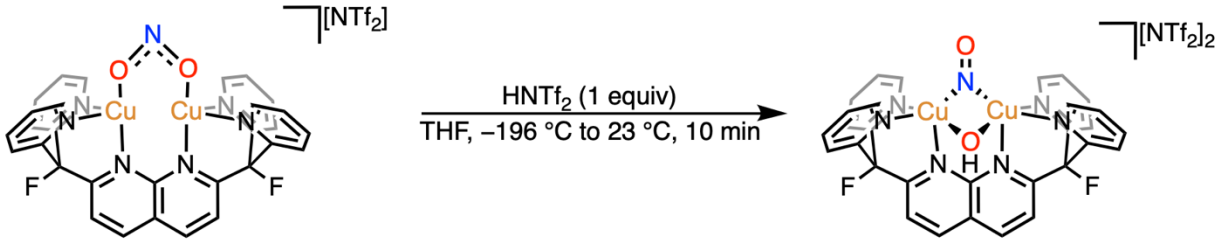

2 **4**

In a N_2-filled glovebox, a scintillation vial containing a solution of **2** (0.100 g, 0.105 mmol) in THF (2 mL) and a magnetic stir bar, was left in a cold well cooled with liquid nitrogen for 10 minutes. The vial with the frozen solution was then removed from the cold well and a solution of bistriflimidic acid (0.029 g, 0.11 mmol) in THF (2 mL) was added dropwise. The black-red solid began to slowly melt and turn dark green. Pentane (16 mL) was quickly added after 10 minutes of stirring under these conditions, which caused precipitation of a dark green solid. The residue was then dried under vacuum for several hours to afford **3** as a dark green powder (0.126 g, 0.103 mmol, 98%). Layering of pentane onto a saturated THF solution of the product in a J. Young NMR tube at 23 °C, afforded X-ray quality, dichroic green/orange needle-shaped crystals of **3** after 3 days. **^{1}H NMR (600 MHz, THF-d_8):** δ 9.15 (d, J = 8.7 Hz, 2H, 4-naphth-C–*H*), 8.98 (d, J = 5.3 Hz, 2H, 6-pyridyl-C–*H*$_a$), 8.93 (d, J = 5.1 Hz, 2H, 6-pyridyl-C–*H*$_b$), 8.67 (dd, J = 8.6, 3.1 Hz, 2H, 3-naphth-C–*H*), 8.27-8.23 (m, 4H, 3-pyridyl-C–*H*$_{a,b}$), 8.21 (dd, J = 8.3, 3.1 Hz, 2H, 4-pyridyl-C–*H*$_a$), 8.15 (td, J = 7.9, 1.6 Hz, 2H, 4-pyridyl-C–*H*$_b$), 7.83 (td, 6.0, 2.2 Hz, 2H, 5-pyridyl-C–*H*$_a$), 7.67 (dd, 7.5, 5.2 Hz, 2H, 5-pyridyl-C–*H*$_b$), 1.22 (s, 1H, O–*H*). **^{19}F{^{1}H} NMR (470 MHz, THF-d_8):** δ –80.25 (s, 6F, –N(SO$_2$CF$_3$)$_2$), –174.41 (s, 2F, (pyridyl)$_2$(naphth)C–*F*). **^{13}C{^{1}H} NMR (125 MHz, THF-d_8):** δ 161.80 (d, J = 30.5 Hz, 2-naphth-*C*), 153.16 (d, J = 9.7 Hz, 2-pyridyl-*C*), 152.97 (d, J = 10.3 Hz, 2-pyridyl-*C*), 151.27 (8a-naphth-*C*), 151.25 (d, J = 11.9 Hz, 6-pyridyl-*C*-H), 145.11 (4-naphth-*C*–H), 142.93 (d, J = 3.6 Hz, 4-pyridyl-*C*–H$_a$), 142.49 (d, J = 3.6 Hz, 4-pyridyl-*C*–H$_b$), 128.33 (5-pyridyl-*C*–H$_a$), 127.50 (5-

pyridyl-*C*–H_b), 125.27 (8-naphth-*C*), 122.56 (d, *J* = 9.7 Hz, 3-pyridyl-*C*–H_b), 122.46 (d, *J* = 11.4 Hz, 3-pyridyl-*C*–H_a), 121.18 (q, *J* = 322.7 Hz, –$N(SO_2CF_3)_2$), 120.36 (d, *J* = 15.2 Hz, 3-naphth-*C*–H), 94.02 (d, *J* = 189.2 Hz, $(pyridyl)_2$(naphth)C–F). **IR (KBr, cm^{-1}):** 3547 (m, br), 3090 (w), 1607 (m), 1579 (w), 1555 (w), 1507 (w), 1473 (m), 1445 (m), 1352 (s), 1193 (s, br), 1134 (s), 1086 (m), 1058 (s), 931 (w), 901 (w), 773 (s), 740 (w), 710 (w), 688 (m), 654 (m), 616 (s), 599 (s), 570 (s), 510 (m). **Anal. Calcd** for $C_{34}H_{21}Cu_2F_{14}N_9O_{10}S_4$: C, 33.02; H, 1.71; N, 10.19. Found: C, 33.40; H, 1.65; N, 9.86.

* The synthesis of $[Cu_2(\mu\text{-}^{15}NO)(\mu\text{-}OH)DPFN][NTf_2]_2$ employed $[Cu_2(\kappa^1,\kappa^1\text{-}O_2{}^{15}N)DPFN][NTf_2]$ instead of $[Cu_2(\kappa^1,\kappa^1\text{-}O_2N)DPFN][NTf_2]$.

3) Reactivity Studies

Monitoring HONO release from the reaction of $[Cu_2(\mu\text{–}\kappa^1\text{:}\kappa^1\text{-}O_2N)DPFN][NTf_2]$ (2) with 4-methylbenzenethiol

2 **3**

In a N_2-filled glovebox, a 4 mL shell vial containing a THF (1 mL) solution of **2** (0.02 g, 0.021 mmol) being stirred by a magnetic stir bar was placed inside a 20 mL scintillation vial containing a THF (2 mL) solution of CoTPP (0.0141 g, 0.021 mmol). The 20 mL scintillation vial was capped with a rubber septum and a THF (1 mL) solution of 4-methylbenzenethiol (0.0026 g, 0.021 mmol) was added dropwise to the shell vial with a syringe. The black-red color of the initial solution turned dark orange upon addition. After an hour, the solution in the 20 mL scintillation vial was transferred to a J. Young NMR tube. An internal standard of hexamethylbenzene (0.002 g, 0.01 mmol) was then added to the NMR tube. ^{1}H NMR spectroscopy indicated generation of $\{CoNO\}^8$ (61%).

Reaction of $[Cu_2(\mu\text{-NO})(\mu\text{-OH})DPFN][NTf_2]_2$ (4) and CoTPP

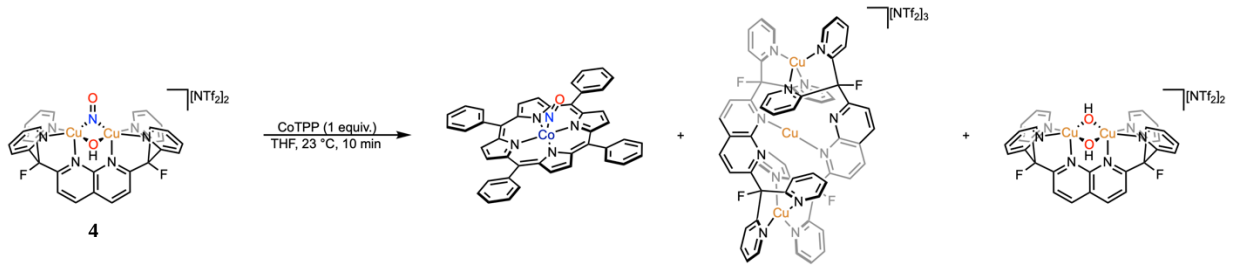

4

In a N_2-filled glovebox, a THF (2 mL) solution of CoTPP (0.005 g, 0.008 mmol) was added dropwise to a scintillation vial containing a THF (2 mL) solution of **4** (0.01 g, 0.008 mmol) being stirred by a magnetic stir bar. The green color of the solution of **4** was eclipsed by the red color of the CoTPP solution. The mixture was stirred for an hour after addition before being filtered through glass wool and Celite (1 cm height in a Pasteur pipette). The solution was then concentrated under vacuum and transferred to a J. Young NMR tube. An internal standard of C_6F_6 (1 µL) was then added to the NMR tube. ^1H, $^{19}F\{^1H\}$) NMR spectroscopy indicated full consumption of **4**, with generation of $Cu_3(DPFN)_2][NTf_2]_3$ (17%), $[Cu_2(\mu\text{-OH})_2DPFN][NTf_2]_2$ (37%), and $\{CoNO\}^8$ (97%). This result suggested that after NO loss to CoTPP, the remaining $[Cu_2(\mu\text{-OH})DPFN][NTf_2]_2$ is unstable under these conditions, and disproportionates to give the aforementioned DPFN-containing products.

Reaction of $[Cu_2(\mu\text{-NO})(\mu\text{-OH})DPFN][NTf_2]_2$ (4) and KO^tBu

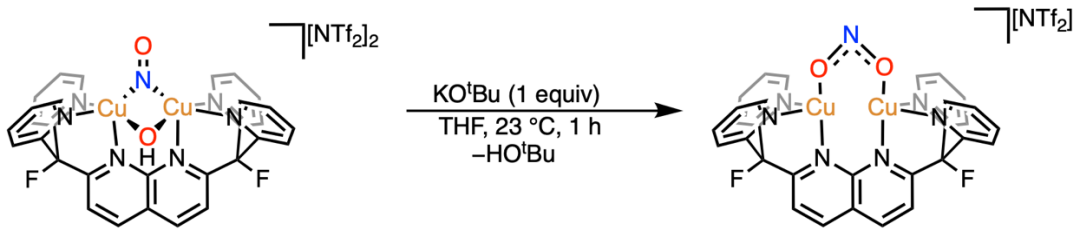

4 2

In a N_2-filled glovebox, a THF (1 mL) solution of **4** (0.020 g, 0.016 mmol) was added dropwise to a scintillation vial containing a mixture of finely crushed KO^tBu (0.0018 g, 0.016 mmol) and THF (1 mL) being stirred by a magnetic stir bar. The green color of the resulting mixture turned black-red a few seconds after addition and a noticeable exotherm was observed. The mixture was stirred for an hour longer before being filtered through glass wool and Celite (1 cm height in a Pasteur pipette). The solution was then transferred to a J. Young NMR tube. An internal standard of C_6F_6 (1 µL) was then added to the NMR tube. Multinuclear (^1H, $^{19}F\{^1H\}$) NMR spectroscopy indicated full consumption of **4**, accompanied by formation of

2 (72%) and HO^{t}Bu (98%). Additionally, trace amount of [Cu$_2$(μ-O^{t}Bu)DPFN][NTf$_2$] (5%) was formed and likely resulted from the reaction of the two aforementioned products formed after deprotonation.

Reaction of [Cu$_2$(μ-NO)(μ-OH)DPFN][NTf$_2$]$_2$ (4) and CO

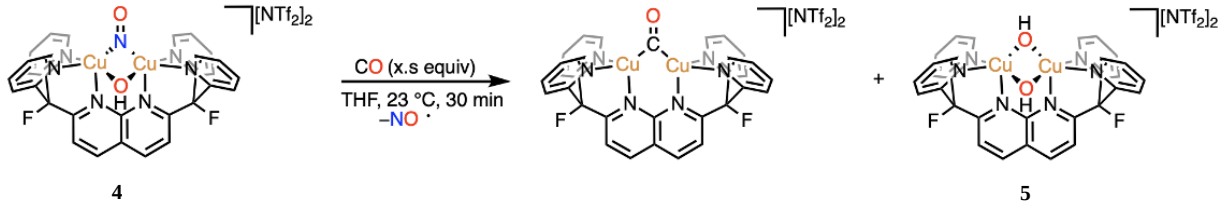

4 5

In a N$_2$-filled glovebox, a THF (1 mL) solution of **4** (0.013 g, 0.011 mmol) was transferred to a J. Young NMR tube. The solution was then degassed by being subjected to three freeze-pump-thaw cycles. Ultra-high purity carbon monoxide was administered to the NMR tube for 20 seconds. After addition, the tube was shaken vigorously for 5 minutes, which caused the solution to turn light blue. After 25 more minutes, the solution was once again degassed by three freeze-pump-thaw cycles. An internal standard of C$_6$F$_6$ (1 µL) was then added to the NMR tube. Multinuclear (^{1}H, ^{19}F{^{1}H}) NMR spectroscopy indicated full consumption of **4**, with generation of [Cu$_2$(μ-OH)$_2$DPFN][NTf$_2$]$_2$ (41%) and [Cu$_2$(μ-CO)DPFN][NTf$_2$]$_2$ (35%). These results imply the formation of an unstable [Cu$_2$(μ-OH)(μ-CO)DPFN][NTf$_2$]$_2$ that disproportionates to give the aforementioned DPFN-containing products.

Reaction of [Cu$_2$(μ-NO)(μ-OH)DPFN][NTf$_2$]$_2$ (4) and [^{n}Bu$_4$N][NO$_2$]

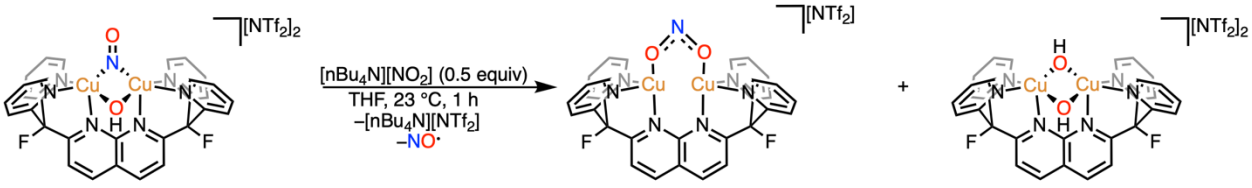

4 2 5

In a N$_2$-filled glovebox, a 4 mL shell vial containing a THF (1 mL) solution of **4** (0.01 g, 0.008 mmol) being stirred by a magnetic stir bar was placed inside a 20 mL scintillation vial containing a THF (2 mL) solution of CoTPP (0.0054 g, 0.008 mmol). The 20 mL scintillation vial was capped with a rubber septum and a THF (1 mL) solution of [^{n}Bu$_4$N][NO$_2$] (0.001 g, 0.004 mmol, 0.5 equiv) was added dropwise to the shell vial with a syringe. The green color of the resulting mixture turned black-red a few seconds after addition. The mixture was stirred for an hour longer before being filtered through glass wool and Celite (1 cm height in a Pasteur pipette). The

solution was then transferred to a J. Young NMR tube. An internal standard of C_6F_6 (1 µL) was then added to the NMR tube. Multinuclear (^{1}H, ^{19}F{^{1}H}) NMR spectroscopy indicated full consumption of **4**, with generation of **2** (31%) and $[Cu_2(\mu\text{-}OH)_2DPFN][NTf_2]_2$ (33%). These results imply the formation of an unstable $[Cu_2(\mu\text{-}OH)(\kappa^1,\kappa^1\text{-}O_2N)DPFN][NTf_2]$ that reacts with the remaining amount of **4** to give the aforementioned DPFN-containing products. The solution of the 20 mL scintillation vial was also transferred to a J. Young NMR tube. An internal standard of hexamethylbenzene (0.0022 g, 0.014 mmol) was then added to the NMR tube. ^{1}H NMR spectroscopy indicated almost quantitative consumption of CoTPP and generation of $\{CoNO\}^8$ (84%).

4) NMR Spectra

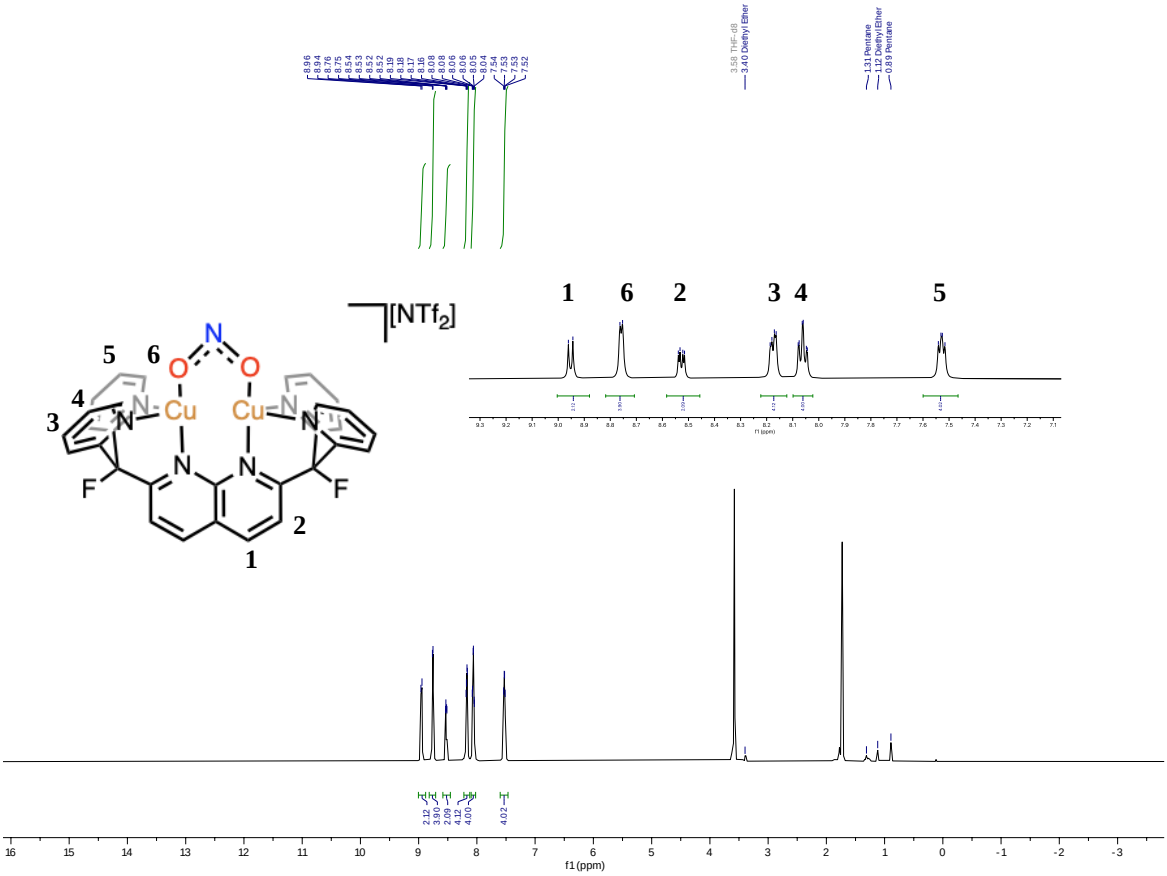

Figure S1. ^{1}H NMR spectrum (THF-d_8, 500 MHz) of complex **2.**

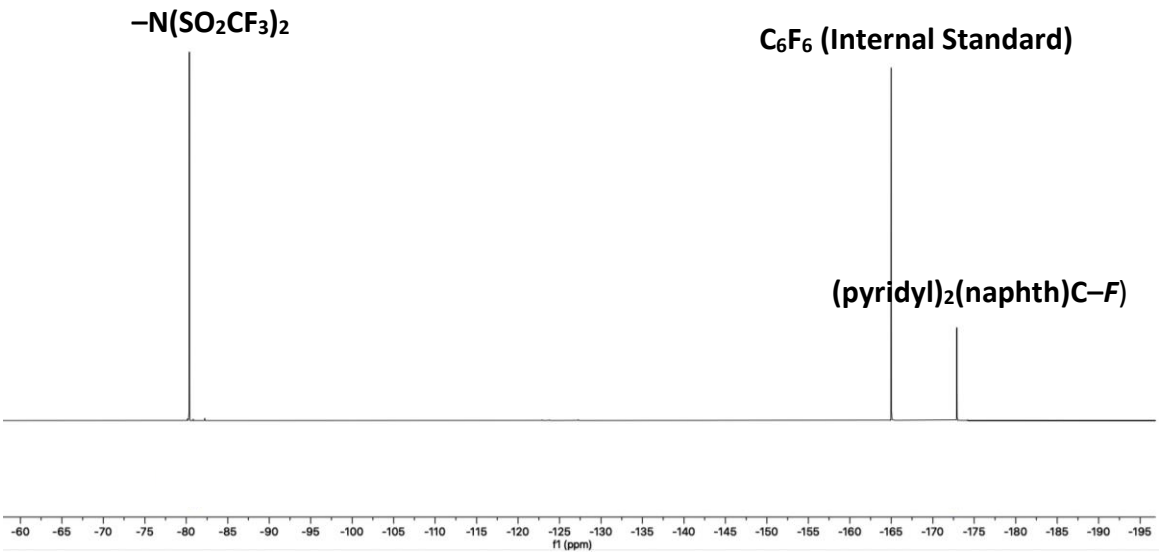

Figure S2. $^{19}F\{^{1}H\}$ NMR spectrum (THF-d_8, 470 MHz) of complex **2.**

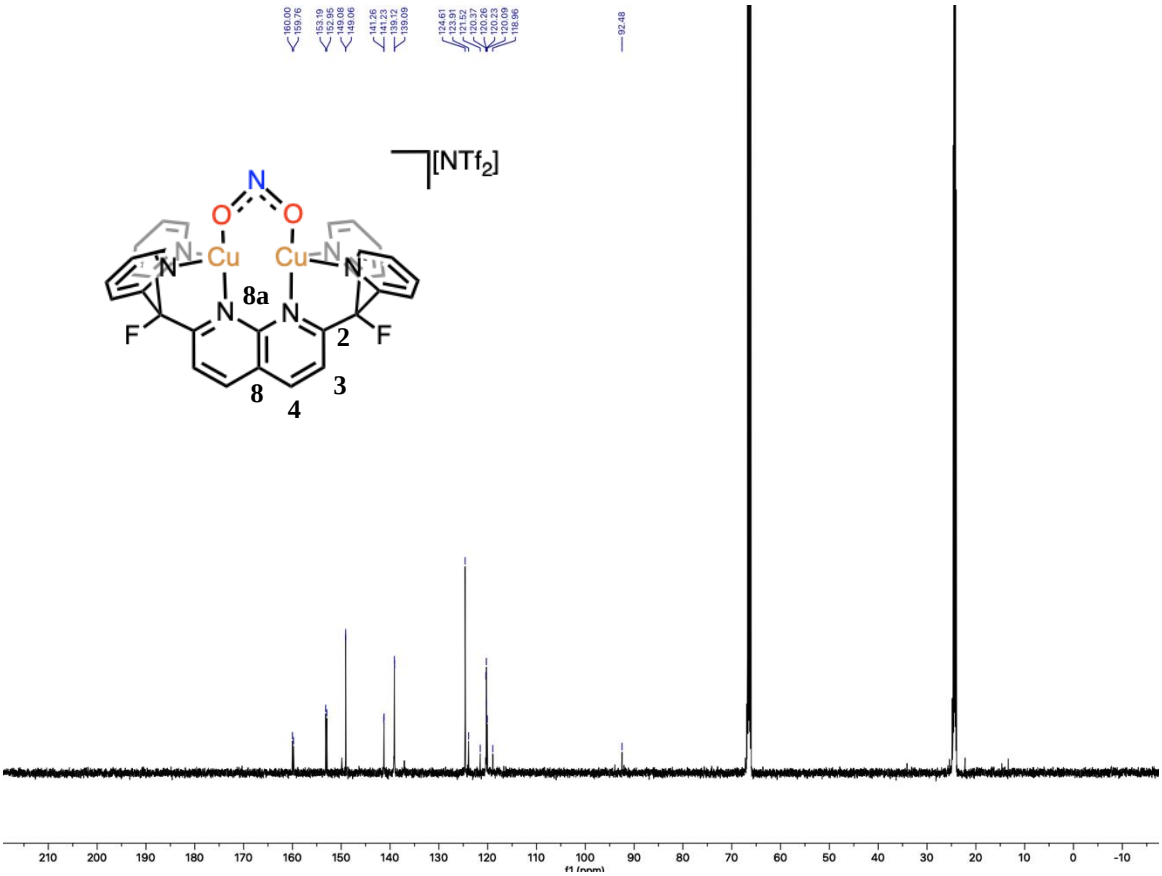

Figure S3. $^{13}C\{^{1}H\}$ NMR spectrum (THF-d_8, 125 MHz) of complex **2.**

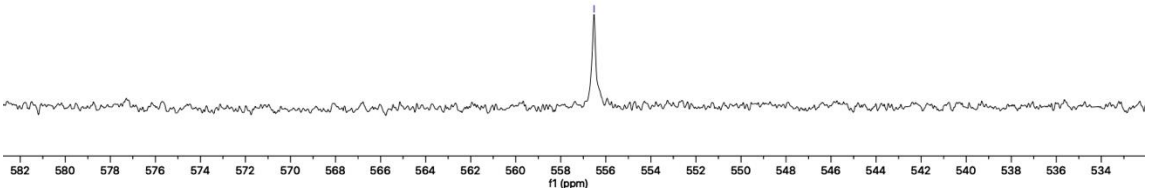

Figure S4. $^{15}N\{^{1}H\}$ NMR spectrum (THF-d_8, 61 MHz) of complex **2.**

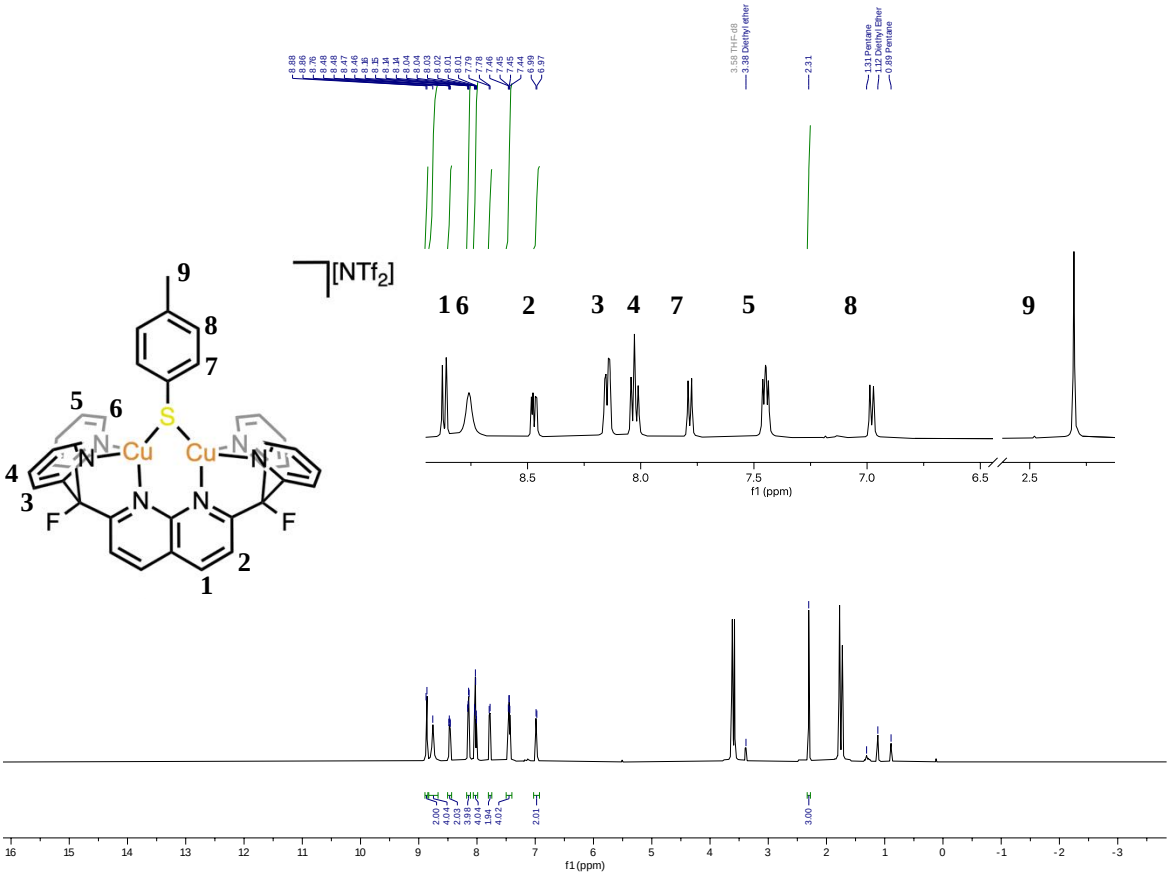

Figure S5. ^{1}H NMR spectrum (THF-d_8, 500 MHz) of complex **3.**

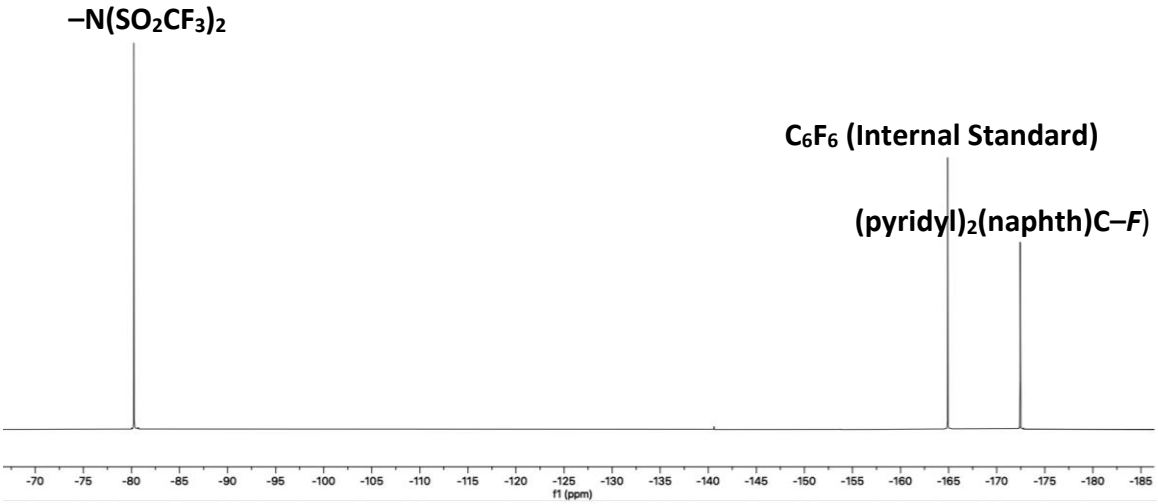

Figure S6. $^{19}F\{^{1}H\}$ NMR spectrum (THF-d_8, 470 MHz) of complex **3.**

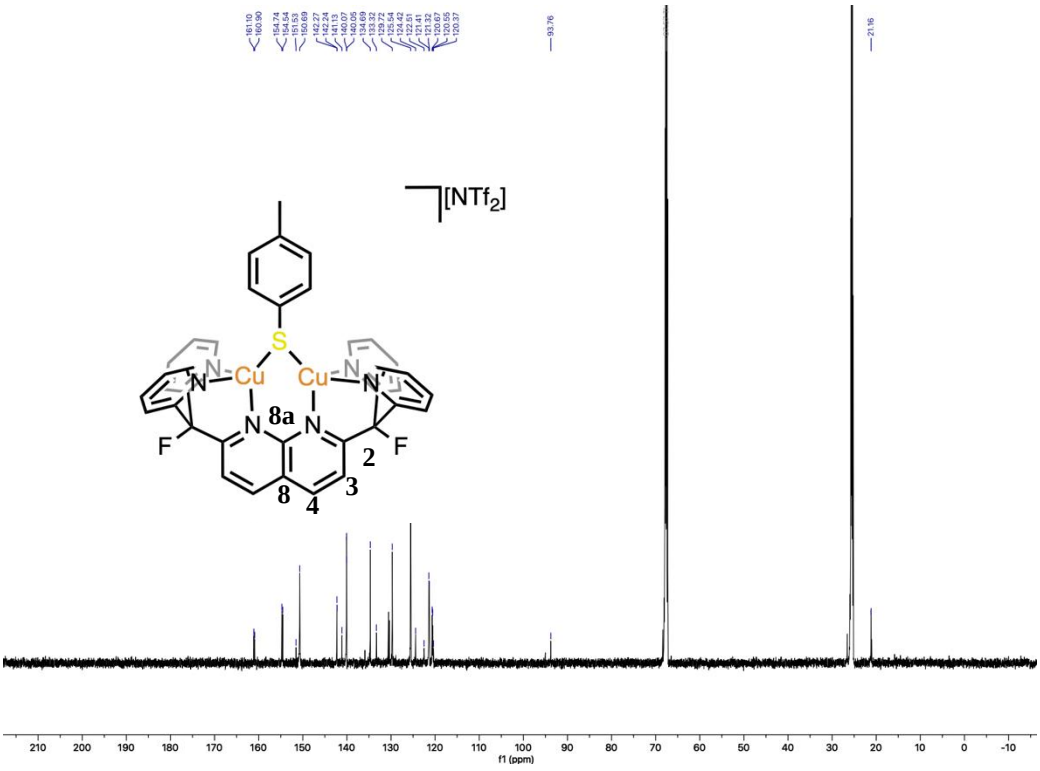

Figure S7. $^{13}C\{^{1}H\}$ NMR spectrum (THF-d_8, 125 MHz) of complex **3.**

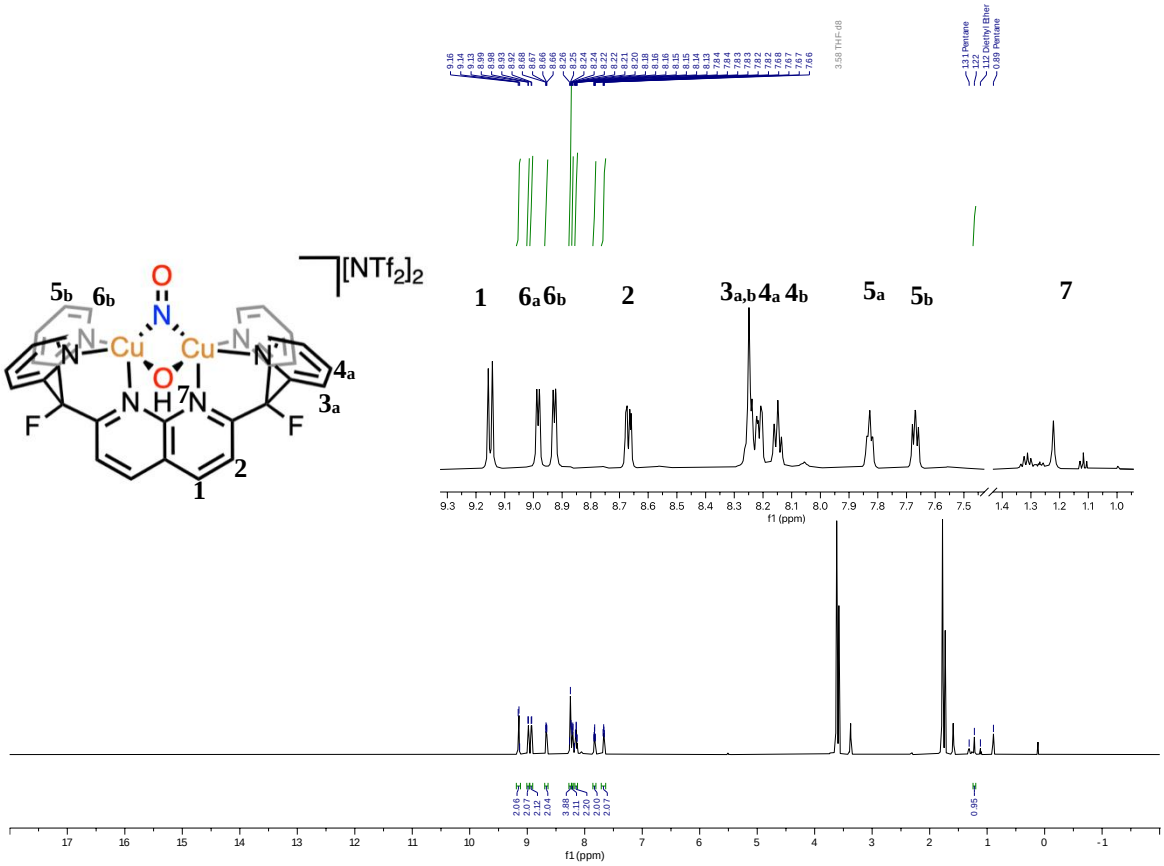

Figure S8. ^{1}H NMR spectrum (THF-d_8, 600 MHz) of complex **4.**

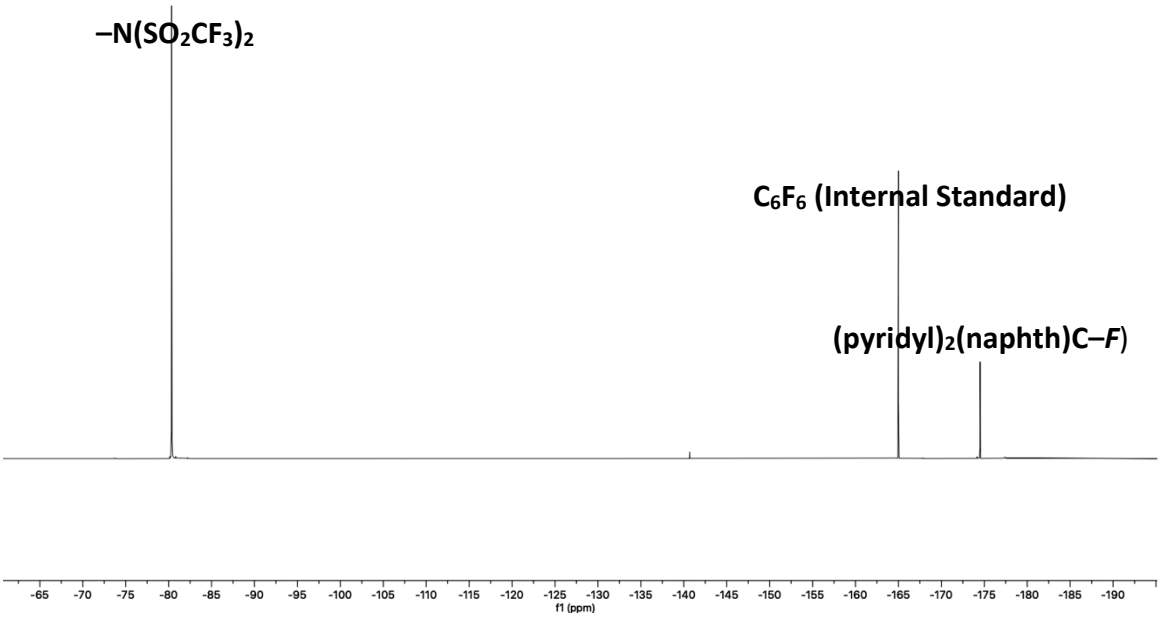

Figure S9. ^{19}F{^{1}H} NMR spectrum (THF-d_8, 470 MHz) of complex **4.**

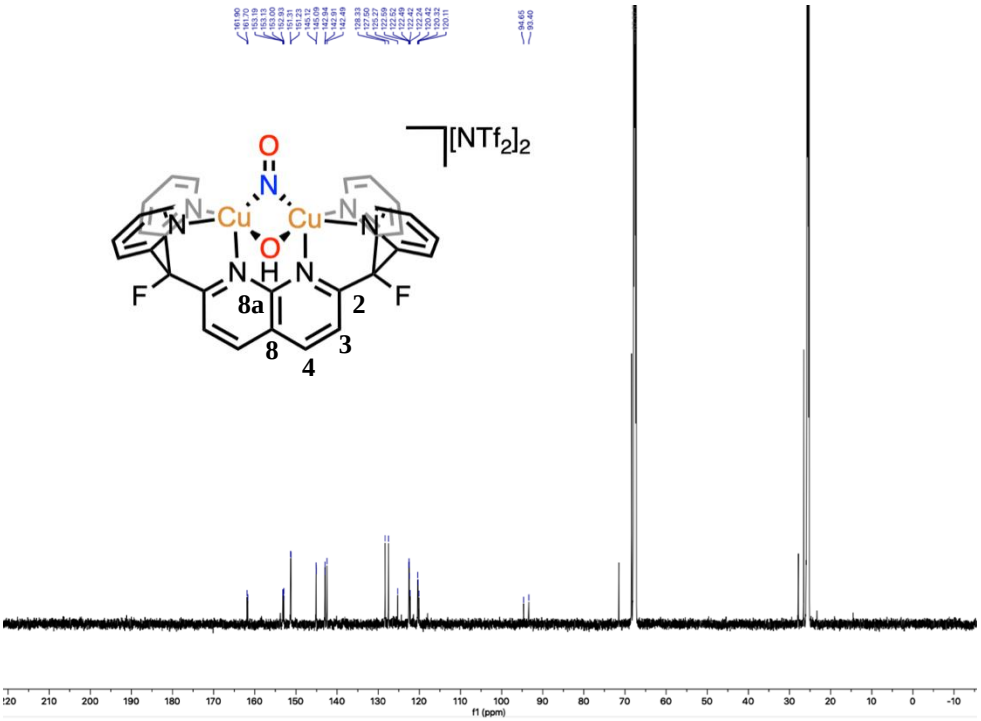

Figure S10. $^{13}C\{^{1}H\}$ NMR spectrum (THF-d_8, 125 MHz) of complex **4.**

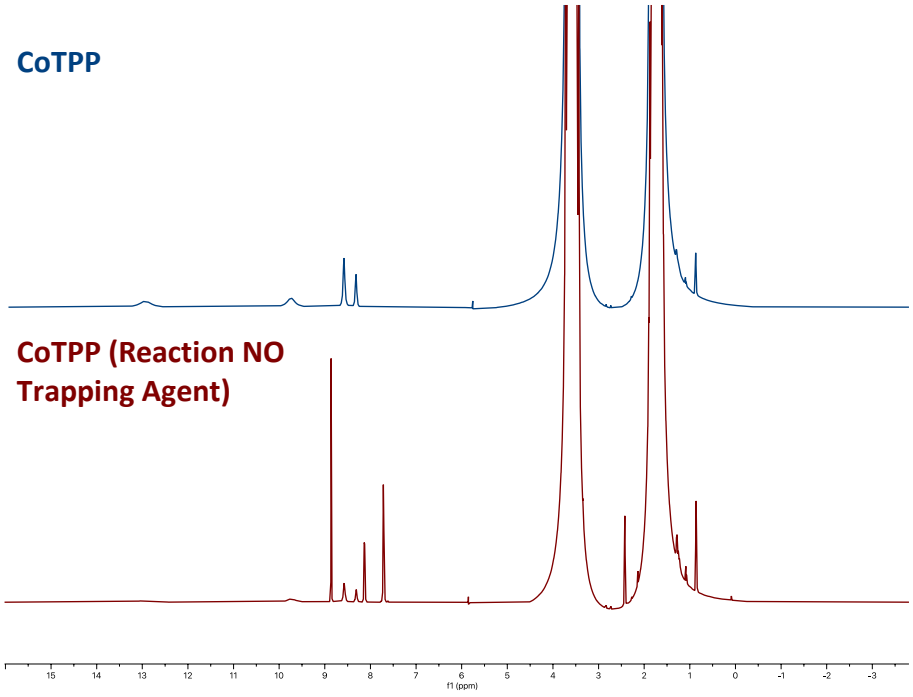

Figure S11. ^{1}H NMR spectra (THF-h_8, 500 MHz) of CoTPP (top) and CoTPP used to trap NO released (nitrous acid decomposition product) by the reaction of **2** and 4-methylbenzenethiol (1 equiv) on a 20 mg scale (bottom).

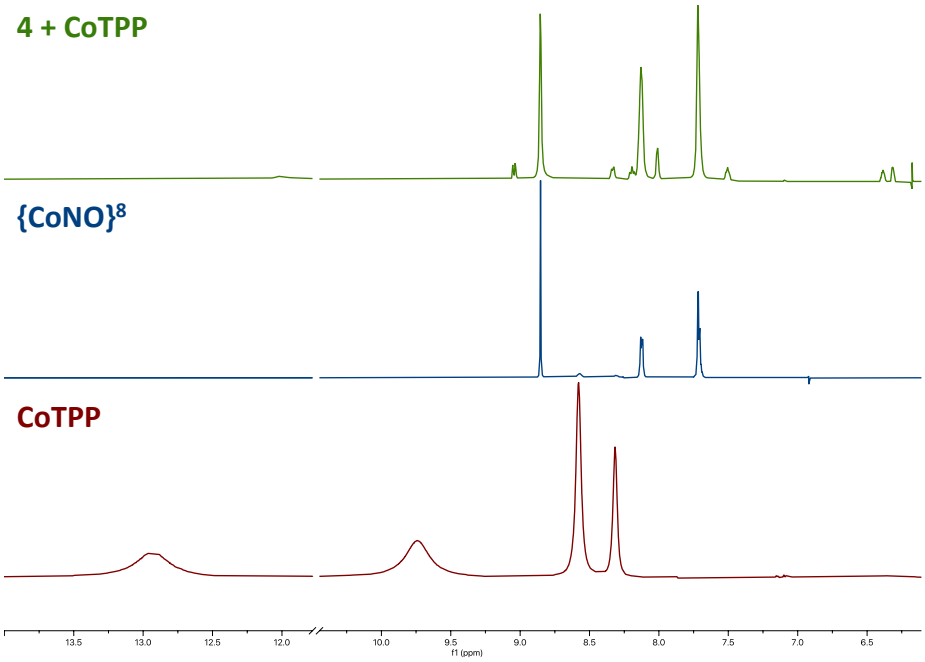

Figure S12. ^{1}H NMR spectra (THF-h_8, 500 MHz) of **4** + CoTPP on a 10 mg scale (top), {CoNO}^{8} (middle), and CoTPP (bottom).

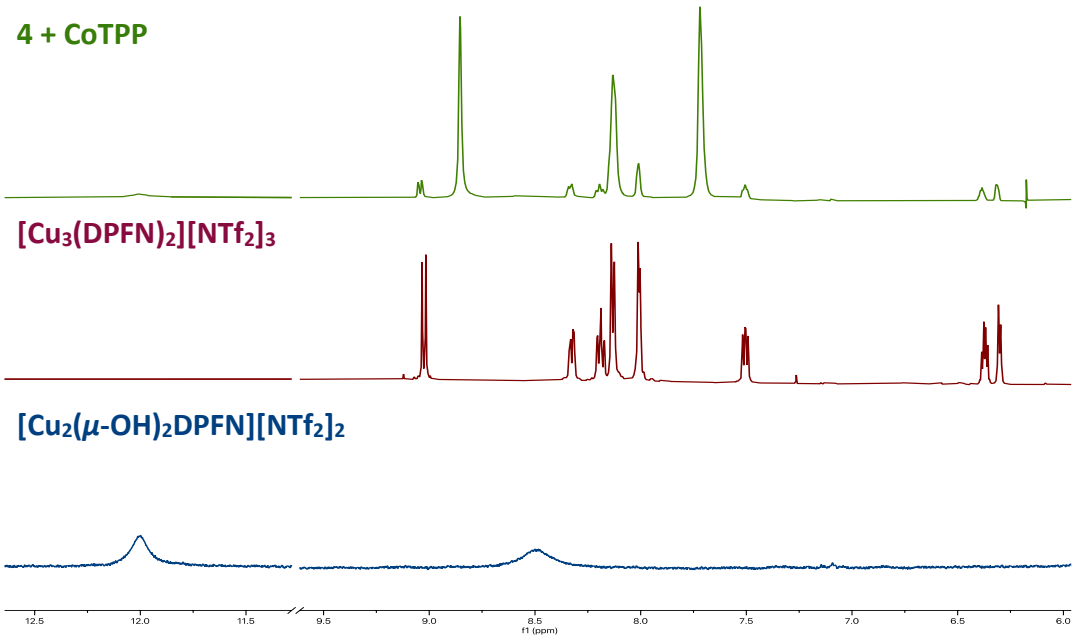

Figure S13. ^{1}H NMR spectra (THF-h_8, 500 MHz) of **4** + CoTPP on a 10 mg scale (top), $[Cu_3(DPFN)_2][NTf_2]_3$ (middle), and $[Cu_2(\mu\text{-}OH)_2DPFN][NTf_2]_2$ (bottom).

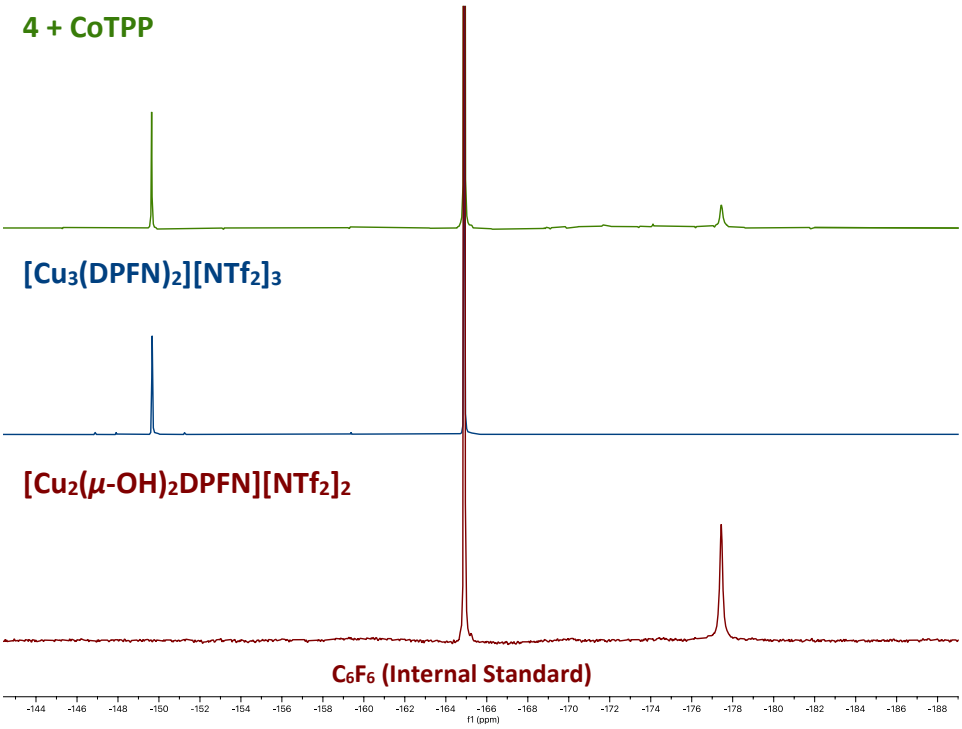

Figure S14. $^{19}F\{^{1}H\}$ NMR spectra (THF-h_8, 470 MHz) of **4** + CoTPP on a 10 mg scale (top), $[Cu_3(DPFN)_2][NTf_2]_3$ (middle), and $[Cu_2(\mu\text{-}OH)_2DPFN][NTf_2]_2$ (bottom).

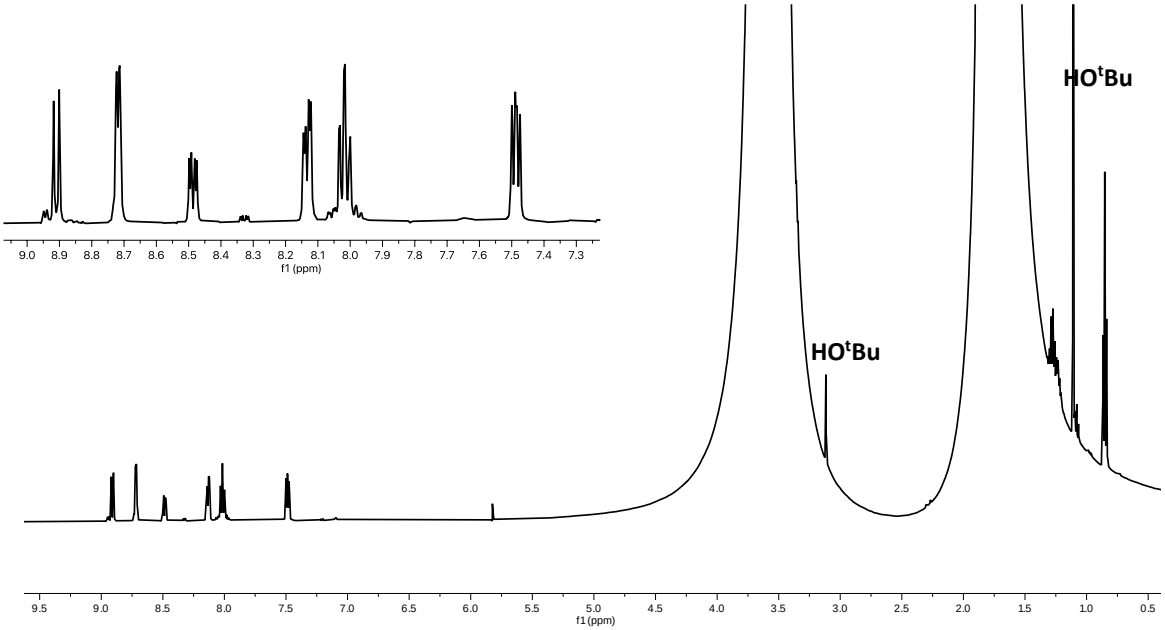

Figure S15. ^{1}H NMR spectrum (THF-h_8, 500 MHz) of **4** + KO^{t}Bu on a 10 mg scale.

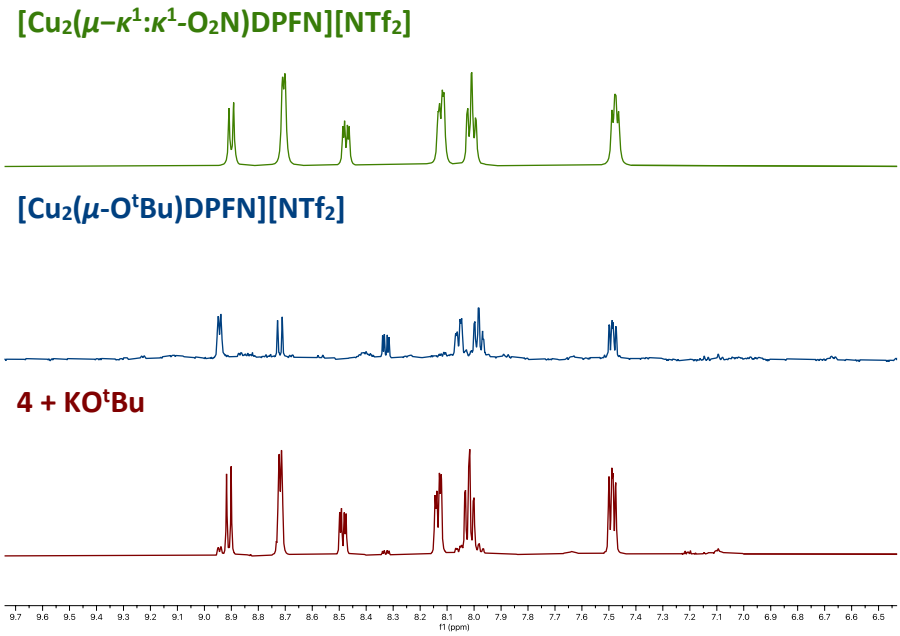

Figure S16. ^{1}H NMR spectra (THF-h_8, 500 MHz) of [Cu$_2$(μ–κ^1:κ^1-O$_2$N)DPFN][NTf$_2$] (top), [Cu$_2$(μ-O^{t}Bu)DPFN][NTf$_2$] (middle), and **4** + KO^{t}Bu on a 10 mg scale (bottom).

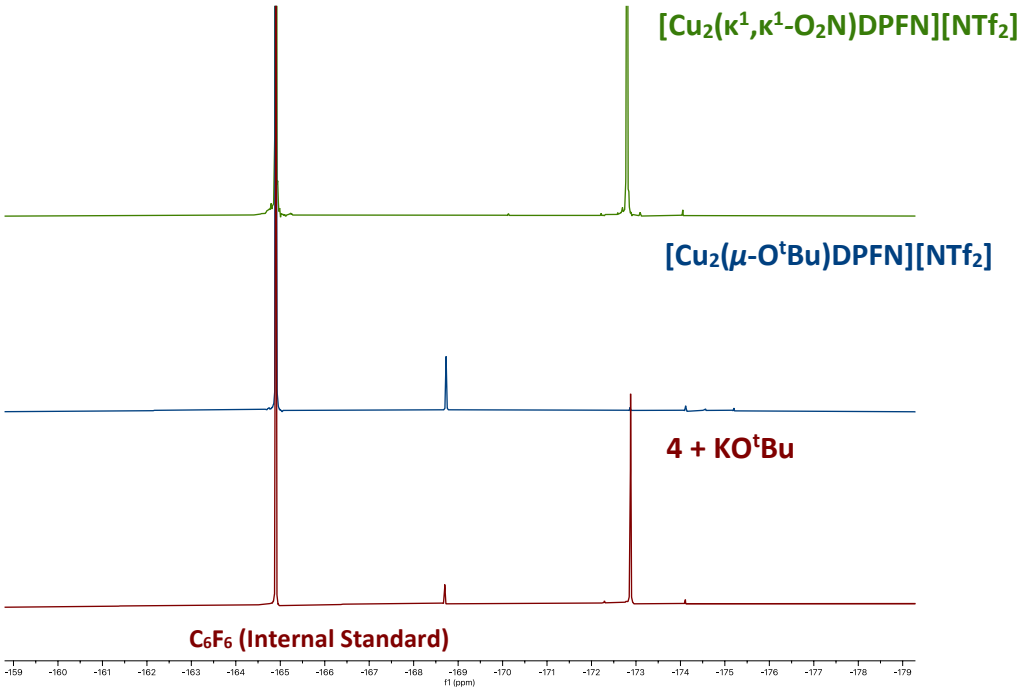

Figure S17. ^{19}F{^{1}H} NMR spectra (THF-h_8, 470 MHz) of [Cu$_2$(μ–κ^1:κ^1-O$_2$N)DPFN][NTf$_2$] (top), [Cu$_2$(μ-O^{t}Bu)DPFN][NTf$_2$] (middle), and **4** + KO^{t}Bu on a 10 mg scale (bottom).

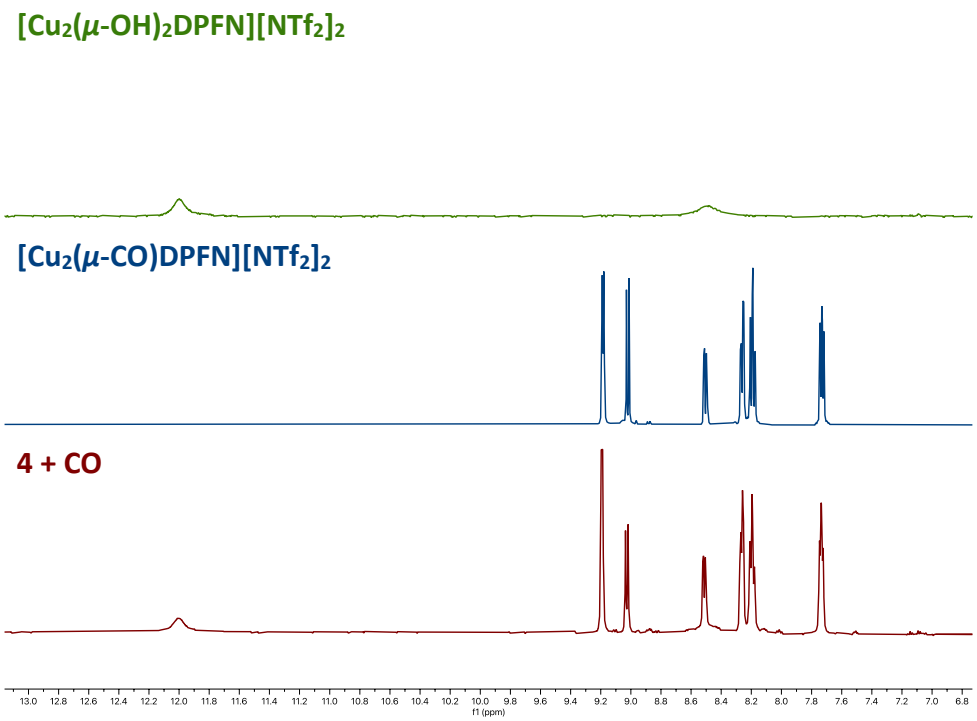

Figure S18. ^{1}H NMR spectra (THF-h_8, 500 MHz) of $[Cu_2(\mu\text{-}OH)_2DPFN][NTf_2]_2$, $[Cu_2(\mu\text{-}CO)DPFN][NTf_2]_2$, and **4** + CO (excess) on a 10 mg scale (bottom).

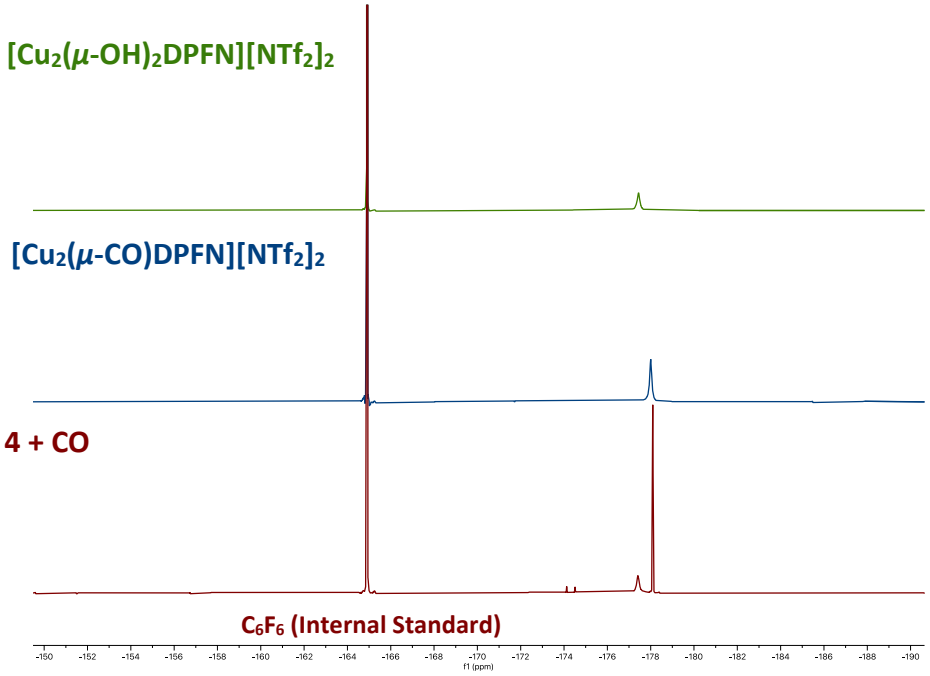

Figure S19. ^{19}F{^{1}H} NMR spectra (THF-h_8, 470 MHz) of $[Cu_2(\mu\text{-}OH)_2DPFN][NTf_2]_2$, $[Cu_2(\mu\text{-}CO)DPFN][NTf_2]_2$, and **4** + CO (excess) on a 10 mg scale (bottom).

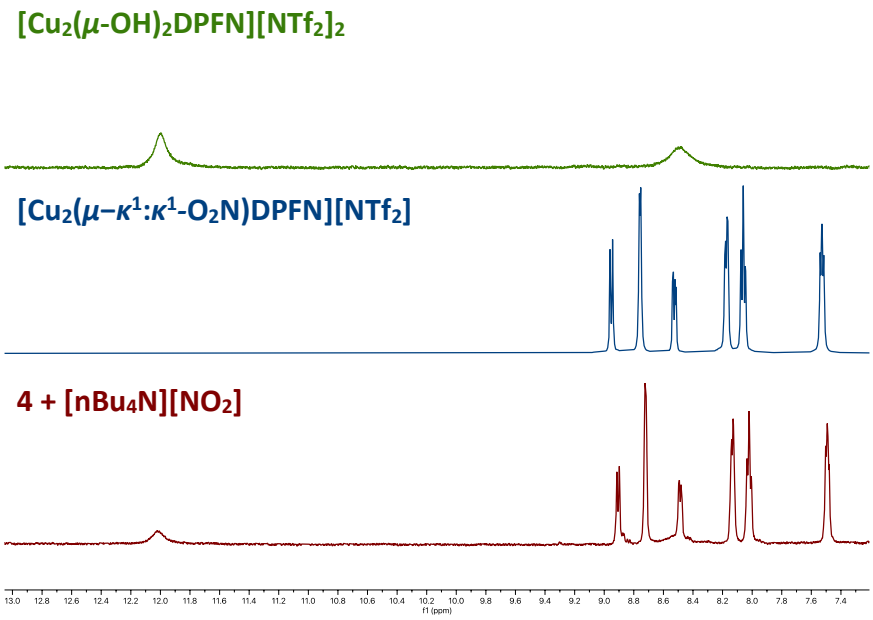

Figure S20. ^{1}H NMR spectra (THF-h_8, 500 MHz) of $[Cu_2(\mu\text{-}OH)_2DPFN][NTf_2]_2$, $[Cu_2(\mu–\kappa^1:\kappa^1\text{-}O_2N)DPFN][NTf_2]$, and **4** + $[nBu_4N][NO_2]$ (0.5 equiv) on a 10 mg scale (bottom).

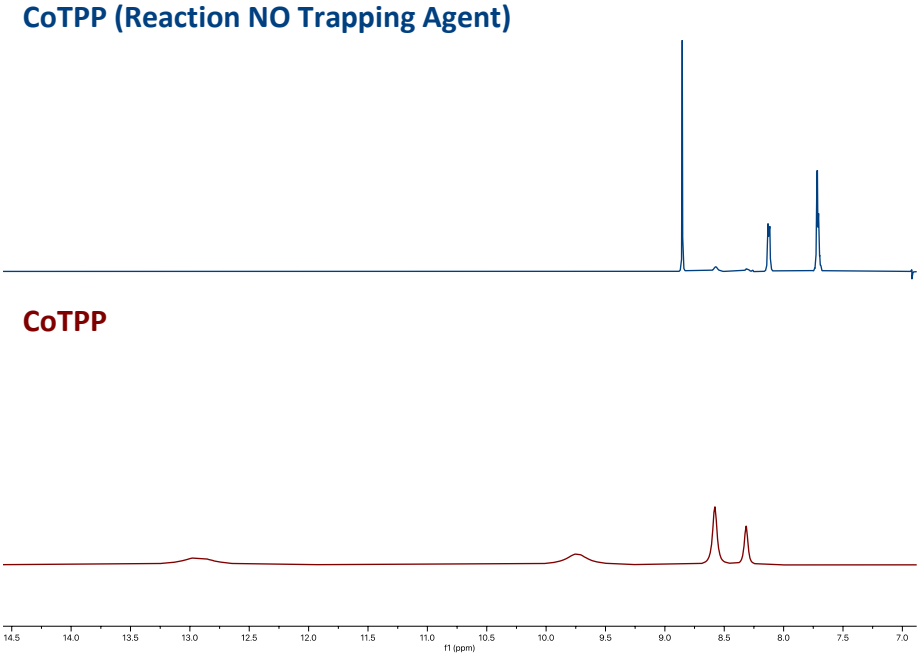

Figure S21. ^{1}H NMR spectra (THF-h_8, 500 MHz) of the CoTPP used to trap NO released by the reaction of **4** + $[nBu_4N][NO_2]$ (0.5 equiv) on a 10 mg scale (top) and CoTPP (bottom).

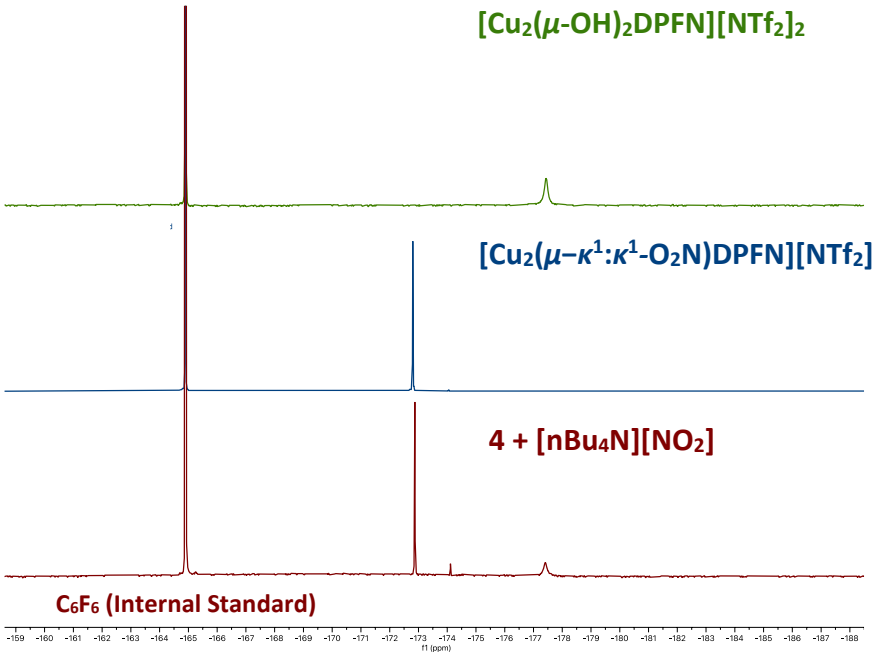

Figure S22. $^{19}F\{^{1}H\}$ NMR spectra (THF-h_8, 470 MHz) of $[Cu_2(\mu\text{-}OH)_2DPFN][NTf_2]_2$, $[Cu_2(\mu–\kappa^1:\kappa^1\text{-}O_2N)DPFN][NTf_2]$, and **4** + $[nBu_4N][NO_2]$ (0.5 equiv) on a 10 mg scale (bottom).

5) Infrared Spectroscopy

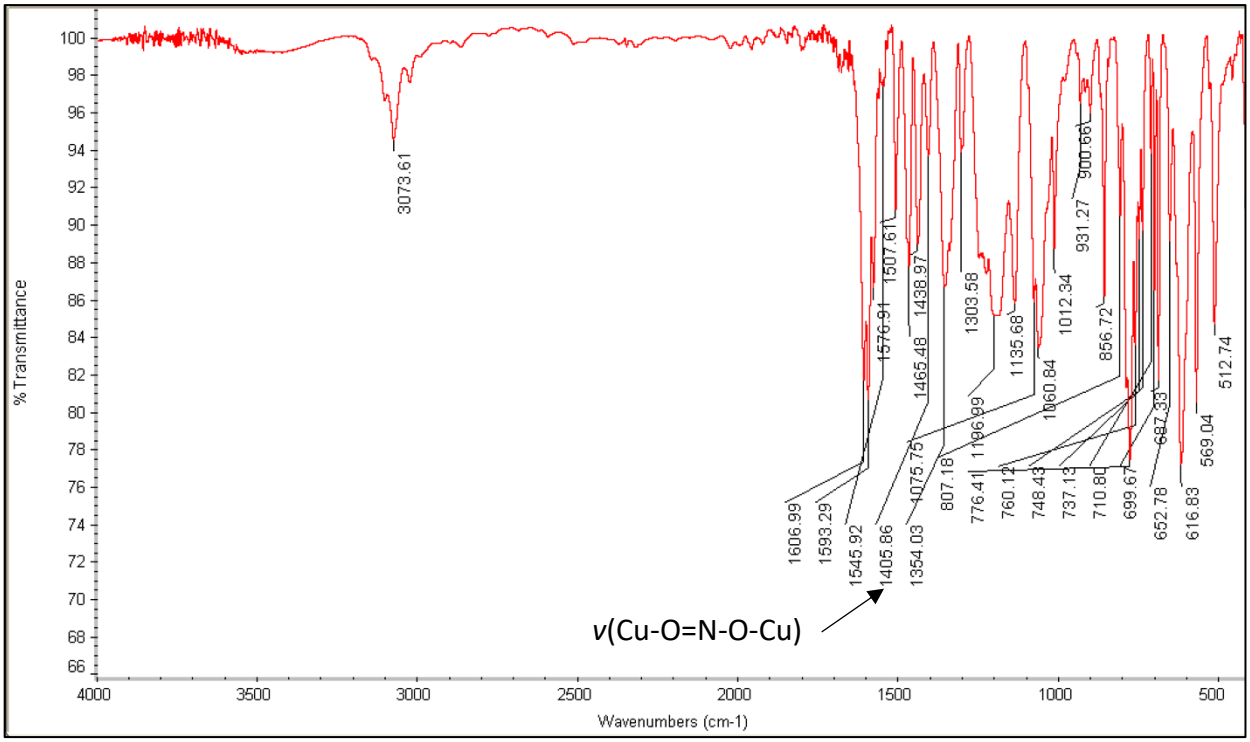

Figure S23. IR spectrum of complex **2.**

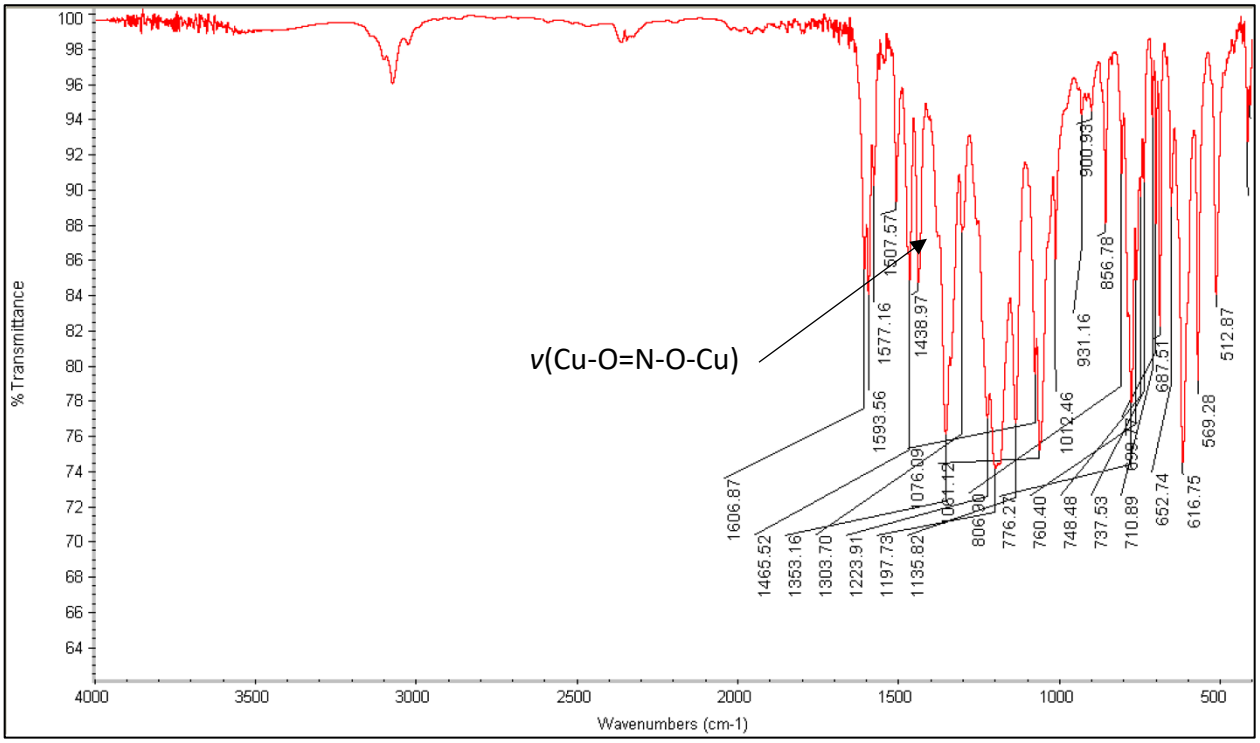

Figure S24. IR spectra of complex **2b.**

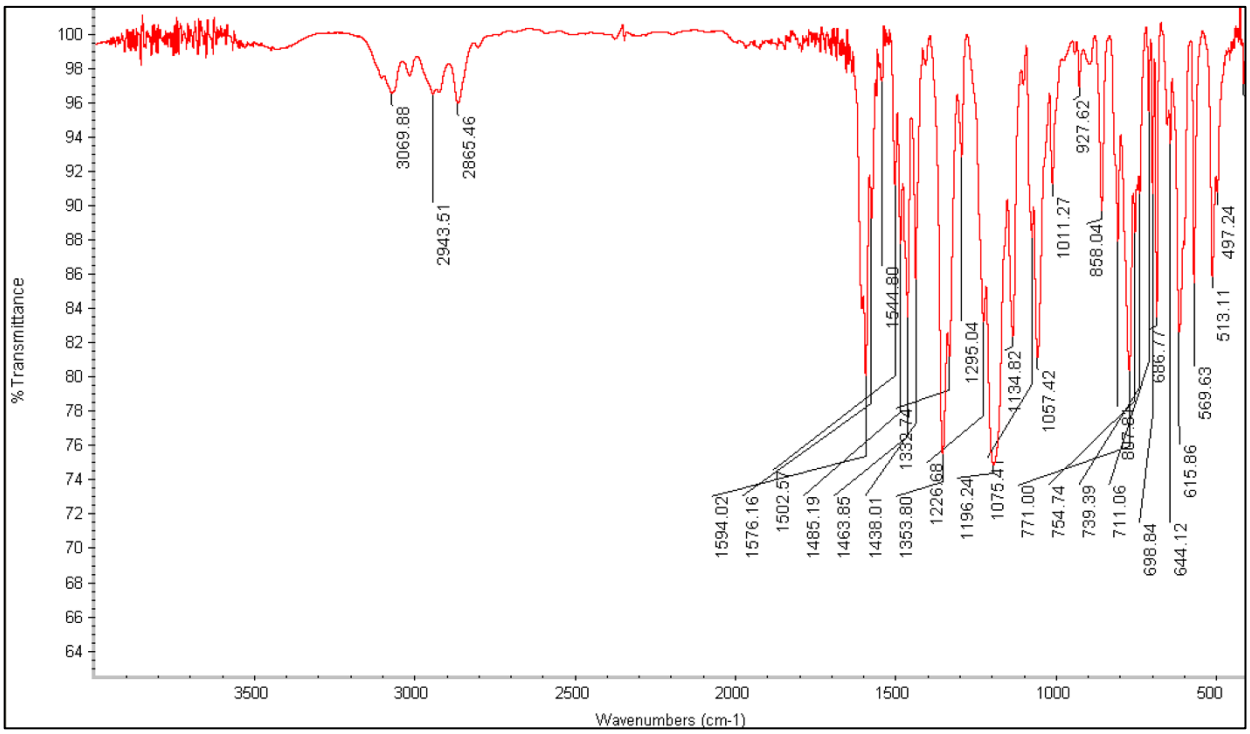

Figure S25. IR spectrum of complex **3.**

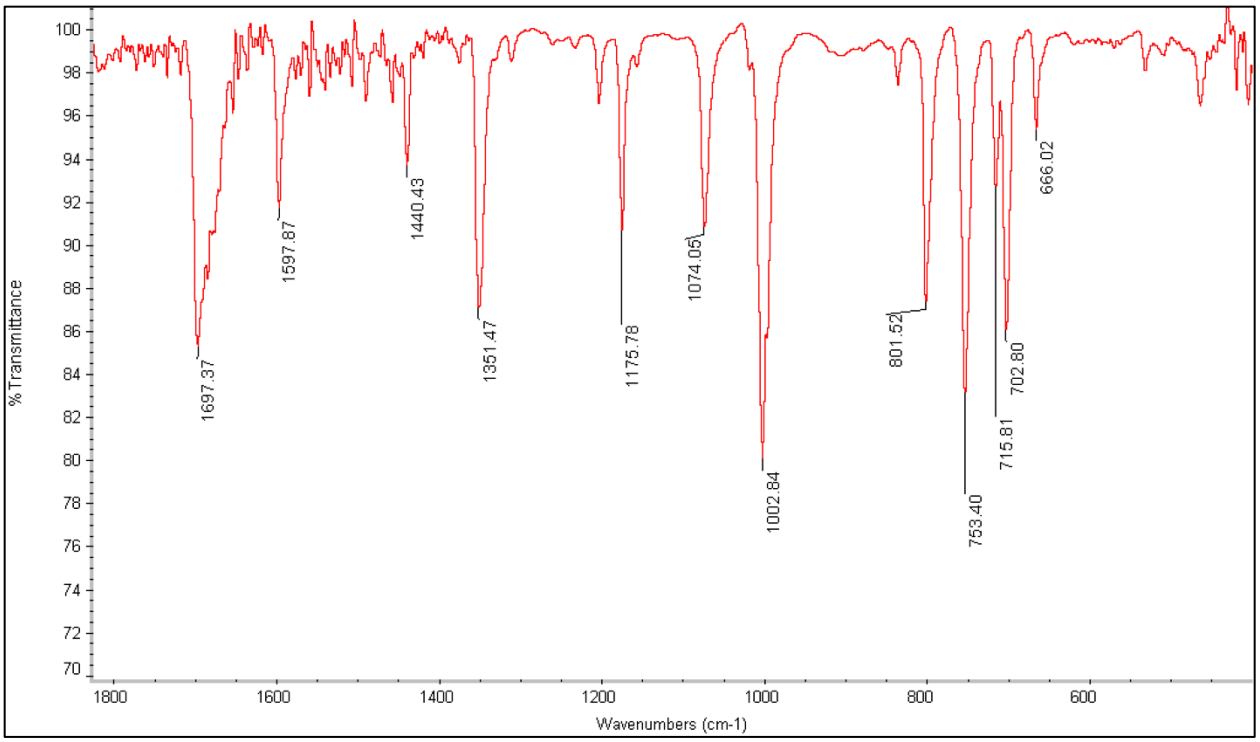

Figure S26. IR spectrum of Co(NO)TPP.

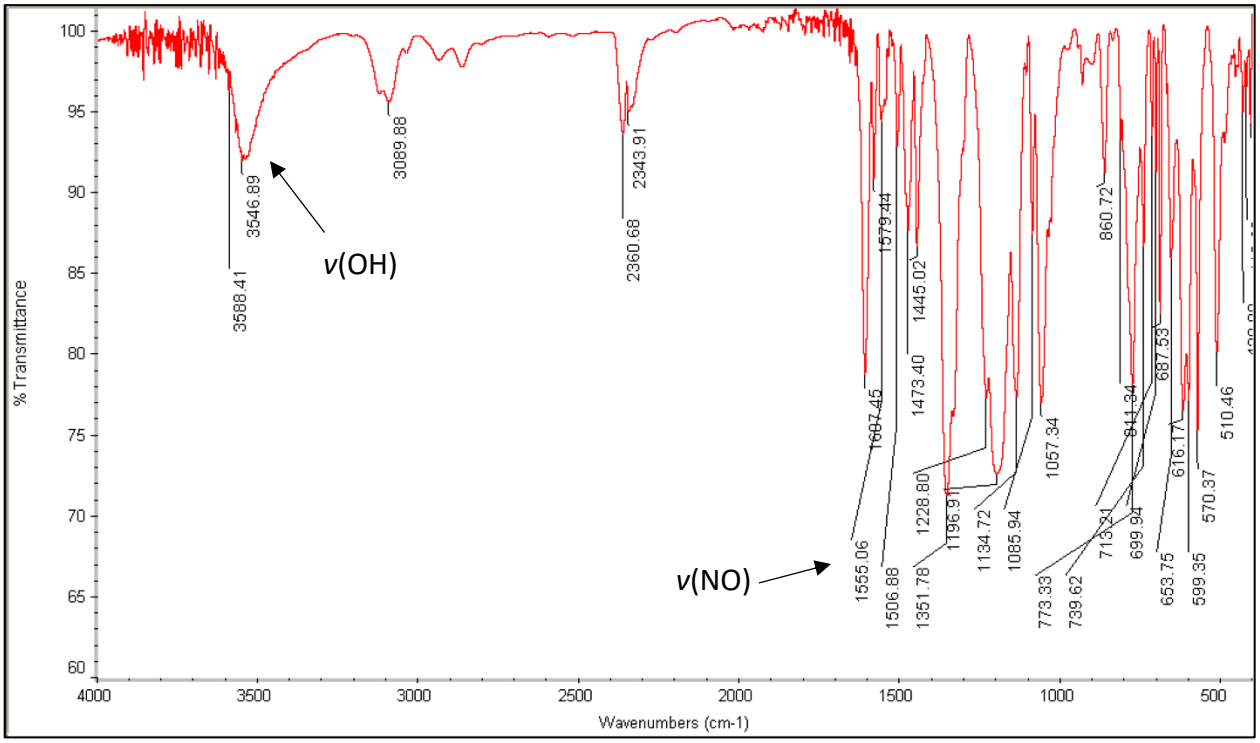

Figure S27. IR spectrum of complex **4.**

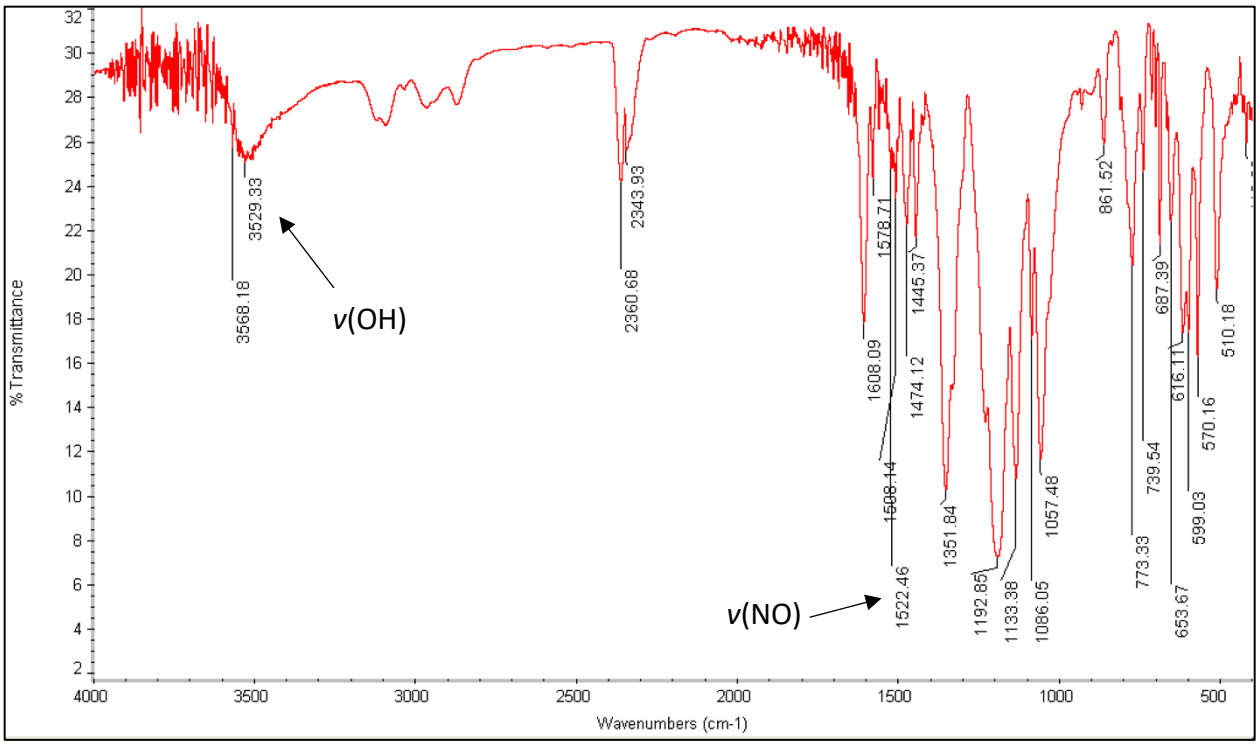

Figure S28. IR spectra of complex **4b.**

6) Mass Spectrometry

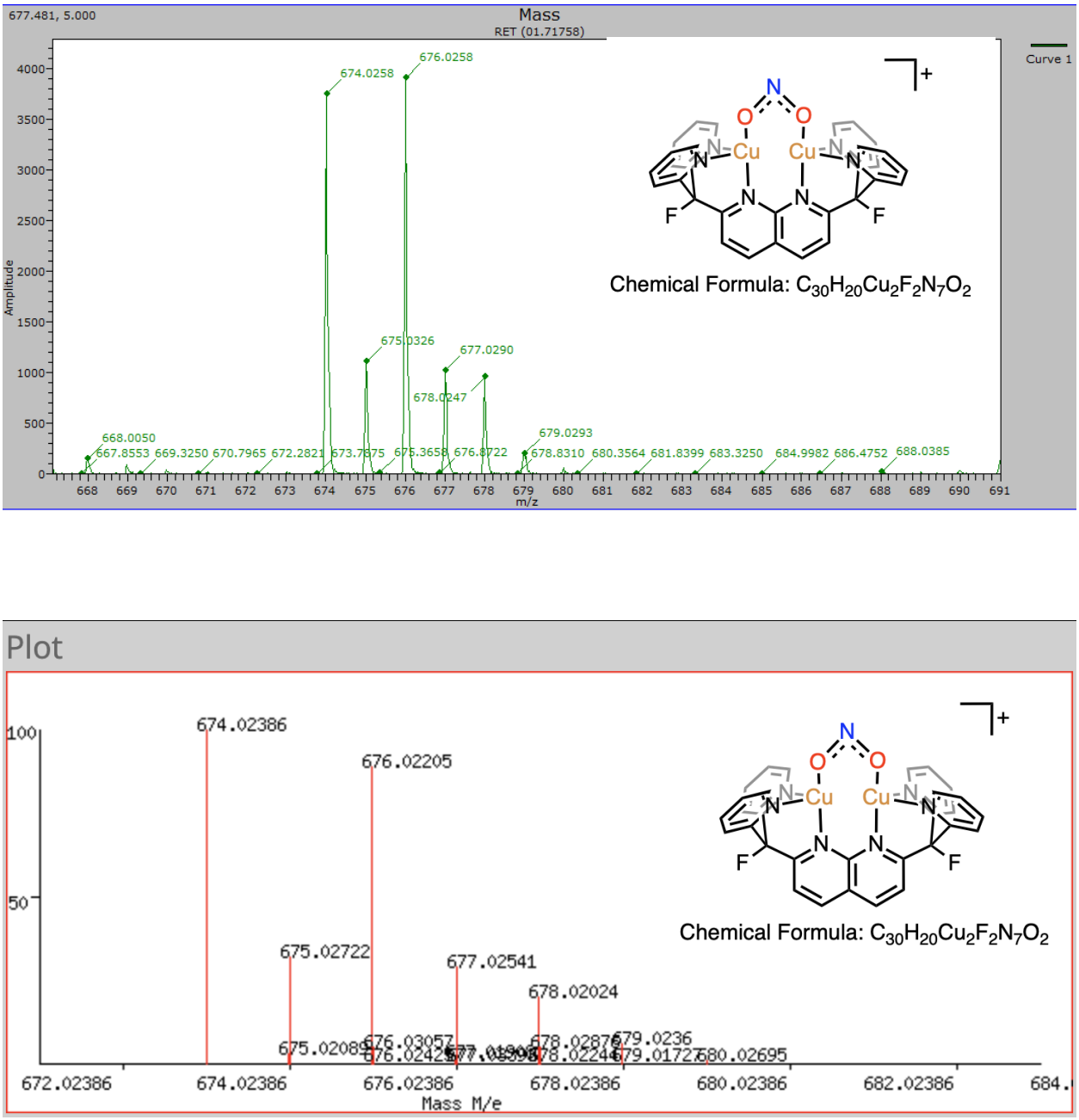

Figure S29. Experimental and predicted MS spectra of complex **2.**[6]

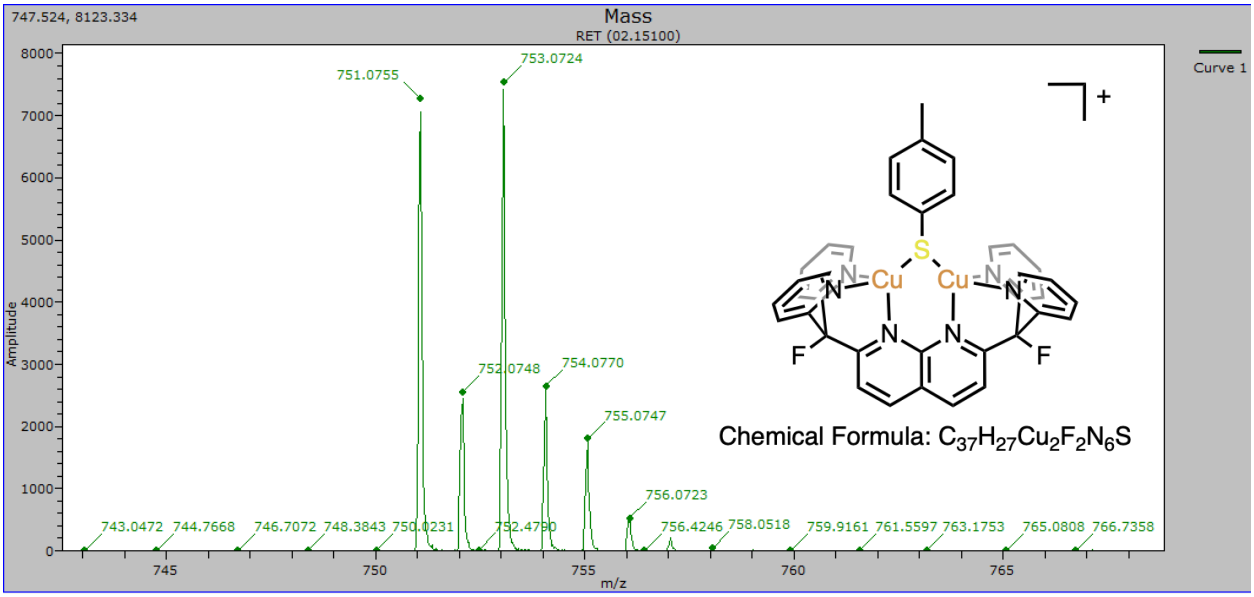

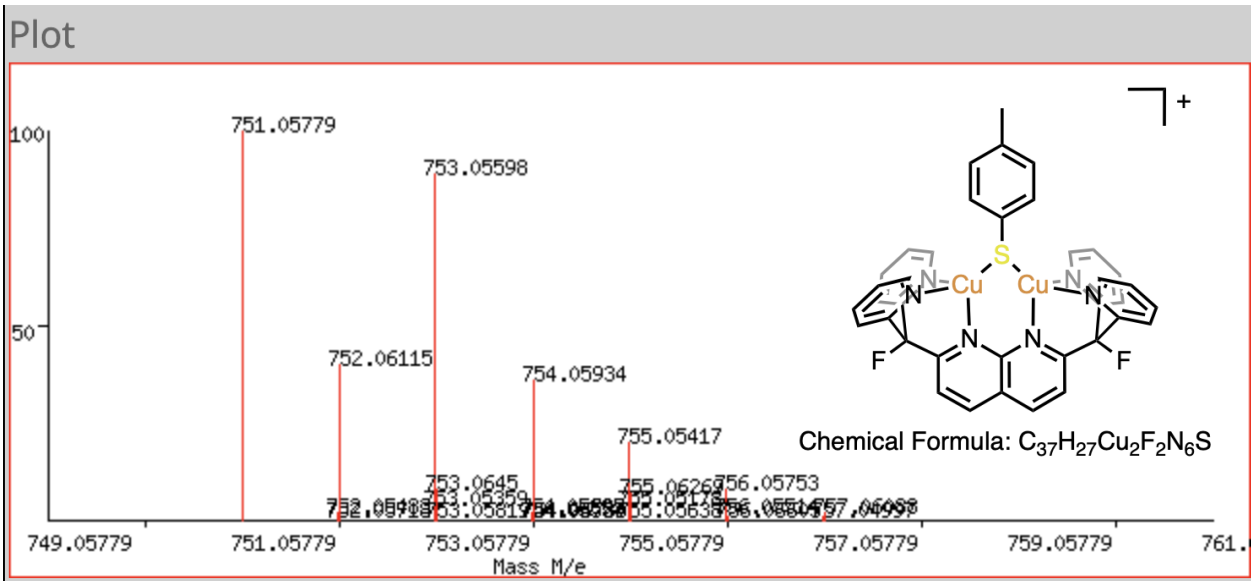

Figure S30. Experimental and predicted MS spectra of complex **3.** [6]

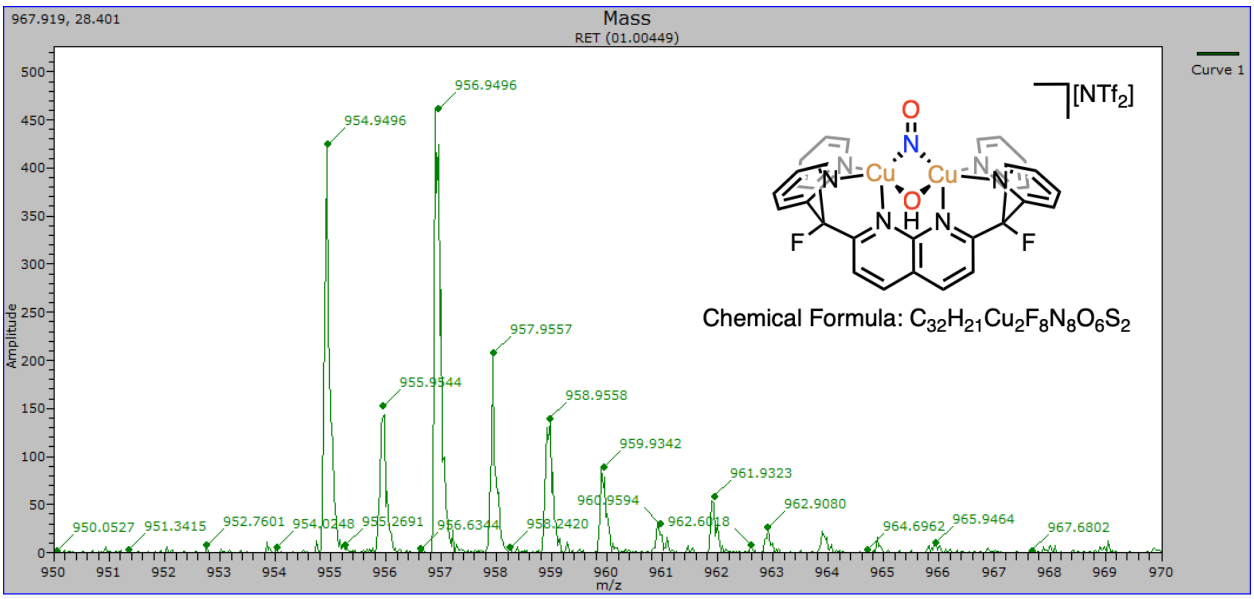

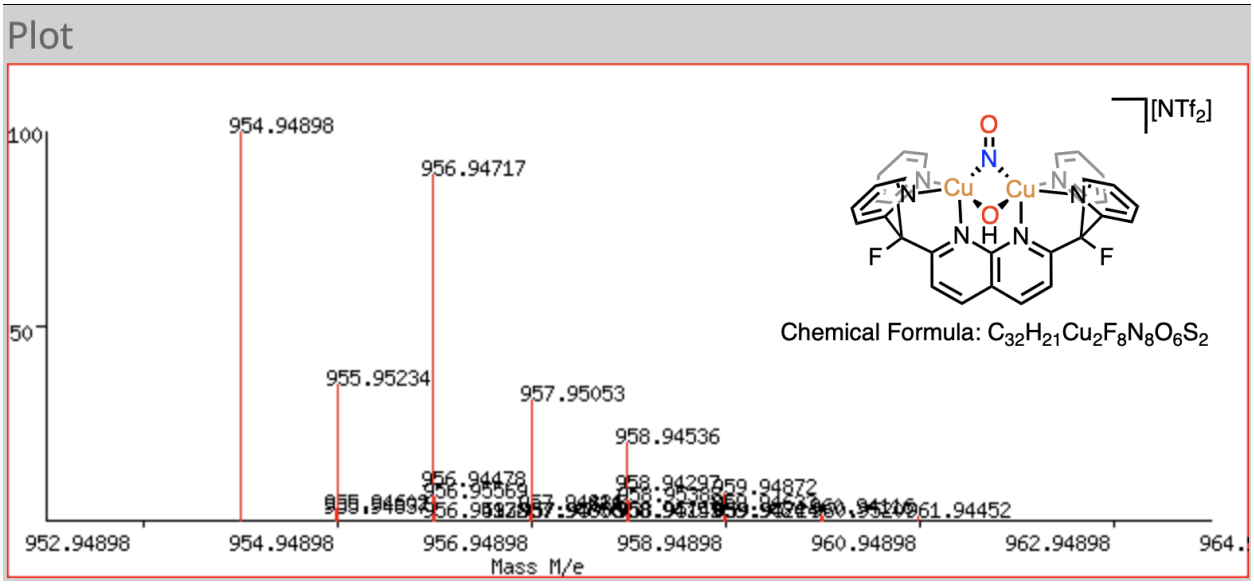

Figure S31. Experimental and predicted MS spectra of complex **4.** [6]

7) Electrochemistry

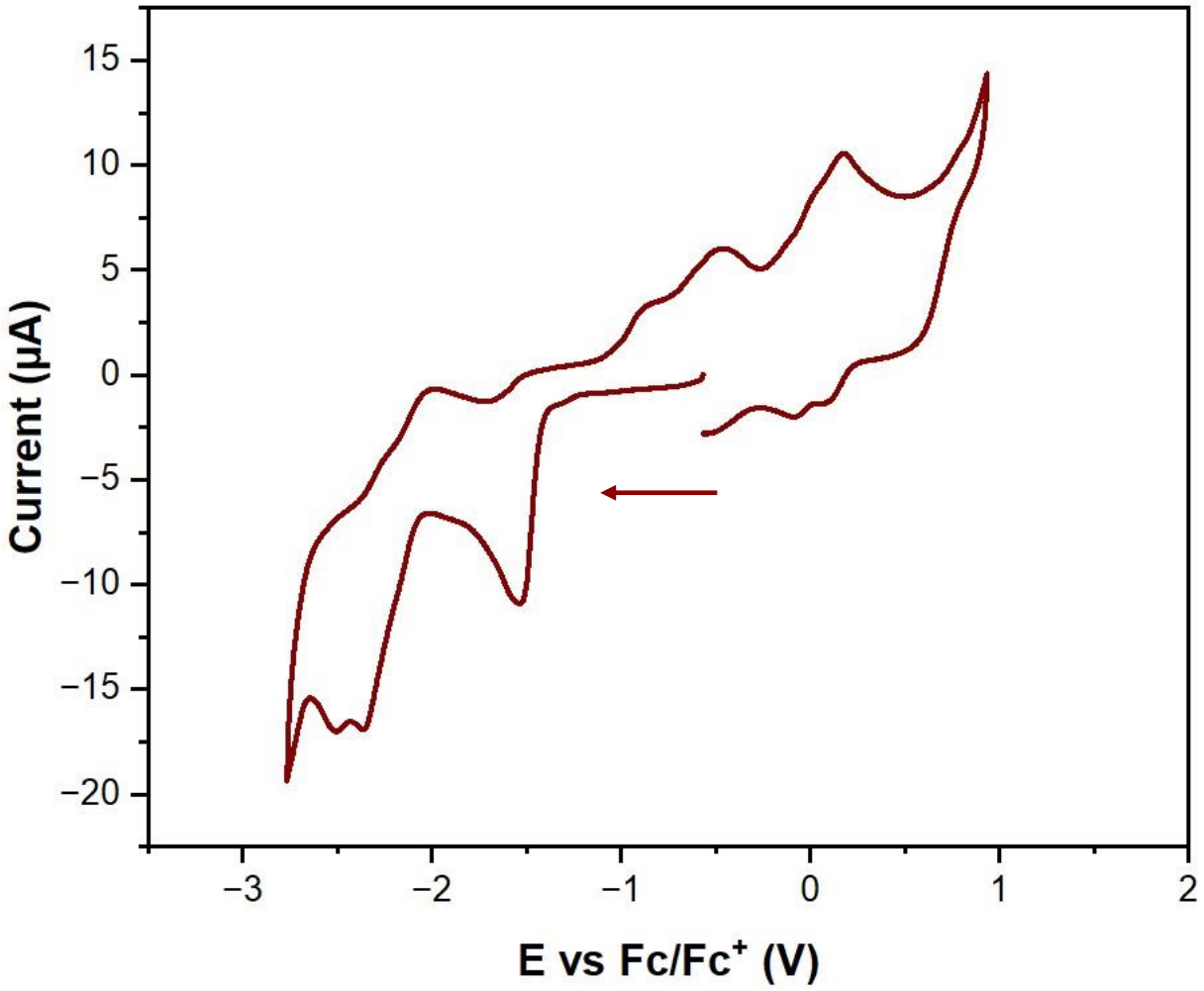

Figure S32. Cyclic voltammogram (100 mV/s scan rate) of a 1 mM solution of **2** in THF with 0.1 M [^{n}Bu$_4$N][PF$_6$] supporting electrolyte. The arrow indicates the initial potential and scanning direction. Baselines were acquired with the same electrodes and electrolyte solution before recording experimental voltammograms. The voltammogram of **2** only displays a series of electrochemically irreversible (up to 1000 mV/s) features.

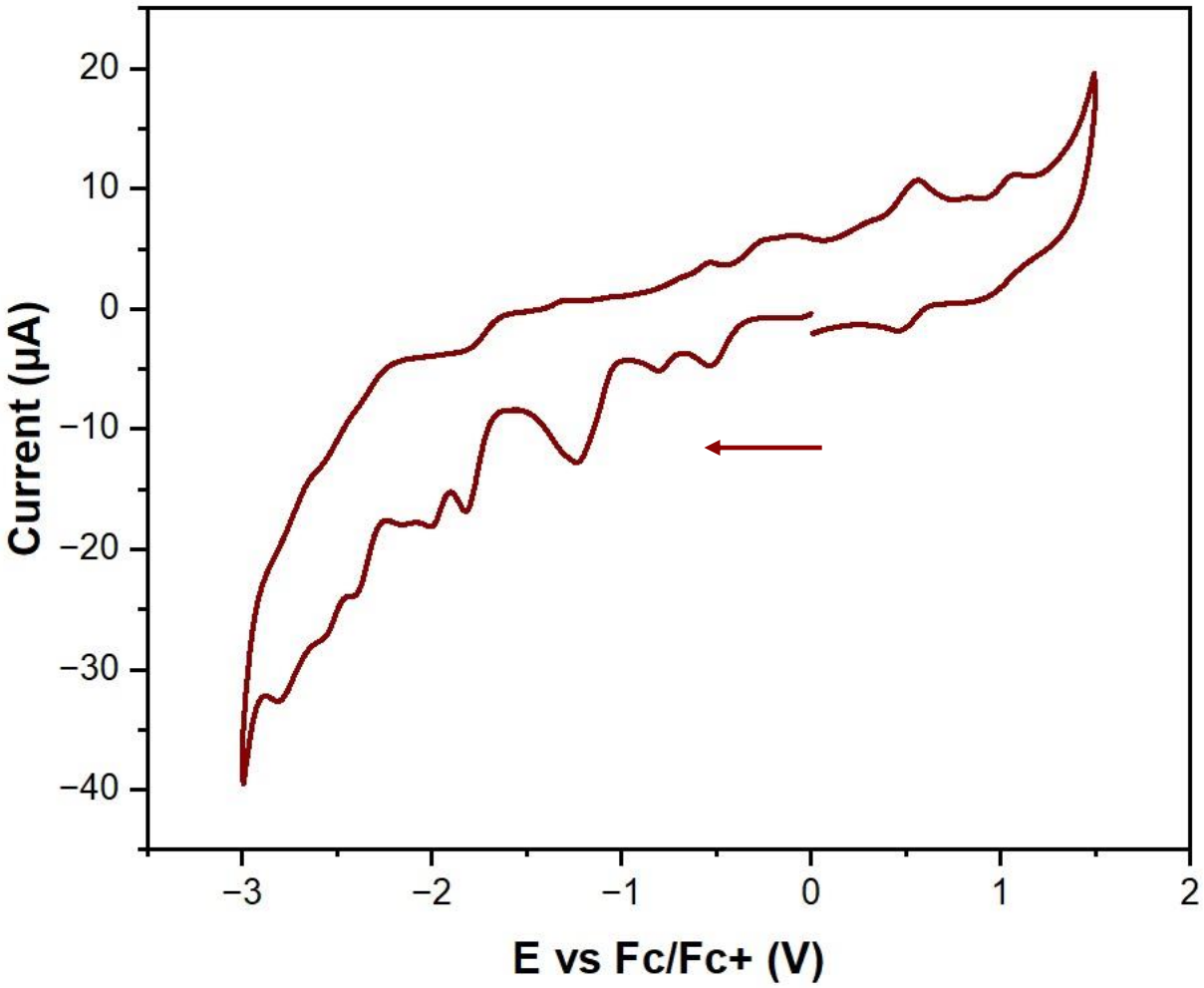

Figure S33. Cyclic voltammogram (100 mV/s scan rate) of a 1 mM solution of **4** in THF with 0.1 M [^{n}Bu$_4$N][PF$_6$] supporting electrolyte. The arrow indicates the initial potential and scanning direction. Baselines were acquired with the same electrodes and electrolyte solution before recording experimental voltammograms. The voltammogram of **4** only displays a series of electrochemically irreversible (up to 1000 mV/s) features.

9) Computational Details

Density functional theory (DFT) calculations were conducted to analyze the electronic structure of complex **2** and its transformation to complex **4** using ORCA 5.[7] The procedure involved a two-step calculation to ensure wavefunction stability. Initially, geometry optimization and vibrational frequency calculations were performed in tetrahydrofuran (THF) solvent with the CPCM solvation model, employing the B3LYP functional and def2-SVP basis sets. This was followed by a single-point energy calculation using the B3LYP functional and def2-TZVPP basis set at the optimized geometry.[8] Multiple spin states (closed-shell, open-shell, broken symmetry singlets, and restricted/unrestricted triplets) were considered. The optimized structures were visualized with ChemCraft.[9]

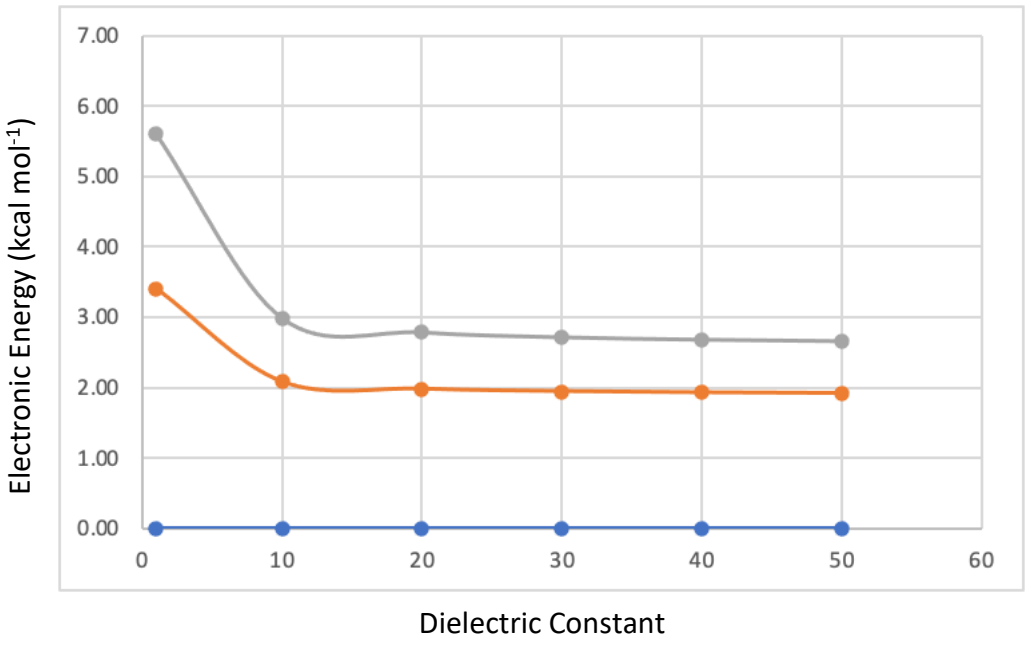

Figure S34. Plot of the electronic energies as a function of the dielectric constant for model complexes **2***(blue), **2***'(orange), and **2*"** (grey). As illustrated, once the dielectric constant surpasses approximately 10 - 20, the relative energies of the isomers level off.

Nitrite Complex		Protonated isomer	Reaction Free Energy (kcal mol^{-1})	Comment
2* (main reactant)	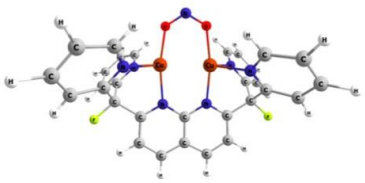		+8.43	---
2*”	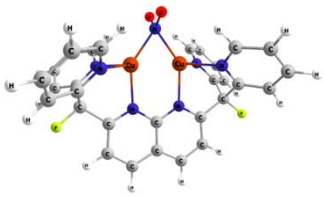		-2.46	---
2*’ (protonation at O bound to Cu)	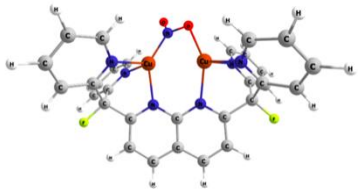		+4.88	After protonation and optimization the structure has been changed from mu NOHO to μ -NO_2H
2*’ (protonation at O bound to N)	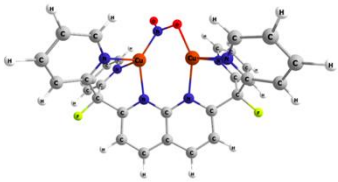	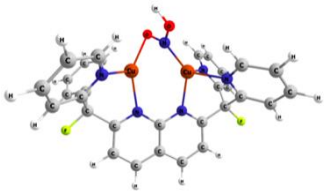	-1.52	---

Figure S35. Table displaying model complexes **2***(top), **2***”(middle), and **2*’** (bottom) as well as the calculated products of their protonation. The reaction free energy (kcal mol^{-1}) for each of these processes is also provided.

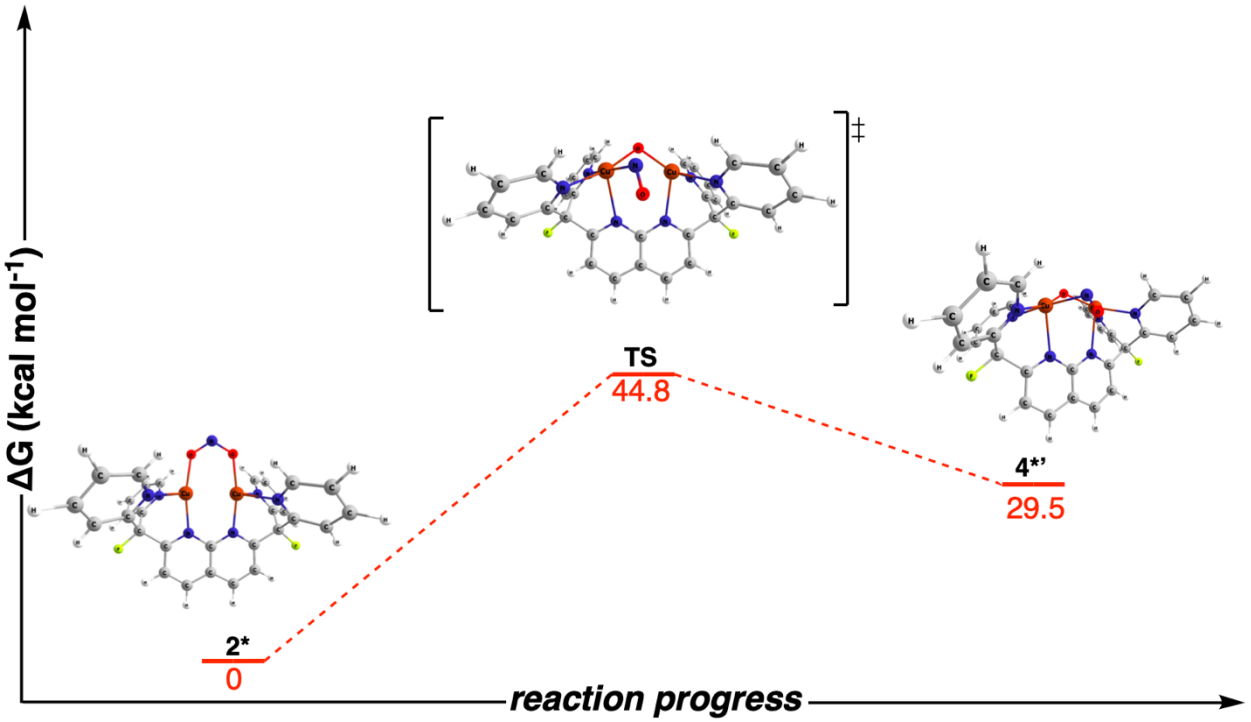

Figure S36. Reaction coordinate diagram for the cleavage of NO_2^- prior to protonation derived by DFT at the B3LYP/def2-TZVPP/CPCM-THF level of theory.

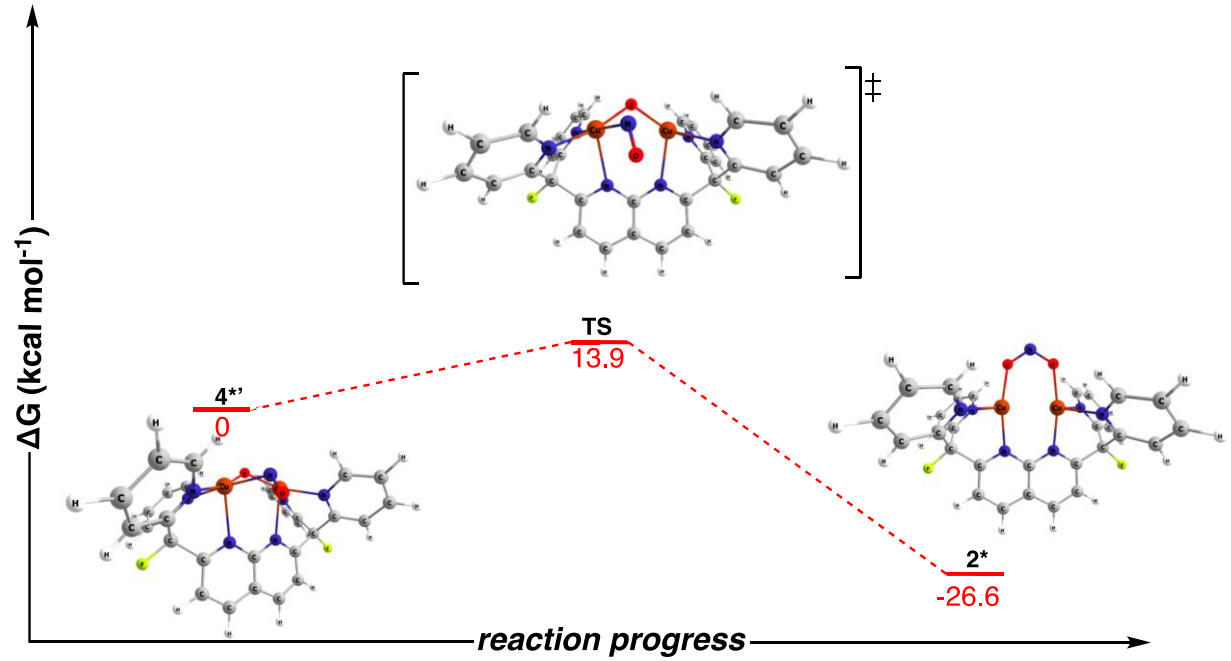

Figure S37. Reaction coordinate diagram for N-O bond formation after deprotonation derived by DFT at the B3LYP/def2-TZVPP/CPCM-THF level of theory.

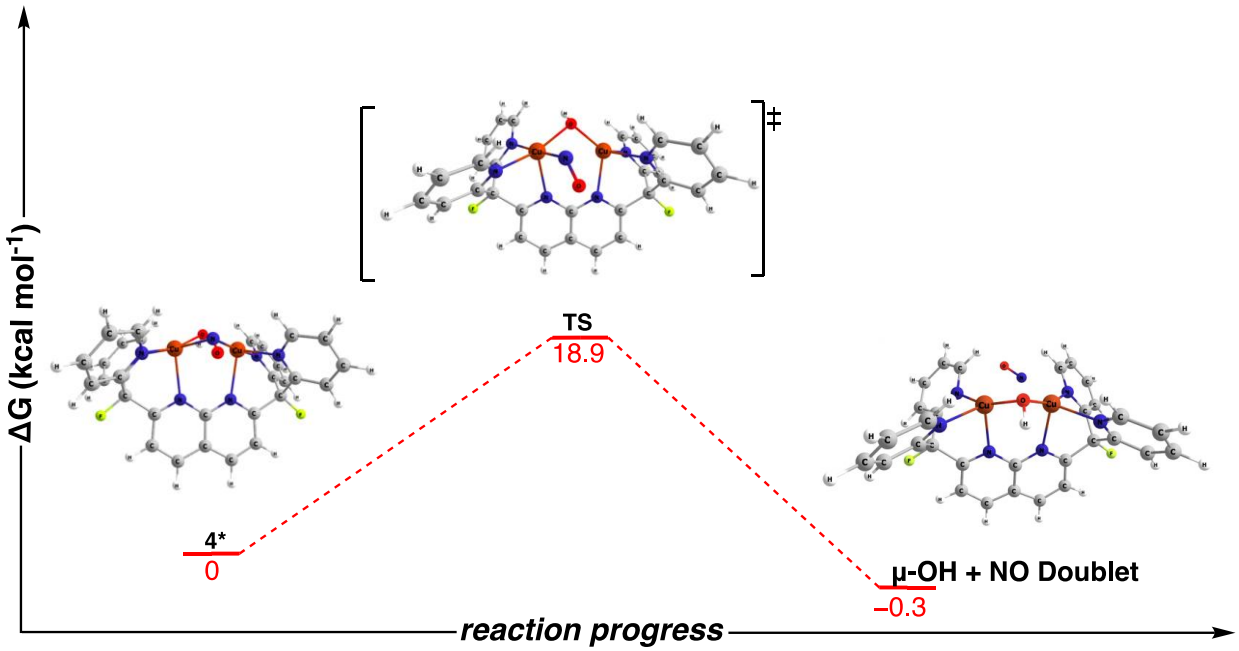

Figure S38. Reaction coordinate diagram for NO loss from **4*** derived by DFT at the B3LYP/def2-TZVPP/CPCM-THF level of theory. All calculated species are dicationic.

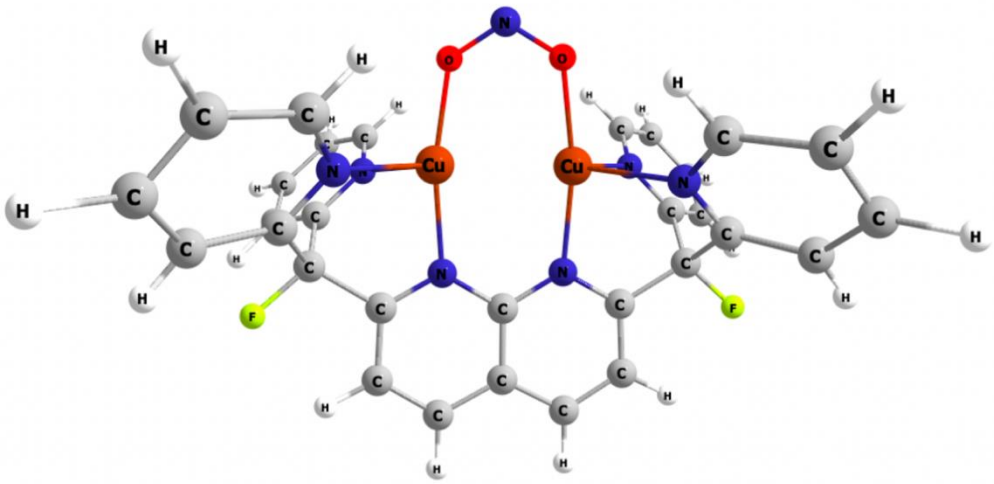

Figure S39. B3LYP/def2-TZVPP/CPCM-THF optimized geometry of complex **2***. The unrestricted singlet wavefunction yields the lowest calculated energy (-3243449.556 kcal mol^{-1}).

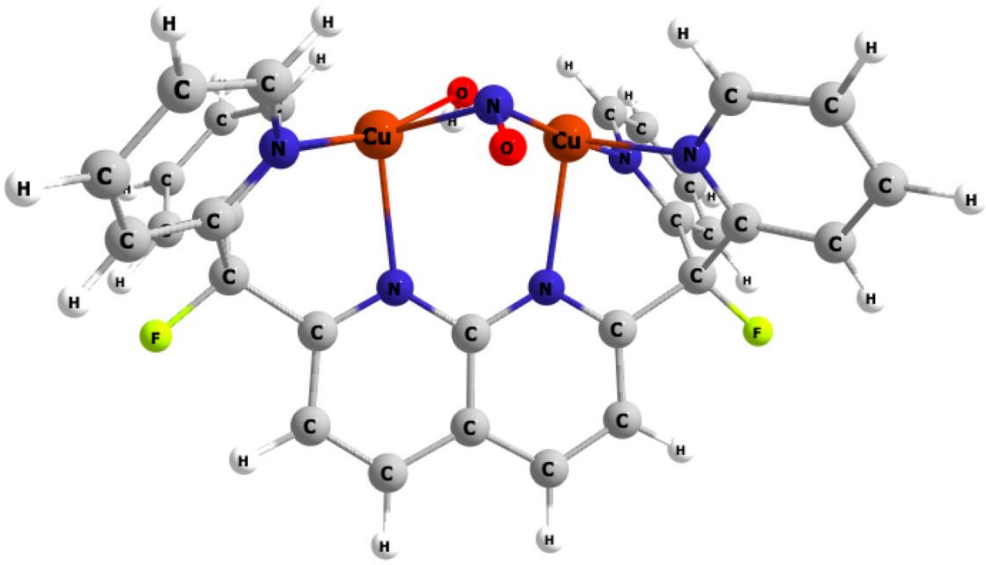

Figure S40. B3LYP/def2-TZVPP/CPCM-THF optimized geometry of complex **4*****.**

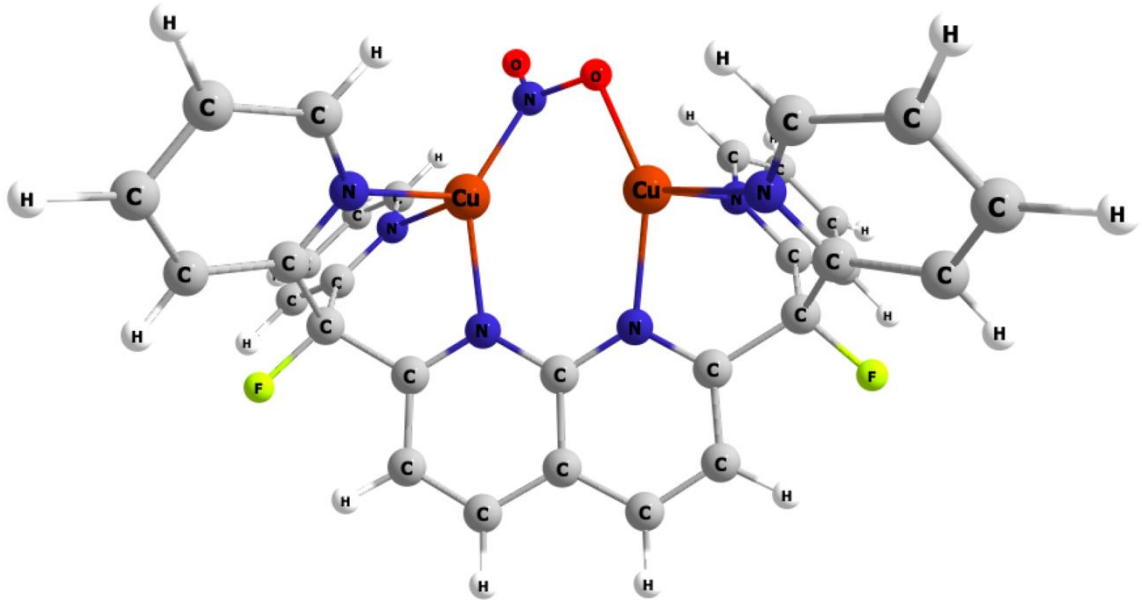

Figure S41. B3LYP/def2-TZVPP/CPCM-THF optimized geometry of the **2*'** linkage isomer. The restricted singlet wavefunction yielded the lowest energy (-3243447.908 kcal mol^{-1}).

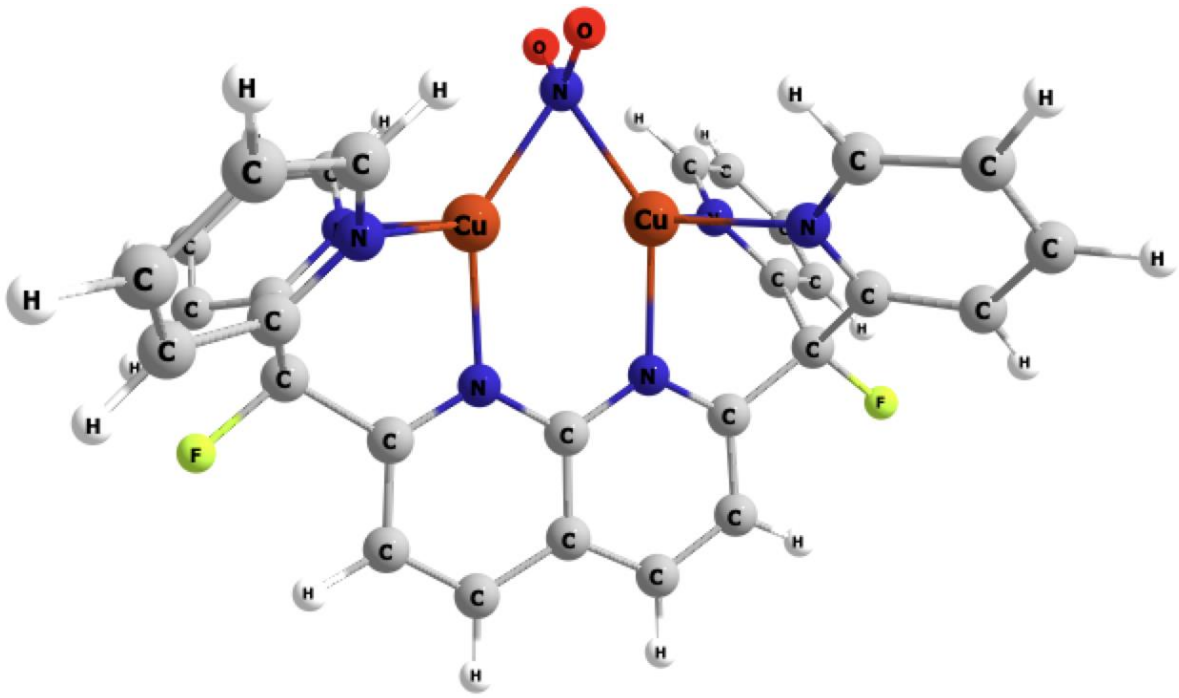

Figure S42. Optimized geometry of **2*"** linkage isomer. The broken-symmetry singlet yielded the lowest calculated energy (-3243449.063 kcal mol^{-1}).

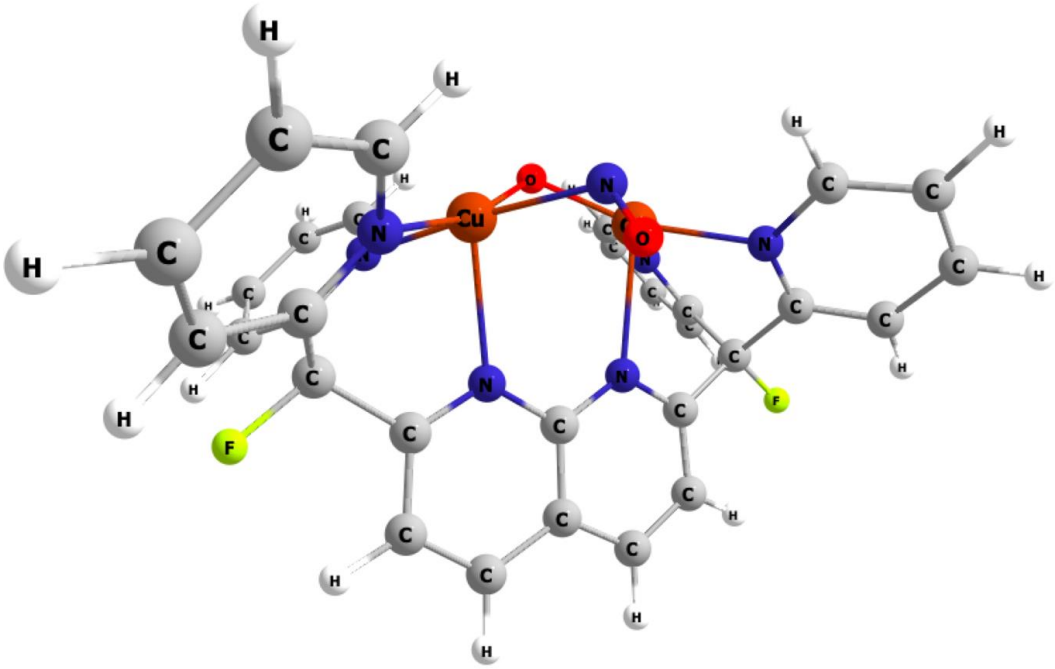

Figure S43. B3LYP/def2-TZVPP/CPCM-THF optimized geometry of **4*'** intermediate.

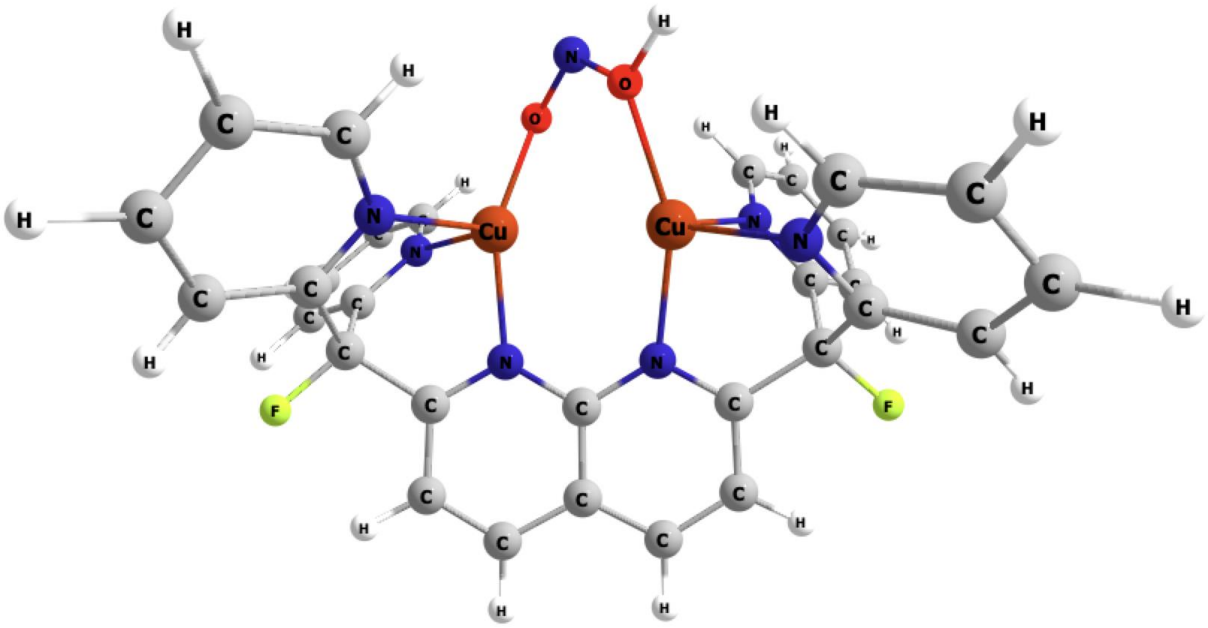

Figure S44. B3LYP/def2-TZVPP/CPCM-THF optimized geometry of intermediate **A**.

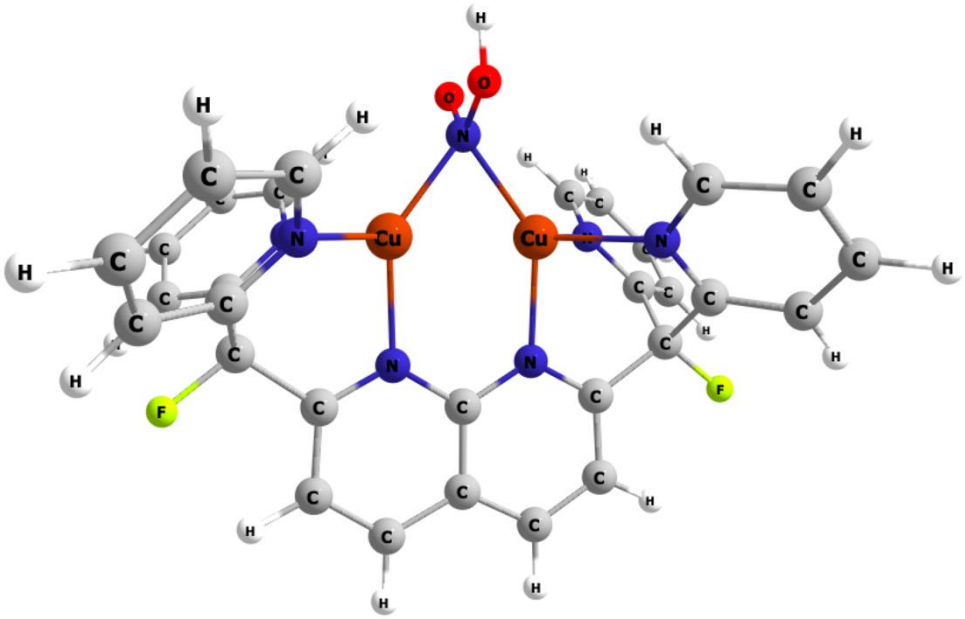

Figure S45. B3LYP/def2-TZVPP/CPCM-THF optimized geometry of intermediate **B**.

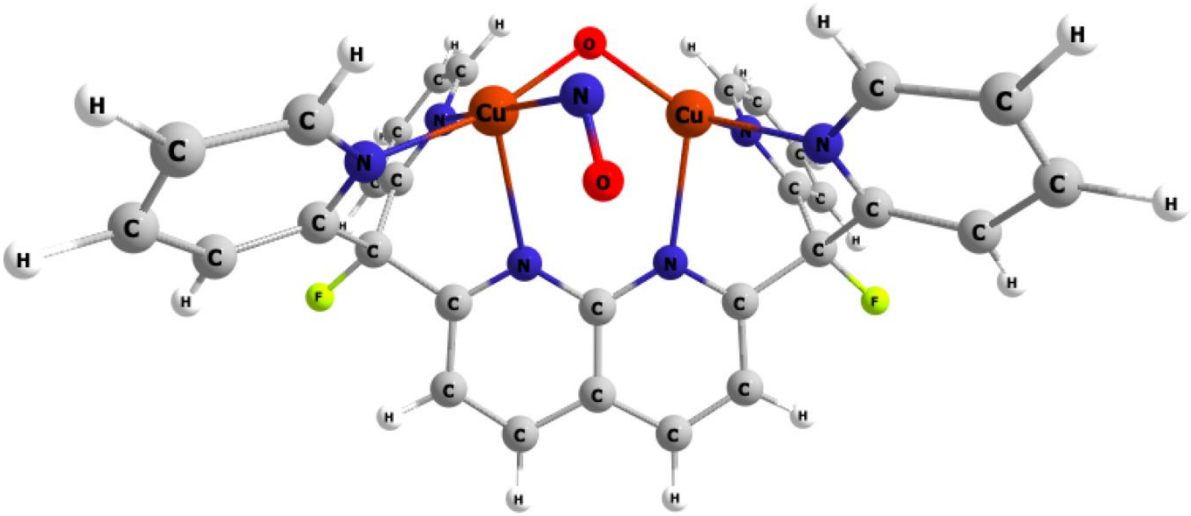

Figure S46. B3LYP/def2-TZVPP/CPCM-THF optimized geometry of the transition state for the cleavage of NO_2^- prior to protonation.

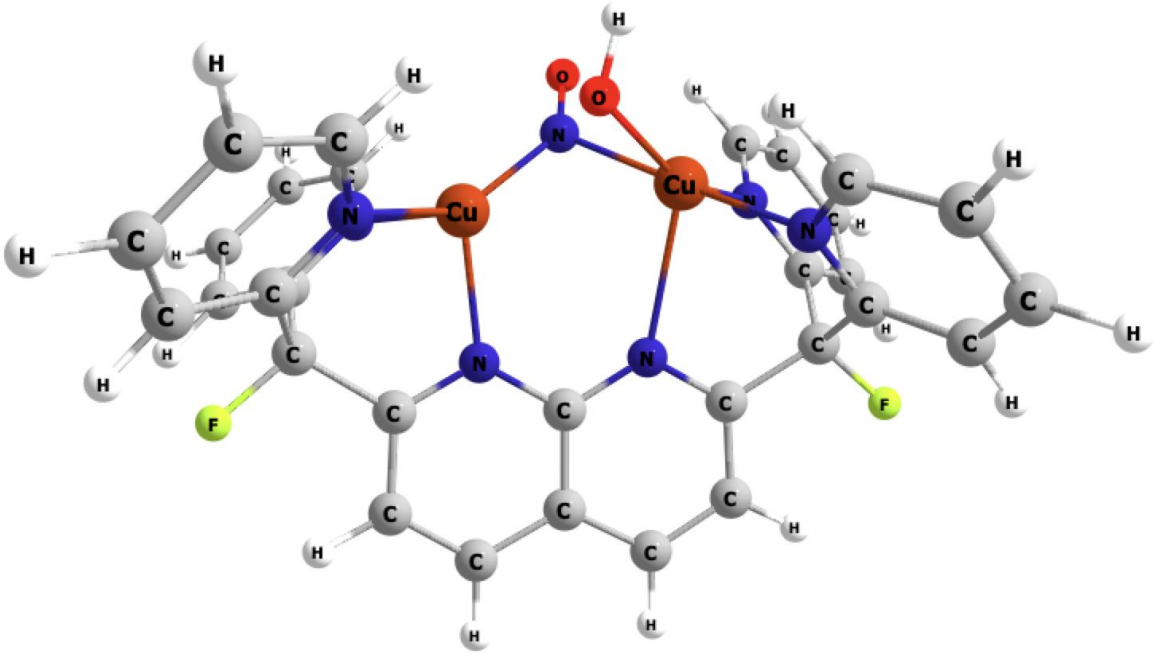

Figure S47. Optimized geometry of HONO cleavage transition state.

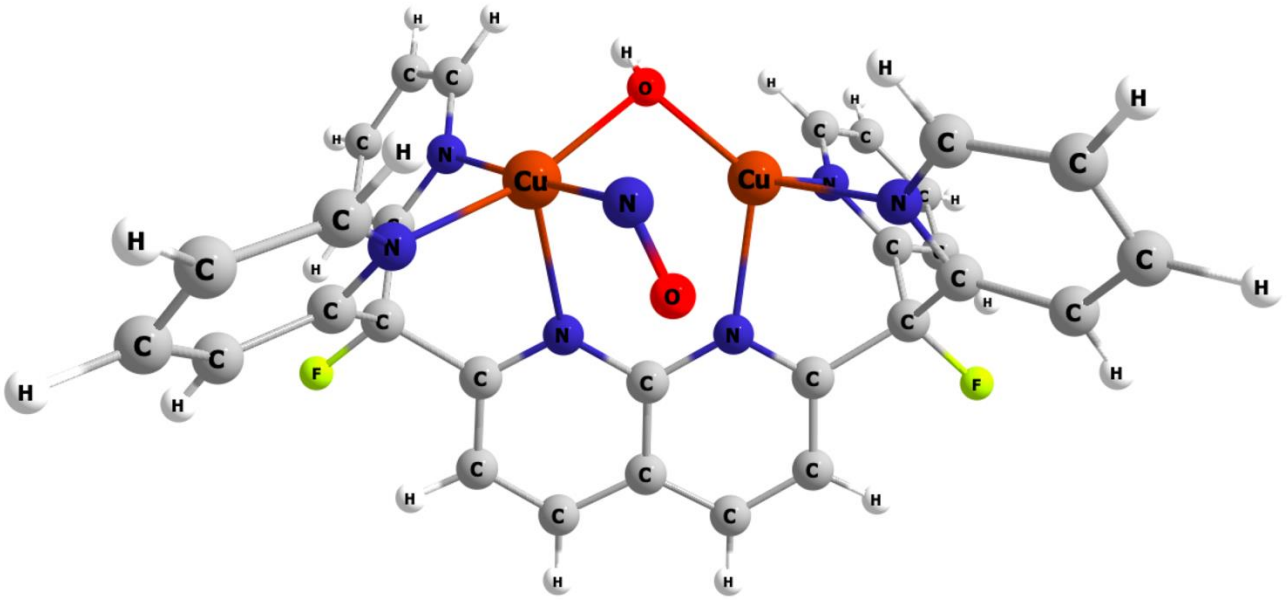

Figure S48. Optimized geometry of NO loss transition state.

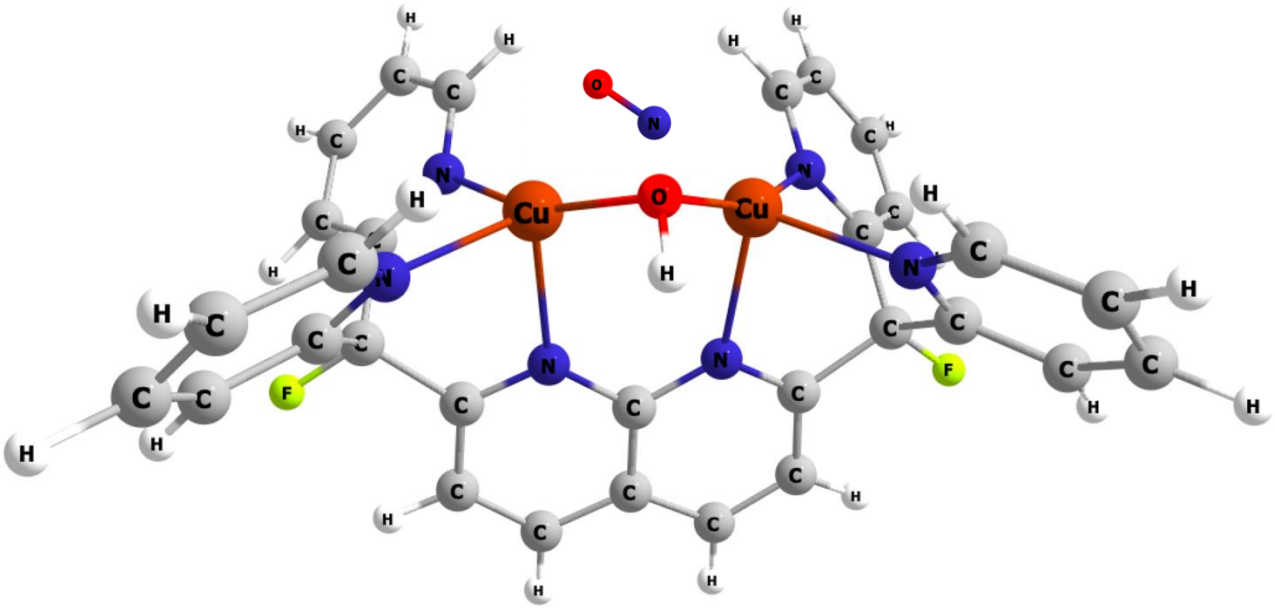

Figure S49. B3LYP/def2-TZVPP/CPCM-THF optimized geometry of μ-OH + NO Doublet.

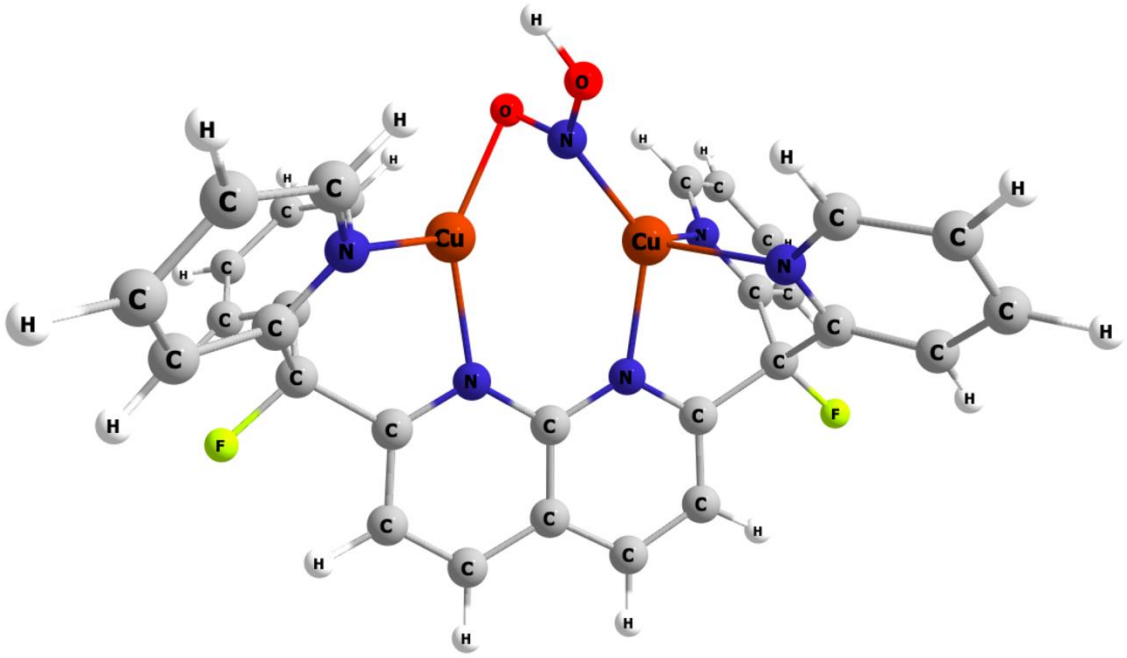

Figure S50. B3LYP/def2-TZVPP/CPCM-THF optimized geometry of the protonated **2*'** complex.

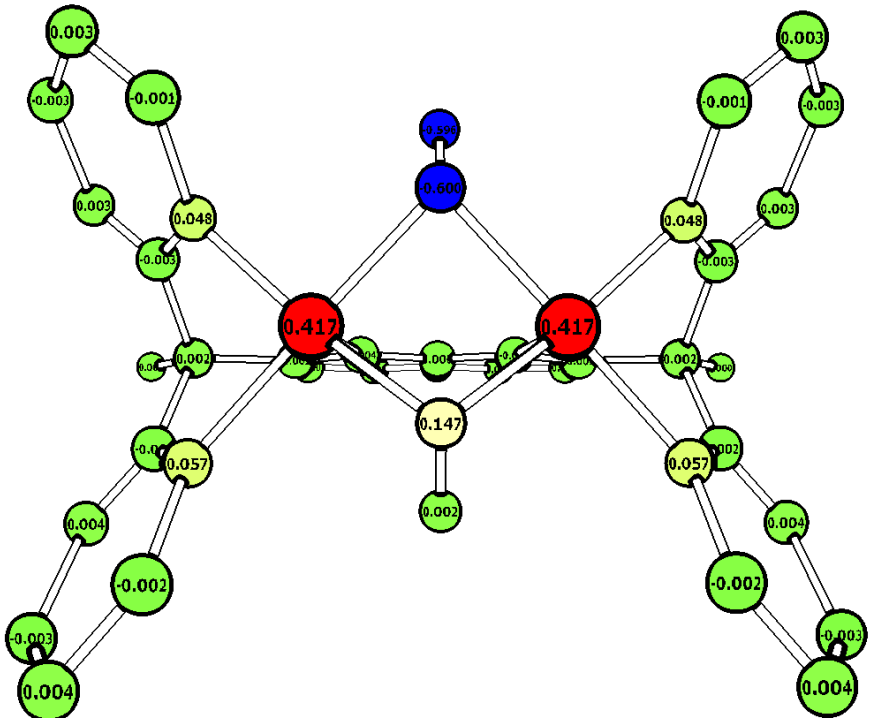

Figure S51. Schematic of the Löwdin spin population of **4***. Spin densities are quoted in e^-.

10) Cartesian Coordinates of the optimized structures

Complex **2***; closed shell singlet

29	-1.306816000	-0.028629000	-0.896300000
29	1.309915000	0.038999000	-0.895219000
9	-4.669947000	0.174020000	1.930767000
8	1.042890000	0.236439000	-2.888428000
7	-1.165584000	0.033915000	1.165424000
7	-2.917209000	-1.496337000	-0.710357000
9	4.671555000	-0.189926000	1.931357000
7	2.923769000	1.501502000	-0.699095000
7	-2.837408000	1.496455000	-0.850119000
7	1.167730000	-0.033351000	1.166104000
6	-3.837498000	-1.203725000	0.213558000
6	0.000897000	-0.000886000	1.871836000
7	2.833689000	-1.491353000	-0.855911000
7	0.003323000	0.019979000	-3.546401000
6	-3.757181000	1.346013000	0.108842000
6	-4.950105000	-2.018817000	0.450757000
6	-3.633051000	0.100884000	1.009674000
6	-4.810067000	2.251109000	0.285493000
6	3.067228000	2.613715000	-1.431989000
6	2.407145000	-0.095664000	3.237531000
6	-2.923045000	2.540320000	-1.685796000
6	0.000513000	-0.003996000	3.298508000
6	-2.321591000	0.077675000	1.820833000
6	-2.406021000	0.089078000	3.236514000
6	4.963016000	2.007033000	0.457977000
6	-4.895814000	3.342593000	-0.582944000
6	2.323374000	-0.080927000	1.821887000
6	-3.058148000	-2.604761000	-1.449431000
6	4.148369000	3.481068000	-1.268054000
6	3.845490000	1.198875000	0.219919000
6	-1.244973000	0.044317000	3.970782000
6	1.245624000	-0.054576000	3.971325000

6	4.796916000	-2.264927000	0.283320000
6	5.110277000	3.169176000	-0.303979000
6	-3.939389000	3.491432000	-1.590378000
6	-5.094470000	-3.177222000	-0.317508000
6	2.912194000	-2.534567000	-1.693037000
6	3.634972000	-0.107598000	1.010742000
6	-4.134565000	-3.478267000	-1.286981000
8	-1.036320000	-0.204850000	-2.891579000
1	-5.682631000	-1.752250000	1.211367000
1	-5.543049000	2.102006000	1.076967000
1	2.289527000	2.808358000	-2.176731000
1	3.380110000	-0.137302000	3.722034000
1	-2.151964000	2.610854000	-2.459298000
1	-3.379154000	0.130106000	3.720610000
1	5.697134000	1.732338000	1.214197000
1	-5.707253000	4.066713000	-0.473224000
1	-2.282700000	-2.790946000	-2.198658000
1	4.229484000	4.379295000	-1.883479000
1	-1.266550000	0.046917000	5.063532000
1	1.266651000	-0.060034000	5.064051000
1	5.529972000	-2.123088000	1.076030000
1	5.971088000	3.823271000	-0.144259000
1	-3.975433000	4.328193000	-2.291368000
1	-5.951899000	-3.836082000	-0.158909000
1	2.141725000	-2.597759000	-2.467853000
1	-4.213610000	-4.372998000	-1.907884000
6	3.920094000	-3.494495000	-1.596711000
1	3.950695000	-4.330681000	-2.298747000
6	4.875863000	-3.355198000	-0.587275000
1	5.681034000	-4.086321000	-0.477404000
6	3.752001000	-1.350777000	0.105996000

Complex **4***; broken symmetry singlet

29	-1.446223000	-0.100740000	-1.121863000
29	1.445634000	-0.096703000	-1.117211000
9	-4.670041000	0.216596000	1.870238000

8	-0.000934000	0.943614000	-1.905956000
7	-1.168838000	0.068831000	1.160665000
7	-2.942855000	-1.432643000	-0.812542000
9	4.665854000	0.236825000	1.876010000
7	2.827209000	1.442710000	-0.951303000
7	-2.833118000	1.433411000	-0.953369000
7	1.166052000	0.074314000	1.162308000
6	-3.818545000	-1.165784000	0.172667000
6	-0.001963000	0.089120000	1.862754000
7	2.947145000	-1.423091000	-0.805588000
7	0.002343000	-1.585315000	-1.442655000
6	-3.702672000	1.366427000	0.065158000
6	-4.892902000	-2.012903000	0.451440000
6	-3.619841000	0.130021000	0.976676000
6	-4.655392000	2.362237000	0.289489000
6	2.861145000	2.485180000	-1.796143000
6	2.409015000	0.169221000	3.229551000
6	-2.869663000	2.477294000	-1.796355000
6	-0.002987000	0.139745000	3.290480000
6	-2.318424000	0.112609000	1.812088000
6	-2.414986000	0.156170000	3.226363000
6	4.648171000	2.377514000	0.289008000
6	-4.695935000	3.451708000	-0.585687000
6	2.314593000	0.124041000	1.815196000
6	-3.106648000	-2.534268000	-1.566365000
6	3.781420000	3.521853000	-1.650285000
6	3.697255000	1.379441000	0.067076000
6	-1.250969000	0.165348000	3.960418000
6	1.243952000	0.172546000	3.962009000
6	4.895915000	-1.996338000	0.463592000
6	4.686271000	3.465283000	-0.588377000
6	-3.791845000	3.511928000	-1.648052000
6	-5.062237000	-3.159547000	-0.328801000
6	3.820428000	-1.152089000	0.180618000
6	3.114523000	-2.526300000	-1.556275000
6	5.068836000	-3.144694000	-0.313300000
6	3.617042000	0.144917000	0.981378000

6	-4.158047000	-3.423993000	-1.358532000
6	4.167115000	-3.413586000	-1.344024000
8	0.002674000	-2.564420000	-0.780188000
1	-5.582893000	-1.774392000	1.259277000
1	-5.348271000	2.283478000	1.126058000
1	2.128202000	2.479968000	-2.607365000
1	3.381665000	0.202717000	3.716167000
1	-2.137564000	2.474675000	-2.608359000
1	-3.388483000	0.184433000	3.711572000
1	5.341771000	2.301535000	1.125228000
1	-5.431643000	4.245751000	-0.435148000
1	-2.374676000	-2.703333000	-2.359118000
1	3.782490000	4.353592000	-2.357615000
1	-1.276789000	0.199505000	5.052656000
1	1.268098000	0.207135000	5.054282000
1	5.583921000	-1.754422000	1.272087000
1	5.420698000	4.260888000	-0.439854000
1	-3.794837000	4.344945000	-2.353867000
1	-5.897167000	-3.836349000	-0.132490000
1	2.384310000	-2.698944000	-2.349889000
1	-4.257824000	-4.304228000	-1.995922000
1	-0.002516000	1.847508000	-1.554843000
1	5.904817000	-3.819249000	-0.113889000
1	4.269777000	-4.295213000	-1.978991000

2*’ linkage isomer; Broken Symmetry Singlet

29	1.411481000	0.186230000	-0.931936000
7	1.168346000	-0.026521000	1.128739000
7	-0.454668000	-0.686000000	-2.618644000
6	-0.002667000	-0.023832000	1.834945000
6	2.323222000	-0.071861000	1.788803000
29	-1.426082000	-0.186731000	-0.970747000
8	0.669508000	-0.093513000	-2.789160000
7	-1.177022000	0.008661000	1.137623000
6	0.001704000	-0.044107000	3.262903000
6	3.647071000	-0.050180000	0.989881000

6	2.407454000	-0.121795000	3.203722000
6	-2.324893000	0.072343000	1.804466000
6	1.245391000	-0.102198000	3.936253000
6	-1.238006000	0.003141000	3.944702000
6	3.795401000	-1.264076000	0.052649000
6	3.848414000	1.286861000	0.245851000
9	4.674412000	-0.145048000	1.919804000
1	3.378753000	-0.164811000	3.690952000
6	-3.648399000	0.141797000	1.009677000
6	-2.403308000	0.074612000	3.220654000
1	1.267052000	-0.125307000	5.028824000
1	-1.252917000	-0.010524000	5.037585000
6	4.814574000	-2.204134000	0.242223000
7	2.915596000	-1.355572000	-0.947976000
6	4.973877000	2.077360000	0.504451000
7	2.917570000	1.639143000	-0.651204000
6	-3.698713000	1.361791000	0.070204000
6	-3.941264000	-1.176569000	0.269120000
9	-4.666312000	0.311670000	1.937610000
1	-3.371255000	0.126272000	3.713975000
6	4.903813000	-3.267625000	-0.660708000
1	5.517774000	-2.104118000	1.067965000
6	3.003046000	-2.370440000	-1.818067000
6	5.122831000	3.272394000	-0.203519000
1	5.714434000	1.764099000	1.238960000
6	3.062064000	2.787322000	-1.330118000
6	-4.678208000	2.346987000	0.234311000
7	-2.777550000	1.424523000	-0.900037000
6	-5.084245000	-1.928761000	0.560206000
7	-3.057958000	-1.547589000	-0.662274000
6	3.986454000	-3.354705000	-1.711632000
1	5.688013000	-4.020046000	-0.542627000
1	2.260863000	-2.382224000	-2.622745000
6	4.151013000	3.637498000	-1.138018000
1	5.991711000	3.910504000	-0.024331000
1	2.276009000	3.029673000	-2.051176000
6	-4.687826000	3.427110000	-0.651959000

1	-5.413440000	2.268022000	1.033862000
6	-2.787221000	2.462369000	-1.750239000
6	-5.297115000	-3.107102000	-0.160578000
1	-5.786964000	-1.602249000	1.325874000
6	-3.266085000	-2.671828000	-1.362254000
1	4.029185000	-4.169171000	-2.438189000
1	4.229518000	4.564006000	-1.709971000
6	-3.726829000	3.488967000	-1.663755000
1	-5.441386000	4.212387000	-0.549687000
1	-2.013922000	2.466056000	-2.524166000
6	-4.376505000	-3.487342000	-1.140232000
1	-6.178845000	-3.720131000	0.042018000
1	-2.519102000	-2.905178000	-2.126683000
1	-3.700151000	4.316523000	-2.375980000
1	-4.512250000	-4.398783000	-1.725597000
8	-0.775027000	-1.516912000	-3.456943000

2*” linkage isomer; closed shell singlet

29	-1.204709000	0.039434000	-0.819166000
29	1.214145000	-0.000127000	-0.816363000
9	-4.667476000	0.098204000	1.880313000
8	0.029376000	1.147961000	-3.099999000
7	-1.153195000	0.032957000	1.267655000
7	-2.744038000	-1.415992000	-0.751354000
9	4.669567000	-0.118837000	1.888585000
7	2.764629000	1.442487000	-0.729063000
7	-2.694883000	1.543824000	-0.752157000
7	1.157083000	-0.020478000	1.270281000
6	-3.704304000	-1.195092000	0.156964000
6	0.001210000	0.005553000	1.982005000
7	2.690010000	-1.517375000	-0.764098000
7	0.003129000	0.057639000	-2.486009000
6	-3.662339000	1.356991000	0.155685000
6	-4.788429000	-2.063242000	0.319519000
6	-3.581637000	0.079948000	1.019838000
6	-4.716942000	2.261228000	0.315315000

6	2.848075000	2.530277000	-1.508483000
6	2.417805000	-0.058774000	3.317370000
6	-2.725900000	2.625910000	-1.542965000
6	-0.000239000	0.002584000	3.404641000
6	-2.315701000	0.057198000	1.896753000
6	-2.418085000	0.059447000	3.312525000
6	4.823505000	2.047506000	0.339016000
6	-4.750379000	3.390788000	-0.508031000
6	2.318251000	-0.052177000	1.901412000
6	-2.812888000	-2.498212000	-1.539829000
6	3.909408000	3.431145000	-1.413646000
6	3.724591000	1.198669000	0.173729000
6	-1.259373000	0.032136000	4.059816000
6	1.257542000	-0.030566000	4.062248000
6	4.690940000	-2.275919000	0.314337000
6	4.911505000	3.182264000	-0.472860000
6	-3.740608000	3.579456000	-1.454627000
6	-4.860632000	-3.192887000	-0.501053000
6	2.709126000	-2.594289000	-1.562313000
6	3.585544000	-0.081369000	1.026479000
6	-3.858665000	-3.417340000	-1.448162000
8	-0.011107000	-1.001983000	-3.151423000
1	-5.555766000	-1.857645000	1.064650000
1	-5.491379000	2.083581000	1.060349000
1	2.033917000	2.668384000	-2.226950000
1	3.395385000	-0.085667000	3.795883000
1	-1.907210000	2.715078000	-2.264226000
1	-3.396755000	0.081765000	3.788993000
1	5.590193000	1.823033000	1.079309000
1	-5.562604000	4.115489000	-0.407980000
1	-1.999989000	-2.616856000	-2.263197000
1	3.944244000	4.307068000	-2.064703000
1	-1.299969000	0.032113000	5.152210000
1	1.295740000	-0.033701000	5.154728000
1	5.462218000	-2.116398000	1.066762000
1	5.759748000	3.863630000	-0.368606000
1	-3.733682000	4.449377000	-2.114751000

1	-5.696745000	-3.889441000	-0.398704000
1	1.894936000	-2.664790000	-2.290654000
1	-3.881775000	-4.288419000	-2.106286000
6	3.706656000	-3.565581000	-1.472347000
1	3.690261000	-4.431058000	-2.138147000
6	4.711693000	-3.400339000	-0.516388000
1	5.510467000	-4.139631000	-0.414503000
6	3.653030000	-1.352876000	0.152724000

4*' intermediate; broken symmetry singlet

29	-1.377473000	-0.262598000	-1.279829000
29	1.378340000	-0.259243000	-1.277985000
9	-4.655462000	0.329060000	1.781196000
8	-0.000026000	0.634601000	-2.148625000
7	-1.161783000	-0.030149000	1.141233000
7	-2.971872000	-1.493205000	-0.816149000
9	4.649905000	0.345078000	1.787630000
7	2.616015000	1.407177000	-0.967033000
7	-2.621542000	1.399389000	-0.970225000
7	1.158434000	-0.026003000	1.142859000
6	-3.853552000	-1.142242000	0.133699000
6	-0.002126000	-0.025471000	1.847782000
7	2.975718000	-1.484801000	-0.810643000
7	0.002911000	-1.835072000	-1.496521000
6	-3.530824000	1.398042000	0.011298000
6	-4.976354000	-1.922740000	0.426803000
6	-3.588944000	0.153296000	0.913874000
6	-4.361319000	2.497020000	0.249429000
6	2.453630000	2.492253000	-1.735595000
6	2.410430000	0.096901000	3.199260000
6	-2.461980000	2.485340000	-1.738188000
6	-0.003255000	0.025907000	3.276318000
6	-2.310168000	0.052403000	1.779057000
6	-2.417083000	0.087206000	3.195958000
6	4.353198000	2.509892000	0.251804000
6	-4.218180000	3.623617000	-0.565900000

6	2.305688000	0.061143000	1.782307000
6	-3.170851000	-2.626604000	-1.510660000
6	3.237423000	3.634148000	-1.569296000
6	3.525145000	1.408863000	0.014622000
6	-1.257095000	0.063188000	3.938501000
6	1.249375000	0.068152000	3.940192000
6	4.980040000	-1.906730000	0.435363000
6	4.207112000	3.635697000	-0.564166000
6	-3.248806000	3.625028000	-1.571353000
6	-5.182024000	-3.099306000	-0.296355000
6	3.855137000	-1.130174000	0.139995000
6	3.179315000	-2.618254000	-1.503686000
6	5.190467000	-3.083294000	-0.286406000
6	3.585393000	0.165288000	0.918525000
6	-4.263641000	-3.460509000	-1.283390000
6	4.274513000	-3.448399000	-1.274211000
8	0.003524000	-2.674866000	-0.637029000
1	-5.671884000	-1.613718000	1.205529000
1	-5.094346000	2.472208000	1.054773000
1	1.652807000	2.418069000	-2.477039000
1	3.385744000	0.154414000	3.679626000
1	-1.661285000	2.413602000	-2.480018000
1	-3.393525000	0.140809000	3.674371000
1	5.086613000	2.487160000	1.056895000
1	-4.854942000	4.497378000	-0.405241000
1	-2.423714000	-2.869527000	-2.269983000
1	3.084308000	4.502437000	-2.213559000
1	-1.290904000	0.092953000	5.031005000
1	1.281697000	0.098076000	5.032742000
1	5.673662000	-1.594585000	1.214572000
1	4.841744000	4.511134000	-0.404208000
1	-3.098613000	4.493791000	-2.215679000
1	-6.051656000	-3.726730000	-0.086411000
1	2.434052000	-2.864395000	-2.263825000
1	-4.384186000	-4.372428000	-1.870736000
1	6.061956000	-3.707612000	-0.074909000
1	4.398691000	-4.360419000	-1.860588000

[Cu_2(μ-(η^1-NO_2H)DPFN]$^{2+}$ intermediate (B); closed shell singlet

29	1.195392000	-0.018386000	-0.793349000
7	1.148823000	-0.033243000	1.252671000
7	-0.021026000	0.100817000	-2.400947000
6	-0.002290000	-0.006019000	1.970774000
6	2.316750000	-0.064433000	1.874160000
29	-1.223708000	0.032905000	-0.780035000
8	0.002189000	1.065590000	-3.129829000
7	-1.160267000	0.031721000	1.264197000
6	0.004317000	-0.012826000	3.391654000
6	3.573102000	-0.083411000	0.985169000
6	2.423188000	-0.077461000	3.287623000
6	-2.321856000	0.068757000	1.896977000
6	1.266711000	-0.052204000	4.039933000
6	-1.251816000	0.023327000	4.052182000
6	3.640273000	-1.354083000	0.109433000
6	3.691416000	1.196272000	0.127397000
9	4.663492000	-0.110650000	1.833156000
1	3.403639000	-0.105973000	3.760145000
6	-3.585649000	0.115485000	1.019880000
6	-2.415207000	0.065805000	3.311398000
1	1.312666000	-0.060280000	5.131926000
1	-1.287229000	0.018961000	5.144586000
6	4.694220000	-2.259145000	0.258292000
7	2.666769000	-1.534123000	-0.797521000
6	4.784071000	2.052543000	0.285466000
7	2.724813000	1.431890000	-0.774389000
6	-3.641076000	1.393062000	0.153274000
6	-3.732455000	-1.155420000	0.153845000
9	-4.667390000	0.154915000	1.878386000
1	-3.390977000	0.096927000	3.793279000
6	4.726880000	-3.383360000	-0.571995000
1	5.470876000	-2.085512000	1.001730000
6	2.699619000	-2.612660000	-1.594959000
6	4.863645000	3.185737000	-0.529350000

1	5.554424000	1.834617000	1.023691000
6	2.802225000	2.518765000	-1.556851000
6	-4.674219000	2.318378000	0.321800000
7	-2.678124000	1.559496000	-0.767186000
6	-4.842021000	-1.989746000	0.312280000
7	-2.775006000	-1.403520000	-0.754637000
6	3.714873000	-3.565487000	-1.516201000
1	5.539760000	-4.107962000	-0.478698000
1	1.884226000	-2.709876000	-2.317274000
6	3.858284000	3.425432000	-1.467959000
1	5.707951000	3.872260000	-0.428656000
1	1.991045000	2.662302000	-2.276943000
6	-4.696061000	3.447355000	-0.502579000
1	-5.443054000	2.157005000	1.076105000
6	-2.700285000	2.641726000	-1.559116000
6	-4.950578000	-3.114723000	-0.510186000
1	-5.603126000	-1.760723000	1.056710000
6	-2.880783000	-2.483384000	-1.544275000
1	3.704975000	-4.430391000	-2.182536000
1	3.885061000	4.299134000	-2.122028000
6	-3.695183000	3.614116000	-1.461565000
1	-5.492300000	4.188060000	-0.393282000
1	-1.893981000	2.727388000	-2.293912000
6	-3.955479000	-3.368004000	-1.456043000
1	-5.808712000	-3.783955000	-0.410473000
1	-2.076949000	-2.637806000	-2.269474000
1	-3.677657000	4.481814000	-2.124067000
1	-4.004613000	-4.235721000	-2.116781000
8	-0.062022000	-1.116432000	-3.053524000
1	-0.060572000	-0.909151000	-4.017650000

[Cu_2(μ–κ^1:κ^1-HONO)DPFN]$^{2+}$ intermediate (A); closed shell singlet

29	-1.336044000	-0.315751000	-0.845446000
29	1.364685000	0.212199000	-0.848361000
9	-4.654640000	0.341458000	1.860818000

8	0.702774000	0.564622000	-2.816692000
7	-1.159702000	-0.017390000	1.176301000
7	-2.957889000	-1.679460000	-0.564121000
9	4.668265000	-0.288095000	1.898776000
7	2.905044000	1.641526000	-0.560600000
7	-2.687587000	1.291443000	-0.992285000
7	1.165359000	-0.079702000	1.175478000
6	-3.881256000	-1.239585000	0.300545000
6	0.002535000	-0.050879000	1.883415000
7	2.815019000	-1.347057000	-0.985195000
7	-0.103502000	-0.379690000	-3.462631000
6	-3.625280000	1.286798000	-0.031853000
6	-5.042829000	-1.962366000	0.587025000
6	-3.612498000	0.120246000	0.978588000
6	-4.597818000	2.286660000	0.061429000
6	3.049768000	2.826160000	-1.174009000
6	2.407640000	-0.184161000	3.239735000
6	-2.677632000	2.282483000	-1.896795000
6	-0.000868000	-0.046547000	3.307416000
6	-2.318166000	0.079284000	1.818042000
6	-2.408815000	0.122894000	3.231730000
6	4.972073000	2.005340000	0.601558000
6	-4.586933000	3.316919000	-0.882361000
6	2.322879000	-0.141699000	1.824869000
6	-3.143798000	-2.853442000	-1.184571000
6	4.144474000	3.658808000	-0.944513000
6	3.840446000	1.236934000	0.310771000
6	-1.250007000	0.043661000	3.971066000
6	1.246138000	-0.125948000	3.976152000
6	4.719956000	-2.271098000	0.142746000
6	5.122367000	3.236400000	-0.041820000
6	-3.611545000	3.317387000	-1.881212000
6	-5.235202000	-3.186504000	-0.059127000
6	2.871496000	-2.343076000	-1.881600000
6	3.627792000	-0.129245000	0.999025000
6	-4.271295000	-3.643432000	-0.960244000
8	-0.729427000	-0.990007000	-2.646772000

1	-5.776787000	-1.578744000	1.294484000
1	-5.345585000	2.256648000	0.852639000
1	2.258083000	3.119827000	-1.869235000
1	3.379361000	-0.246358000	3.725124000
1	-1.893674000	2.246182000	-2.658566000
1	-3.381247000	0.206031000	3.712908000
1	5.716040000	1.650236000	1.313227000
1	-5.336442000	4.111073000	-0.833739000
1	-2.362859000	-3.167803000	-1.882766000
1	4.221192000	4.616285000	-1.462679000
1	-1.280683000	0.054337000	5.063580000
1	1.273677000	-0.135667000	5.068713000
1	5.438643000	-2.210093000	0.958633000
1	5.996063000	3.859036000	0.165366000
1	-3.568213000	4.103982000	-2.637497000
1	-6.132439000	-3.776450000	0.143117000
1	2.117869000	-2.338278000	-2.674710000
1	-4.384551000	-4.595213000	-1.482156000
6	3.837563000	-3.346879000	-1.825540000
1	3.848010000	-4.138896000	-2.577408000
6	4.775923000	-3.308093000	-0.792262000
1	5.548575000	-4.076962000	-0.711052000
6	3.718054000	-1.305271000	0.005080000
1	1.232156000	0.994757000	-3.521324000

HONO cleavage transition state; closed-shell singlet

29	1.406906000	0.228387000	-0.999655000
7	1.190442000	0.004446000	1.059331000
7	0.036027000	0.976567000	-2.073653000
6	0.010419000	0.045403000	1.741819000
6	2.338686000	-0.085403000	1.715519000
29	-1.538958000	-0.077847000	-1.393769000
8	-0.062959000	1.731629000	-2.941426000
7	-1.144808000	0.094050000	1.021493000
6	0.004791000	0.026916000	3.169485000

6	3.641993000	-0.141261000	0.885390000
6	2.415868000	-0.124976000	3.129553000
6	-2.295908000	0.138757000	1.672816000
6	1.245060000	-0.059248000	3.850103000
6	-1.244575000	0.090569000	3.832460000
6	3.666088000	-1.349511000	-0.073190000
6	3.904601000	1.185996000	0.144069000
9	4.681344000	-0.313810000	1.780976000
1	3.382176000	-0.200450000	3.624163000
6	-3.606723000	0.139344000	0.849160000
6	-2.399558000	0.151129000	3.088262000
1	1.257922000	-0.076409000	4.942963000
1	-1.279159000	0.085768000	4.924913000
6	4.640177000	-2.342542000	0.056442000
7	2.720860000	-1.397413000	-1.023428000
6	5.046789000	1.941699000	0.422527000
7	3.003647000	1.569485000	-0.773135000
6	-3.719946000	1.348041000	-0.092889000
6	-3.784434000	-1.201809000	0.118077000
9	-4.649123000	0.242602000	1.751367000
1	-3.375005000	0.198161000	3.567486000
6	4.616239000	-3.414352000	-0.840707000
1	5.396495000	-2.277261000	0.837478000
6	2.689333000	-2.431221000	-1.878309000
6	5.245909000	3.130308000	-0.284695000
1	5.762405000	1.607472000	1.172461000
6	3.194689000	2.710569000	-1.451971000
6	-4.709344000	2.311413000	0.118137000
7	-2.858979000	1.436923000	-1.122569000
6	-4.799471000	-2.090872000	0.477942000
7	-2.904546000	-1.488483000	-0.850445000
6	3.625047000	-3.463808000	-1.823094000
1	5.366700000	-4.205629000	-0.766017000
1	1.875928000	-2.419813000	-2.608385000
6	4.306025000	3.524952000	-1.238780000
1	6.130079000	3.741542000	-0.088557000
1	2.432375000	2.978780000	-2.189070000

6	-4.806936000	3.383392000	-0.772387000
1	-5.391139000	2.218220000	0.961594000
6	-2.956783000	2.462951000	-1.983112000
6	-4.882584000	-3.311491000	-0.198822000
1	-5.503087000	-1.834667000	1.268769000
6	-2.970214000	-2.665101000	-1.494003000
1	3.570578000	-4.289291000	-2.535958000
1	4.424404000	4.447235000	-1.810096000
6	-3.918412000	3.461046000	-1.845370000
1	-5.574916000	4.147058000	-0.626746000
1	-2.244411000	2.487910000	-2.812352000
6	-3.951543000	-3.609025000	-1.196224000
1	-5.667706000	-4.026218000	0.059449000
1	-2.204317000	-2.837534000	-2.254271000
1	-3.962510000	4.276430000	-2.569909000
1	-3.978849000	-4.556070000	-1.737982000
8	-0.304593000	-1.118263000	-2.474061000
1	-0.538507000	-1.115367000	-3.419168000

Nitrite cleavage first transition state; closed shell singlet

29	-1.400299000	0.010903000	-1.416055000
29	1.538901000	-0.569726000	-1.529387000
9	-4.607945000	0.327295000	1.717053000
8	0.127499000	0.106357000	-2.479935000
7	-1.143643000	-0.064505000	0.928414000
7	-3.067686000	-1.237157000	-1.122354000
9	4.647350000	0.263609000	1.614438000
7	2.659443000	1.162365000	-1.227771000
7	-2.635359000	1.700476000	-0.946807000
7	1.180597000	-0.144257000	0.916517000
6	-3.939457000	-0.937670000	-0.149435000
6	0.019983000	-0.220240000	1.618528000
7	3.126978000	-1.711417000	-0.972612000
7	0.237691000	-2.070326000	-1.856778000
6	-3.513240000	1.582833000	0.056794000
6	-5.135521000	-1.642959000	0.026205000

6	-3.578866000	0.226980000	0.788666000
6	-4.339062000	2.641584000	0.453160000
6	2.445989000	2.227356000	-2.010977000
6	2.440045000	-0.366751000	2.961894000
6	-2.532674000	2.867974000	-1.597065000
6	0.026351000	-0.401966000	3.036891000
6	-2.286036000	-0.052908000	1.587756000
6	-2.381166000	-0.261613000	2.991695000
6	4.217522000	2.415169000	0.082625000
6	-4.234101000	3.856960000	-0.228453000
6	2.329501000	-0.177671000	1.558317000
6	-3.347331000	-2.249441000	-1.960132000
6	3.113284000	3.434987000	-1.806513000
6	3.505478000	1.244627000	-0.194657000
6	-1.221442000	-0.444771000	3.709101000
6	1.279939000	-0.496106000	3.692808000
6	5.167871000	-1.952128000	0.260327000
6	4.019019000	3.523142000	-0.746891000
6	-3.314391000	3.976790000	-1.272698000
6	-5.422436000	-2.695850000	-0.845410000
6	3.412469000	-2.838867000	-1.647687000
6	3.617872000	0.014524000	0.720342000
6	-4.512495000	-3.008416000	-1.857841000
8	-0.017911000	-2.660090000	-0.882145000
1	-5.823800000	-1.373051000	0.825774000
1	-5.043879000	2.516774000	1.274019000
1	1.700964000	2.083821000	-2.799512000
1	3.417461000	-0.402197000	3.440599000
1	-1.793209000	2.908767000	-2.402600000
1	-3.352860000	-0.264077000	3.481995000
1	4.901073000	2.459502000	0.929659000
1	-4.865268000	4.701757000	0.058356000
1	-2.606113000	-2.453945000	-2.737829000
1	2.920711000	4.285609000	-2.463600000
1	-1.248694000	-0.600619000	4.790771000
1	1.312532000	-0.647085000	4.775094000
1	5.843589000	-1.570785000	1.024324000

1	4.562414000	4.451818000	-0.555619000
1	-3.199497000	4.910177000	-1.827571000
1	-6.348655000	-3.264449000	-0.732020000
1	2.688880000	-3.155276000	-2.403498000
1	-4.696627000	-3.824927000	-2.559060000
6	4.567698000	-3.579572000	-1.409980000
1	4.755359000	-4.491368000	-1.979291000
6	5.460922000	-3.124552000	-0.439135000
1	6.379861000	-3.675097000	-0.224375000
6	3.984417000	-1.270320000	-0.036427000

NO loss transition state; Restricted Singlet

29	-1.427849000	0.403855000	-1.152093000
29	1.506779000	-0.513523000	-1.379410000
9	-4.657927000	0.015019000	1.745087000
8	0.058746000	0.202773000	-2.413409000
7	-1.165220000	-0.036879000	0.943287000
7	-2.979445000	-1.055150000	-1.235396000
9	4.666817000	0.198890000	1.602173000
7	2.809424000	1.089645000	-1.329640000
7	-2.795803000	1.887128000	-0.690204000
7	1.172643000	-0.094007000	0.911132000
6	-3.853413000	-0.982277000	-0.223104000
6	0.012993000	-0.105477000	1.628729000
7	3.034447000	-1.750436000	-0.925019000
7	0.341299000	-2.173171000	-1.560985000
6	-3.728977000	1.536793000	0.208407000
6	-4.947429000	-1.847842000	-0.117503000
6	-3.626754000	0.124158000	0.824413000
6	-4.761994000	2.400146000	0.587118000
6	2.809186000	2.075821000	-2.239884000
6	2.440215000	-0.119418000	2.968813000
6	-2.850596000	3.107826000	-1.248471000
6	0.030937000	-0.166358000	3.055905000
6	-2.308778000	-0.037790000	1.614674000
6	-2.379459000	-0.133298000	3.029181000

6	4.484947000	2.250524000	-0.075147000
6	-4.816316000	3.668996000	0.004808000
6	2.327794000	-0.076933000	1.556906000
6	-3.158483000	-1.977481000	-2.192910000
6	3.631614000	3.194091000	-2.122508000
6	3.632680000	1.162062000	-0.272231000
6	-1.207305000	-0.194683000	3.744669000
6	1.284403000	-0.180855000	3.713305000
6	5.055350000	-2.085361000	0.309343000
6	4.478495000	3.283029000	-1.016628000
6	-3.844237000	4.032446000	-0.929406000
6	-5.129246000	-2.811603000	-1.112939000
6	3.262686000	-2.885696000	-1.608394000
6	3.626116000	-0.013570000	0.719602000
6	-4.222428000	-2.878461000	-2.173476000
8	-0.139057000	-2.598468000	-0.628498000
1	-5.640302000	-1.765531000	0.718591000
1	-5.504807000	2.086207000	1.319080000
1	2.141671000	1.961731000	-3.098365000
1	3.418486000	-0.107987000	3.445267000
1	-2.069010000	3.349290000	-1.973901000
1	-3.345684000	-0.143058000	3.528952000
1	5.140031000	2.284682000	0.794183000
1	-5.611516000	4.365342000	0.281939000
1	-2.422352000	-1.989894000	-3.003300000
1	3.604441000	3.972638000	-2.887532000
1	-1.216616000	-0.254085000	4.835991000
1	1.321446000	-0.228732000	4.804734000
1	5.748720000	-1.736861000	1.073421000
1	5.135421000	4.146446000	-0.885925000
1	-3.849689000	5.014458000	-1.405966000
1	-5.976666000	-3.499773000	-1.059435000
1	2.529005000	-3.165684000	-2.369863000
1	-4.333786000	-3.612555000	-2.974357000
6	4.382064000	-3.678467000	-1.369945000
1	4.530224000	-4.593691000	-1.945053000
6	5.289840000	-3.270928000	-0.391359000

1	6.178930000	-3.867412000	-0.174356000
6	3.911314000	-1.344212000	0.008800000
1	0.289173000	1.082683000	-2.745010000

μ-OH Complex; Doublet

29	-1.354838000	0.364232000	-1.104128000
29	1.352616000	0.368145000	-1.102184000
9	-4.631827000	-0.098767000	1.799812000
8	-0.002265000	1.486442000	-1.838289000
7	-1.158704000	0.360245000	1.161556000
7	-2.476206000	-1.297364000	-0.825549000
9	4.627191000	-0.086593000	1.805894000
7	3.030229000	1.582596000	-0.935579000
7	-3.035895000	1.573617000	-0.940507000
7	1.153589000	0.363073000	1.163029000
6	-3.433012000	-1.235384000	0.119760000
6	-0.003095000	0.433586000	1.868146000
7	2.477758000	-1.290724000	-0.822204000
6	-3.897662000	1.280465000	0.044151000
6	-4.281919000	-2.313993000	0.377021000
6	-3.568640000	0.068146000	0.933500000
6	-5.047876000	2.040509000	0.270046000
6	3.260131000	2.637588000	-1.733587000
6	2.411817000	0.408011000	3.214287000
6	-3.267806000	2.627313000	-1.739612000
6	-0.004118000	0.510291000	3.291962000
6	-2.311127000	0.303750000	1.799653000
6	-2.419695000	0.402797000	3.211196000
6	5.039015000	2.055005000	0.278322000
6	-5.294688000	3.135497000	-0.562788000
6	2.305368000	0.309236000	1.802551000
6	-2.330680000	-2.422671000	-1.547004000
6	4.381534000	3.451016000	-1.576354000
6	3.891456000	1.291617000	0.050195000
6	-1.261378000	0.522395000	3.950341000
6	1.252248000	0.524722000	3.951925000

6	4.289769000	-2.299922000	0.377187000
6	5.283782000	3.151217000	-0.553494000
6	-4.391889000	3.437398000	-1.584538000
6	-4.128092000	-3.483966000	-0.371269000
6	3.435035000	-1.225334000	0.122420000
6	2.336593000	-2.416104000	-1.544403000
6	4.140983000	-3.469708000	-0.372415000
6	3.564804000	0.077674000	0.938025000
6	-3.136281000	-3.541935000	-1.351087000
6	3.147835000	-3.531663000	-1.350629000
1	-5.046751000	-2.236860000	1.148333000
1	-5.731798000	1.780719000	1.076866000
1	2.519285000	2.828771000	-2.514438000
1	3.387727000	0.379236000	3.696536000
1	-2.526454000	2.819984000	-2.519569000
1	-3.396303000	0.372192000	3.691898000
1	5.722566000	1.796526000	1.085866000
1	-6.187237000	3.747009000	-0.410451000
1	-1.544947000	-2.421585000	-2.306622000
1	4.537328000	4.300441000	-2.243945000
1	-1.300187000	0.596915000	5.040262000
1	1.289389000	0.598588000	5.041991000
1	5.055380000	-2.219702000	1.147389000
1	6.174305000	3.765237000	-0.399384000
1	-4.549240000	4.286070000	-2.252736000
1	-4.780205000	-4.340965000	-0.185991000
1	1.549930000	-2.417966000	-2.302997000
1	-2.982843000	-4.435575000	-1.958767000
1	-0.003799000	2.333934000	-1.366692000
1	4.797898000	-4.323508000	-0.189248000
1	2.997490000	-4.425689000	-1.958526000

NO; Doublet

8	0.280701000	0.727763000	0.000000000
7	-0.867432000	0.727763000	0.000000000

Protonated Linkage Isomer 2*'; Restricted Singlet

29	1.416112000	0.174424000	-0.981598000
7	1.145308000	-0.026712000	1.117269000
7	-0.219529000	-0.334185000	-2.380307000
6	-0.016908000	-0.012259000	1.833368000
6	2.306481000	-0.080440000	1.762901000
29	-1.454784000	-0.104859000	-0.910527000
8	0.532155000	0.536990000	-2.833113000
7	-1.197578000	0.029305000	1.150819000
6	-0.000785000	-0.033145000	3.259956000
6	3.616171000	-0.080567000	0.940175000
6	2.405997000	-0.126901000	3.175411000
6	-2.342847000	0.085060000	1.822668000
6	1.250005000	-0.097690000	3.919264000
6	-1.236223000	0.016852000	3.951004000
6	3.725444000	-1.312234000	0.018415000
6	3.812469000	1.243378000	0.175989000
9	4.656185000	-0.171306000	1.847816000
1	3.381807000	-0.176908000	3.653198000
6	-3.663677000	0.138898000	1.022985000
6	-2.409615000	0.085647000	3.237813000
1	1.283794000	-0.120298000	5.011440000
1	-1.242307000	0.003680000	5.043812000
6	4.752991000	-2.242035000	0.201769000
7	2.806849000	-1.440990000	-0.950462000
6	4.925641000	2.051251000	0.421196000
7	2.879424000	1.574351000	-0.729469000
6	-3.737298000	1.369073000	0.097539000
6	-3.917004000	-1.174728000	0.255828000
9	-4.686013000	0.270741000	1.946021000
1	-3.373869000	0.133423000	3.739112000
6	4.817531000	-3.339715000	-0.660744000
1	5.484221000	-2.108612000	0.997427000
6	2.868161000	-2.498951000	-1.773645000
6	5.058695000	3.237057000	-0.306286000
1	5.669024000	1.758002000	1.160935000

6	3.004534000	2.714019000	-1.428626000
6	-4.732576000	2.334734000	0.270907000
7	-2.820566000	1.456892000	-0.876934000
6	-5.052630000	-1.945967000	0.518664000
7	-3.010376000	-1.523965000	-0.666863000
6	3.858642000	-3.474219000	-1.666381000
1	5.611009000	-4.081987000	-0.542804000
1	2.093677000	-2.570665000	-2.541477000
6	4.083465000	3.577586000	-1.246040000
1	5.919443000	3.888329000	-0.136485000
1	2.215724000	2.935269000	-2.152474000
6	-4.763933000	3.420328000	-0.608733000
1	-5.464031000	2.236850000	1.071782000
6	-2.849497000	2.500206000	-1.721030000
6	-5.238254000	-3.120736000	-0.215086000
1	-5.772425000	-1.634945000	1.274629000
6	-3.189192000	-2.652404000	-1.370872000
1	3.870510000	-4.319180000	-2.357852000
1	4.151034000	4.496759000	-1.830612000
6	-3.808154000	3.507355000	-1.623376000
1	-5.531221000	4.190924000	-0.498695000
1	-2.078908000	2.525938000	-2.496904000
6	-4.292172000	-3.483508000	-1.176234000
1	-6.116327000	-3.745489000	-0.034489000
1	-2.421930000	-2.892135000	-2.112083000
1	-3.799105000	4.340541000	-2.329161000
1	-4.400832000	-4.394559000	-1.767486000
8	-0.226944000	-1.488442000	-3.086685000
1	0.345892000	-1.348497000	-3.877249000

11) X-Ray Crystallography

Crystalline samples were prepared in a glovebox by decanting the supernatant and covering the crystals with a layer of Paratone N oil. The samples were then placed in a cold-well, which was previously cooled by liquid nitrogen, until they were frozen. All samples were then transferred to a container of dry ice prior to data collection. Data for complex **3** was collected at the UC Berkeley CheXRay crystallographic facility on a Rigaku Pilatus 200K diffractometer using Mo Kα radiation (λ = 0.7107 Å). Data for complexes **2** and **4** was collected at the advanced Light Source (ALS) on the 12.2.1 beamline using a Bruker D85 three-circle diffractometer with a PHOTON II CCD area detector and synchrotron radiation (λ = 0.7288 Å). The structure was solved by intrinsic phasing using the SHELXT[10] software package and refined using SHELXL[11] in the OLEX2 interface.[12]

CCDC 2391275-2391277 contain the supplementary crystallographic data for this paper.

Structure Determination of 2

All non-hydrogen atoms were refined anisotropically. Hydrogen atoms were placed geometrically, then constrained and refined using a riding model. Displacement parameter restraints were used in the modelling of the structure.

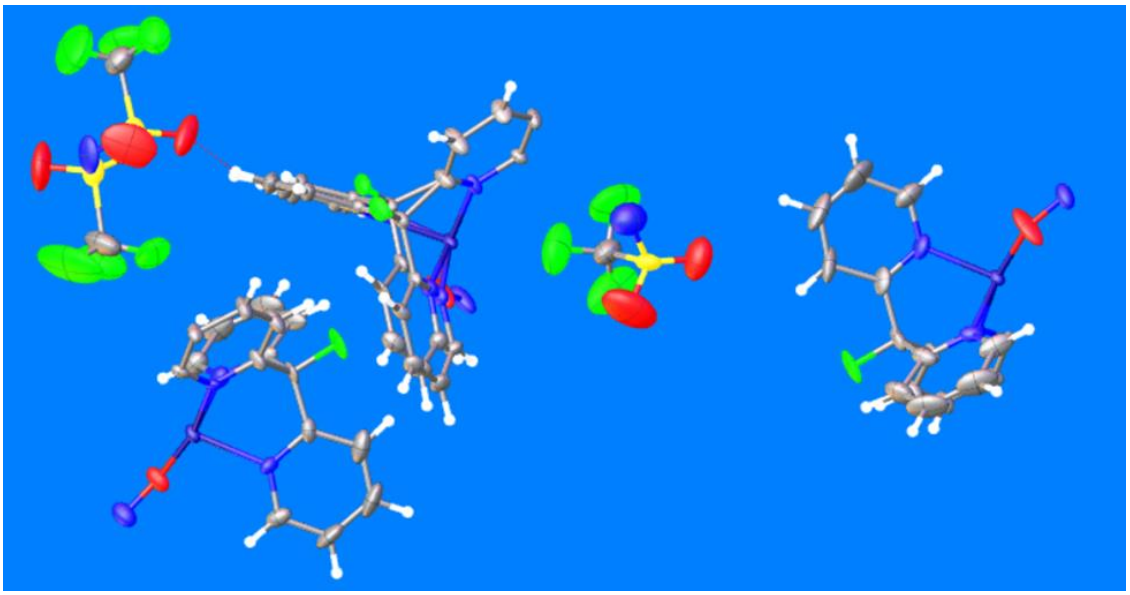

Figure S45. Asymmetric unit of **2**. Color Scheme: C, grey; H, white; N, blue; O, red; S, yellow; F, green; Cu, dark blue.

Table S1. Crystal data and structure refinement for **2**.

Compound	2
Empirical formula	$C_{32}H_{20}N_8O_6F_8S_2Cu_2$
Formula weight	955.76
Temperature/K	100.15
Crystal system	orthorhombic
Space group	$C222_1$
a/Å	17.478(2)
b/Å	31.697(4)
c/Å	19.903(3)
α/°	90
β/°	90
γ/°	90
Volume/Å^3	11026(3)
Z	12
ρ_{calc}g/cm^3	1.727
μ/mm^{-1}	1.462
F(000)	5736.0
Crystal size/mm^3	0.32 × 0.3 × 0.26
Radiation	synchrotron (λ = 0.7288)
2Θ range for data collection/°	4.62 to 62.91
Index ranges	-25 ≤ h ≤ 25, -45 ≤ k ≤ 44, -27 ≤ l ≤ 28
Reflections collected	88123
Independent reflections	16860 [R_{int} = 0.0579, R_{sigma} = 0.0523]
Data/restraints/parameters	16860/1235/916
Goodness-of-fit on F^2	1.085
Final R indexes [I>=2σ (I)]	R_1 = 0.0695, wR_2 = 0.2029
Final R indexes [all data]	R_1 = 0.1257, wR_2 = 0.2441

Structure Determination of 3

Complex **3** crystallized with a single molecule (composed of a cationic and anionic component) in the asymmetric unit. The molecule exhibits no discernable disorder. All hydrogen atoms were placed in calculated positions and refined isotopically.

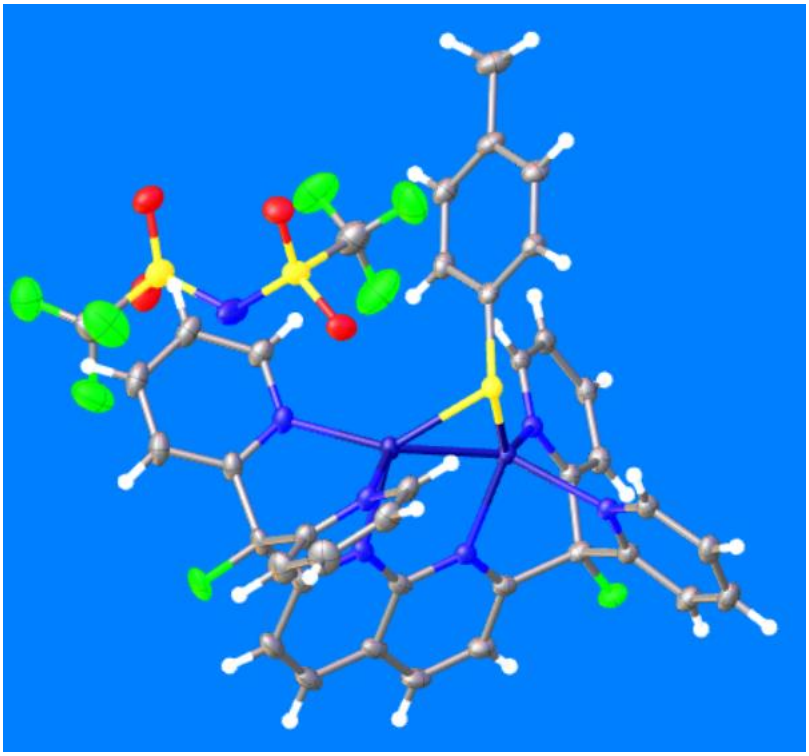

Figure S46. Asymmetric unit of **3**. Color Scheme: C, grey; H, white; N, blue; O, red; S, yellow; F, green; Cu, dark blue.

Table S2. Crystal data and structure refinement for **3**.

Empirical formula	$C_{39}H_{27}Cu_2F_8N_7O_4S_3$
Formula weight	1032.970
Temperature/K	100.15
Crystal system	triclinic
Space group	P-1
a/Å	12.5183(3)
b/Å	12.9638(3)
c/Å	14.4285(3)
α/°	78.142(2)

β/°	88.589(2)
γ/°	61.291(2)
Volume/Å^3	2002.36(9)
Z	2
ρ_{calc}g/cm^3	1.713
μ/mm^{-1}	1.309
F(000)	1043.0
Crystal size/mm^3	0.381 × 0.214 × 0.198
Radiation	Mo Kα (λ = 0.71073)
2Θ range for data collection/°	6.38 to 61
Index ranges	-17 ≤ h ≤ 17, -18 ≤ k ≤ 18, -20 ≤ l ≤ 20
Reflections collected	60298
Independent reflections	12198 [R_{int} = 0.0511, R_{sigma} = 0.0370]
Data/restraints/parameters	12198/0/569
Goodness-of-fit on F^2	1.030
Final R indexes [I>=2σ (I)]	R_1 = 0.0394, wR_2 = 0.1075
Final R indexes [all data]	R_1 = 0.0504, wR_2 = 0.1134
Largest diff. peak/hole / e Å^{-3}	1.58/-0.72

Structure Determination of 4

All non-hydrogen atoms were refined anisotropically. Hydrogen atoms were also placed geometrically, constrained and refined using a riding model. Geometrical and displacement parameter restraints were used to model the highly disordered counter ions. Displacement constraints were used to model the OH/NO disorder. After the model had converged, SQUEEZE was used to remove the electron density from the void space as no recognizable solvent molecules could be discerned. Before SQUEEZE R1 = 10.03% after R1 = 7.92%

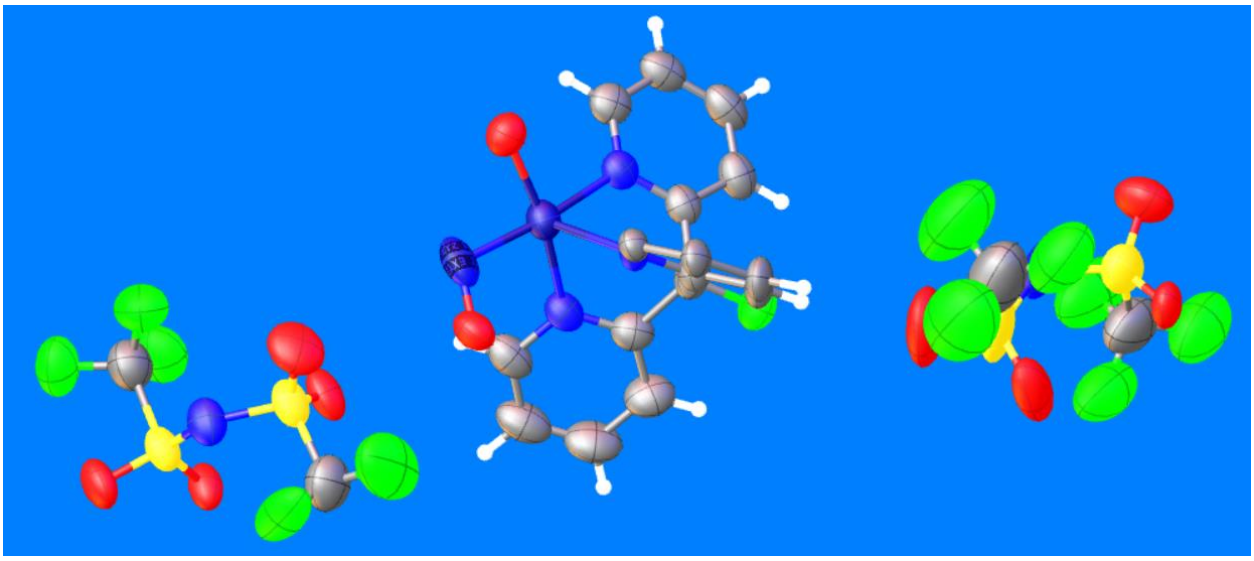

Figure S47. Asymmetric unit of **4**. Color Scheme: C, grey; H, white; N, blue; O, red; S, yellow; F, green; Cu, dark blue.

Table S3. Crystal data and structure refinement for **4**.

Empirical formula	$C_{34}H_{20}Cu_2F_{13}N_{8.30}O_{10}S_4$
Formula weight	1207.10
Temperature/K	150(2)
Crystal system	Monoclinic
Space group	$P2_1/m$
a/Å	12.7416(14)
b/Å	17.5952(19)
c/Å	13.3578(15)
α/°	90
β/°	112.534(4)
γ/°	90
Volume/Å^3	2766.1(5)
Z	2
ρ_{calc}g/cm^3	1.449
μ/mm^{-1}	1.084
F(000)	1202
Crystal size/mm^3	0.100 x 0.040 x 0.030

Radiation	0.72880
2Θ range for data collection/°	1.926 to 26.162
Index ranges	-15<=h<=15, -21<=k<=21, -16<=l<=16
Reflections collected	67245
Independent reflections	5268 [R(int) = 0.0570]
Data/restraints/parameters	5268 / 370 / 449
Goodness-of-fit on F^2	1.077
Final R indexes [I>=2σ (I)]	R_1 = 0.0736, wR2 = 0.2289
Final R indexes [all data]	R_1 = 0.0801, wR2 = 0.2378
Largest diff. peak/hole / e $Å^{-3}$	1.721/-0.893

12) References

1) Ziegler, M. S.; Levine, D. S.; Lakshmi, K. V.; Tilley, T. D. *J. Am. Chem. Soc.* **2016**, *138*, 6484-6491.
2) Desnoyer, A. N.; Nicolay, A.; Ziegler, M. S.; Lakshmi, K. V.; Cundari, T. R.; Tilley, T. D. *J. Am. Chem. Soc.* **2021**, *143*, 7135-7143.
3) Desnoyer, A. N.; Nicolay, A.; Ziegler, M. S.; Torquato, N. A.; Tilley, T. D. *Angew. Chem. Int. Ed.* **2020**, *59*, 12769.
4) Ríos, P.; See, M. S.; Handford, R. C.; Teat, S. J.; Tilley, T. D. *Chem. Sci.,* **2022**, *13*, 6619-6625.
5) Ziegler, M. S.; Torquato, N. A.; Levine, D. S.; Nicolay, A.; Celik, H.; Tilley,T. D. *Organometallics*. **2018**, *37*, 2807-2823.
6) Mass Spec Tools – isotope distribution calculator and mass spec plotter. https://www.sisweb.com/mstools/isotope.htm
7) Weigend, F. and Ahlrichs, R. *Phys. Chem. Chem. Phys.* **2005**, *7*, 3297.
8) Neese, F. Software update: The ORCA program system-Version 5.0. *WIREs Comput Mol Sci.* **2022**; 12:e1606
9) Chemcraft - graphical software for visualization of quantum chemistry computations. https://www.chemcraftprog.com
10) Sheldrick, M. G. *Acta Crystallogr.* **2015**, *A71*, 3–8.
11) Sheldrick, M. G. *Acta Cryst.* **2015**, *C71*, 3–8.
12) Dolomanov, O. V.; Bourhis, J. L.; Gildea, J. R.; Howard, K. A. J.; Puschmann, H. *J Appl Cryst.* **2009**, *42*, 339–341.